



Trinity College Dublin

Coláiste na Tríonóide, Baile Átha Cliath

The University of Dublin

**Functional characterisation of small RNAs
in *Acinetobacter baumannii* using
Hi-GRIL-seq**

Moyne Institute of Preventive Medicine

MSc Microbiology, 2021

Submitted by:

Fergal Hamrock

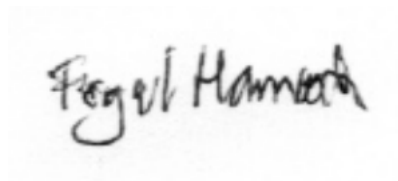
Supervisor: Carsten Kröger

Submission Declaration

I declare that this thesis has not been submitted as an exercise for a degree at this or any other university and it is entirely my own work.

I agree to deposit this thesis in the University's open access institutional repository or allow the Library to do so on my behalf, subject to Irish Copyright Legislation and Trinity College Library conditions of use and acknowledgement.

I consent to the examiner retaining a copy of the thesis beyond the examining period, should they so wish (EU GDPR May 2018).

A handwritten signature in black ink that reads "Fergal Hamrock". The signature is written in a cursive style with a large initial 'F'.

Fergal Hamrock

April 2021

Acknowledgments

I would like to express my gratitude to my supervisor, Asst. Prof. Carsten Kröger, whose guidance, expertise and patience was vital for developing my skill as a postgraduate student. I would also like to thank my postgraduate committee members Alastair Fleming and Marta Martins for their support.

I would also like to thank all the staff, students and members of the Moyne Institute of Preventive Medicine for helping me develop my technical skills and for their friendliness. I would especially like to thank Ali Bakheet and Anna Ershova for their camaraderie.

Table of Contents

| | |
|---|-----------|
| Summary | 1 |
| 1 Introduction | 3 |
| 1.1 <i>A. baumannii</i> as a cause of disease | 3 |
| 1.2 Posttranscriptional regulation by sRNAs | 6 |
| 1.3 Characterisation of posttranscriptional regulation in <i>A. baumannii</i> | 11 |
| 1.4 Identification of sRNA-mRNA interactions..... | 14 |
| 1.5 Aims and Experimental approach..... | 19 |
| 2 Materials and Methods | 21 |
| 2.1 General laboratory techniques | 21 |
| 2.1.1 Media | 21 |
| 2.1.2 Bacterial strains and plasmids..... | 21 |
| 2.1.3 Bacterial culture conditions | 21 |
| 2.1.4 Preparation of antibiotics | 24 |
| 2.1.5 Plasmid preparations | 24 |
| 2.1.6 Genomic DNA extraction | 24 |
| 2.1.7 Polymerase Chain Reactions | 25 |
| 2.1.8 Agarose gel electrophoresis..... | 30 |
| 2.1.9 PCR purification..... | 31 |
| 2.1.10 SLiCE cloning procedure | 31 |
| 2.1.11 Preparation and transformation of competent <i>E. coli</i> | 32 |
| 2.1.12 Sanger sequencing of plasmid DNA..... | 32 |
| 2.1.13 Measurement of fluorescence in 96-well plates | 33 |
| 2.2 Hi-GRIL-seq in <i>A. baumannii</i> AB5075 | 34 |
| 2.2.1 Generation of chimeric molecules | 34 |
| 2.2.2 RNA isolation, reverse-transcription and sequencing..... | 35 |
| 2.2.3 Hi-GRIL-seq analysis | 37 |
| 2.2.4 Bioinformatic analysis | 37 |
| 2.3 Construction of plasmids | 39 |
| 2.3.1 Amplification of pP _L backbone | 39 |
| 2.3.2 Amplification of pXG10 backbone..... | 40 |
| 2.3.3 Amplification of candidate sRNAs | 41 |
| 2.3.4 Amplification of mRNA targets | 41 |
| 2.3.5 Cloning sRNAs into pP _L backbone | 42 |
| 2.3.6 Cloning targets into pXG10 backbone..... | 43 |
| 2.4 GFP based two-plasmid sRNA and target validation | 45 |
| 2.4.1 Plasmids | 45 |
| 2.4.2 Validation of sRNA-mRNA interactions..... | 45 |
| 3 Analysis of RNA-RNA interactions using Hi-GRIL-seq | 46 |
| 3.1 Identification of potential sRNA-mRNA interactions..... | 46 |
| 3.2 Characterisation of candidate sRNAs..... | 50 |
| 3.3 Characterisation of potential mRNA targets | 54 |

| | | |
|----------|--|-----------|
| 3.4 | Prediction of sRNA-mRNA duplex structures..... | 61 |
| 3.5 | Comparison of Hi-GRIL-seq to target prediction tools | 63 |
| 4 | <i>Validation of sRNA-mRNA interactions.....</i> | 66 |
| 4.1 | Construction of overexpression vectors | 66 |
| 4.2 | Verification of sRNA-mRNA interactions | 73 |
| 5 | <i>Discussion</i> | 75 |
| 6 | <i>Bibliography</i> | 82 |

List of Figures

| | |
|--|----|
| Figure 1.1 Antimicrobial resistance strategies in <i>A. baumannii</i> | 5 |
| Figure 1.2 Bacterial trans-encoded sRNA mechanisms of action | 9 |
| Figure 1.3 Regulation of antimicrobial resistance mechanisms by sRNAs..... | 10 |
| Figure 1.4 <i>A. baumannii</i> candidate sRNAs predicted by dRNA-seq..... | 13 |
| Figure 1.5 Hi-GRIL-seq protocol | 18 |
| Figure 3.1 Identification of optimal L-arabinose concentration for T4 RNA ligase expression | 49 |
| Figure 3.2 Two-dimensional display of chimeras identified by Hi-GRIL-seq | 49 |
| Figure 3.3 Mapping Hi-GRIL-seq ligation sites to sRNAs under investigation | 52 |
| Figure 3.4 Mapping Hi-GRIL-seq ligation sites to targets under investigation..... | 58 |
| Figure 3.5 Number of chimera formed in each condition | 60 |
| Figure 3.6 Duplex structure of sRNA-mRNA interactions under investigation | 62 |
| Figure 3.7 Comparison of computational and experimental target predictions..... | 65 |
| Figure 4.1 Model of the two-plasmid RNA-RNA interaction confirmation system | 68 |
| Figure 4.2 Backbone amplification of pP _L and pXG10..... | 68 |
| Figure 4.3 Amplification of sRNAs under investigation | 69 |
| Figure 4.4 Amplification of targets under investigation | 71 |
| Figure 4.5 Co-expression of sRNA and target vectors compared to pJV300 control | 74 |

List of Tables

| | |
|---|----|
| Table 2.1 Bacterial strains used in study | 22 |
| Table 2.2 Plasmids used in study | 23 |
| Table 2.3 Primers used in this study | 26 |
| Table 2.4 Taq polymerase PCR reactants..... | 28 |
| Table 2.5 Ranger-Mix PCR reactants | 29 |
| Table 2.6 PCR cycling conditions | 29 |
| Table 2.7 Colony PCR cycling conditions..... | 30 |
| Table 2.8 SLiCE reaction components | 31 |
| Table 2.9 Details of samples supplied to Vertis Biotechnologie AG | 35 |
| Table 2.10 Properties of cDNA samples..... | 36 |
| Table 2.11 pP _L modified PCR cycling condition | 39 |
| Table 2.12 pXG10 modified PCR cycling condition..... | 40 |
| Table 2.13 sRNA amplification cycling conditions..... | 41 |
| Table 2.14 Target amplification cycling conditions | 42 |
| Table 2.15 sRNA SLiCE cloning..... | 43 |
| Table 2.16 Target SLiCE cloning | 44 |
| Table 3.1 Total number of Hi-GRIL-seq reads per condition | 47 |
| Table 3.2 Genomic structure of sRNAs under investigation | 51 |
| Table 3.3 Hi-GRIL-seq Targets under investigation | 54 |
| Table 3.4 Interaction pair hybridisation strengths | 61 |
| Table 4.1 pP _L and pXG10 amplification results | 69 |
| Table 4.2 sRNA amplification results..... | 70 |
| Table 4.3 Target amplification results | 72 |

Summary

Acinetobacter baumannii is a priority pathogen that is a leading source of nosocomial multidrug resistant (MDR) infections worldwide. A key to the success of *A. baumannii* is the ability to quickly adapt to changing environmental conditions by regulating gene expression programmes which includes genes that are important antimicrobial resistance (AMR), environmental persistence and virulence. This study examines how an MDR strain of *A. baumannii* is capable of persisting in adverse conditions using posttranscriptional regulatory mechanisms. Understanding these mechanisms will inform future research into how this organism causes disease and how it has evolved into an MDR opportunistic pathogen.

To identify the posttranscriptional regulatory mechanisms that promote bacterial survival, we experimentally identified mRNA targets of candidate regulatory sRNAs by employing the proximity ligation procedure Hi-GRIL-seq that ligates RNA-RNA interaction pairs into chimeric molecules independently of RNA chaperones. The sRNA-containing chimeras were identified and mapped to the *A. baumannii* genome to identify mRNA targets. Hi-GRIL-seq procedure was performed during growth in rich medium and following iron starvation and exposure to antibiotics to identify potential targets regulated under such conditions.

Filtering Hi-GRIL-seq generated chimeras based on abundance identified the most likely targets for each sRNA, which led to the identification of over 1500 potential sRNA-mRNA interactions many of which are expected to play essential roles in virulence, metabolism, iron responses and AMR. Eight sRNA-mRNA interaction partners were selected for further mechanistic investigation by analysing ligation junctures of the chimeras for these interaction partners and predicting their duplex structures. By

integrating the Hi-GRIL-seq output with bioinformatic sRNA-target mRNA predictions tools CopraRNA and TargetRNA2, we identified 16S rRNA pseudouridine synthetase as target for regulation by sRNA21. The identified sRNA-mRNA interactions were experimentally tested by using a previously established two-plasmid approach. This system uses a translational fusion of GFP with the target RNA as a reporter of sRNA-based posttranscriptional regulation. By measuring the GFP abundance in *E. coli* co-expressing the sRNA and the cognate target mRNA-GFP compared to controls, we confirmed two sRNA-mRNA interaction. The sRNA21 suppresses the expression of 16S rRNA pseudouridine synthase and sRNA97 enhances the expression of an alpha-keto acid decarboxylase family protein. Recent evidence suggests that these targets may be involved in regulating persistence and amino acid metabolism.

This study demonstrates the power Hi-GRIL-seq can play in elucidating novel sRNA-mRNA interactions. The combination of this procedure with computational predictions and experimental validation promises to enable description of the entire *A. baumannii* targetome.

1 Introduction

1.1 *A. baumannii* as a cause of disease

The Gram-negative bacterium *Acinetobacter baumannii* is a leading source of nosocomial infections. This opportunistic pathogen is a member of the of the *Moraxellaceae* family within the Pseudomonadales order and is one of the few clinically significant *Moraxellaceae* species along with closely related *Acinetobacter calcoaceticus-Acinetobacter baumannii* (*Acb*) complex members *A. nosocomialis* and *A. pittii* (Diancourt et al., 2010). *A. baumannii* infections account for up to 10% of hospital-acquired infections in developed countries and over 20% of hospital-acquired infections in developing countries (Lob et al., 2016; Magill et al., 2014). Outbreaks are frequently observed following military conflict or after natural disasters (Fily et al., 2019; Joly-Guillou, 2005).

A. baumannii infects opportunistically and primarily causes disease in critically ill patients confined to hospital environments (Antunes et al., 2014). Diseases manifest differently depending on the site of infection, but are generally associated with intrusive medical devices such as mechanical ventilators and catheters (Dijkshoorn et al., 2007). The most common presentations include ventilator-associated pneumonia and bacteraemia. These infections are serious with mortality rates of up to 50% (Weiner et al., 2016). Other common infections include catheter-associated urinary tract infections, skin infections, secondary meningitis and burn wound infections (Sievert et al., 2013). Previous traumas or the length of hospital stay can increase the probability of infection (Wu et al., 2020). Community-acquired infections are highly fatal but are rare and largely confined to patients with prior health risk factors and in tropical environments (Dexter et al., 2015).

The exact *A. baumannii* reservoir is unclear, however, it is evident that the pathogen thrives in hospital environments (Towner, 2009), which is attributed to the antimicrobial resistance (AMR) and environmental persistence strategies allowing survival in adverse environmental conditions for extended periods of time (Roca et al., 2012). The accumulation of AMR genes through horizontal gene transfer enables *A. baumannii* to utilise multiple resistance mechanisms, these mechanisms are depicted and described in **Figure 1.1** (Lee et al., 2017; Partridge et al., 2018). The emergence of multi-drug resistant (MDR) strains of *A. baumannii* has a devastating impact on healthcare systems; infections with these strains have mortality rates of up to 20% and cost the US economy \$1.6 billion annually (Butler et al., 2019; Cornejo-Juárez et al., 2020; Nelson et al., 2016). The Centers for Disease Control and the World Health Organisation have recently declared carbapenem-resistant *A. baumannii* as a priority threat (Centers for Disease Control and Prevention, 2019; Tacconelli et al., 2018), because it has developed multiple environmental survival strategies including AMR, many of which aid in host colonisation and infection, for example by withstanding desiccation (Zeidler et al., 2019b) and exposure to oxidative stress (Fiester et al., 2013), creating biofilms (Eze et al., 2018) and surviving in low nutrient concentration conditions (Runci et al., 2019).

A. baumannii modulates the expression of genes underlying these survival strategies to rapidly adapt to changing environmental conditions (Wood et al., 2018). Changes in gene expression are frequently mediated by protein transcriptional regulators and several transcriptional regulators of AMR, environmental persistence and virulence genes in *A. baumannii* have already been defined (Farrow et al., 2018; Gaddy et al., 2009; Kröger et al., 2017; Lucidi et al., 2018). Conversely, post-transcriptional regulation of *A. baumannii* pathophysiology is poorly understood and may offer future strategies for overcoming AMR and virulence.

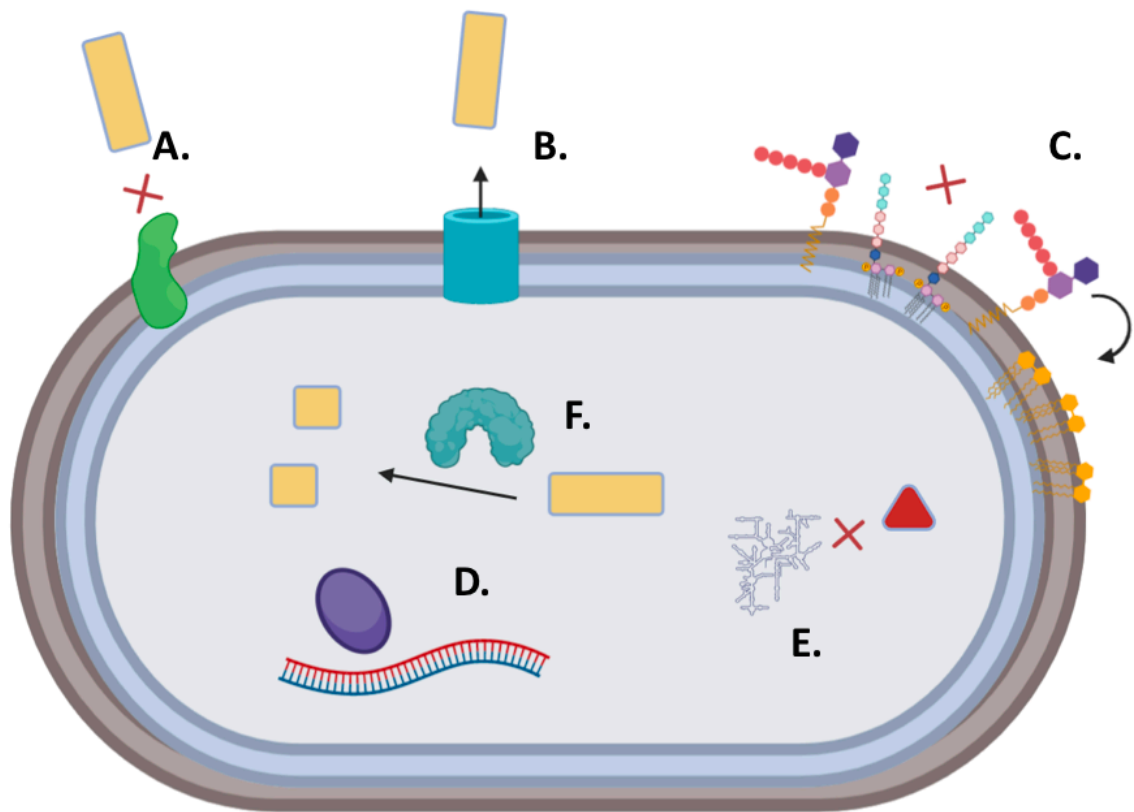


Figure 1.1 Antimicrobial resistance strategies in *A. baumannii*

Diagram depicting major antimicrobial resistance strategies utilised by *A. baumannii* including; A. Modification of outer membrane proteins, B. Use of efflux pumps to remove antimicrobial agents, C. Loss or modification of LPS (colistin resistance), D. Mutations in DNA topoisomerase and gyrase (quinolone resistance), E. Modification of ribosomal binding proteins (aminoglycoside resistance) and F. Generation of β -lactamase (β -lactam resistance). Figure adapted from Asif (Asif et al., 2018).

1.2 Posttranscriptional regulation by sRNAs

The characterisation of posttranscriptional regulatory systems that modulate expression of AMR genes and virulence factors will enhance our understanding of pathogenesis in *A. baumannii*. Bacterial small RNAs (sRNAs) are a class of posttranscriptional regulators of bacterial physiology in numerous species. These are non-coding RNA molecules, ranging from ~50 – 500 nucleotides, that alter translation of specific genes through antisense base-pairing with RNA molecules or through interactions with proteins (Woodson et al., 2018). RNA-RNA interactions between an sRNA and an mRNA target allow formation of an sRNA-mRNA duplex through base-pairing between conserved sRNA “seed” regions and complementary mRNA binding regions (Hör et al., 2018). Bacterial sRNAs are divided into two categories; *cis*-encoded sRNAs and *trans*-encoded sRNAs. *Cis*-encoded sRNAs are transcribed from the complementary strand of the mRNA targets, while *trans*-encoded sRNAs are transcribed at a distance from their mRNA targets. *Trans*-encoded sRNA are capable of interacting with RNA molecules or proteins, for instance 6S RNA interacts with the σ^{70} subunit of RNA polymerase (Wassarman, 2018). Bacterial sRNA can be located within intergenic regions (IGRs), 5' or 3' untranslated regions (UTRs) (Chao et al., 2012; Heidrich et al., 2017; Miyakoshi et al., 2015).

Trans-encoded sRNAs are capable of enhancing or suppressing the expression of mRNA targets using a myriad of mechanisms as shown in **Figure 1.2** (Wagner et al., 2015). Most sRNAs canonically base-pair to the 5'-UTR of their target near or overlapping the ribosome binding site (RBS). This generally blocks the 30S ribosomal subunit from binding to the mRNA preventing translation, however, there are instances when this can stabilise the mRNA molecule for translation (Fröhlich et al., 2009; Papenfort et al., 2009). Typically, sRNA-mRNA interactions induce RNase-mediated (typically RNaseE)

degradation of both molecules. In some circumstances, sRNA-mRNA interactions can block the complex from degradation, enhancing expression of the target (Fröhlich et al., 2013). Many of the *trans*-encoded sRNAs, particularly those in the *Enterobacteriaceae*, require the activity of the RNA-binding protein Hfq (Santiago-Frangos et al., 2018). Hfq is composed on a homo-hexamer, with a proximal face that binds to the A-rich tails of mRNA targets and a distal face that binds to the uridine base-pairs located in the sRNA terminators (Morita et al., 2019). Hfq often acts as a platform for bringing sRNAs and their cognate mRNA targets into close contact, however, it also stabilises these molecules protecting them from degradation, or creating structural rearrangements in sRNAs and mRNAs to expose seed regions and sRNA binding region or enhance the degradation of mRNA targets (Hoekzema et al., 2019). There are several other RNA-binding proteins that sometimes can act as sRNA-mRNA chaperones in Gram-negative pathogens including ProQ, CsrA and CspC/E. ProQ is a chaperone, similar in structure to the RNA-binding protein FinO which mostly highly structured sRNAs bind (Smirnov et al., 2016, 2017). It was shown to work in parallel with Hfq in *Salmonella enterica* Typhimurium to modulate flagellar and SPI-1 component expression, (Westermann et al., 2019). Unlike Hfq, ProQ positively regulates SPI-2 expression highlighting its importance as a chaperone involved in *Salmonella* pathogenicity, but it is absent in *A. baumannii*. CsrA is an RNA chaperone that regulates mRNA transcripts involved in physiology and pathogenesis in multiple bacterial species including *Salmonella* and *E. coli* (Holmqvist et al., 2016) and CspC and CspE are functionally redundant cold-shock proteins that are implicated in regulating *Salmonella* Typhimurium biofilm generation, motility and stress responses (Michaux et al., 2017). CsrA and CspC/E homologues exist in *A. baumannii*, but their role for RNA biology has not been studied, yet.

Trans-encoded sRNAs are important posttranscriptional regulators of bacterial physiology (Holmqvist et al., 2017). The disruption of sRNAs or RNA binding proteins has been shown to enhance antibiotic susceptibility and hinder expression of numerous virulence factors in many bacterial species (Oliva et al., 2015; Yamada et al., 2010). Bacterial sRNAs modulate antibiotic resistance using several strategies by altering antibiotic efflux through efflux pumps (Du et al., 2018), affecting antibiotic uptake through transporters (Di Noto et al., 2019), modifying LPS (Klein et al., 2015) or cell wall biosynthesis (Khan et al., 2016), enhancing DNA mutagenesis (Gutierrez et al., 2013) and biofilm synthesis (Andreassen et al., 2018) leading to resistance to a broad spectrum of antibiotics. Examples of these mechanisms and how they impact AMR are depicted in **Figure 1.3**. *Trans*-encoded sRNAs also modulate expression of virulence factors involved in environmental persistence and host colonisation (Matos et al., 2017). For instance, sRNAs RyhB and PrrF are involved in nutrient acquisition in nutrient poor conditions and in controlling expression of iron acquisition genes, and sRNA SgrS represses glucose transporters in toxic intracellular levels of glucose-6-phosphate (Chareyre et al., 2018; Görke et al., 2008; Reinhart et al., 2017). Bacterial sRNAs also regulate a vital colonisation factor, SgrS negatively regulates SopD, a virulence factor secreted by both *Salmonella* Type III secretion systems and the PhoP-activated sRNA PinT coordinates the transition of *Salmonella* host cell invasion to an intracellular host replicative state (Papenfert et al., 2012; Westermann et al., 2016). Other sRNAs frequently regulate quorum sensing molecules and outer membrane protein expression (Chen et al., 2004; Liu et al., 2020; Vogel et al., 2006).

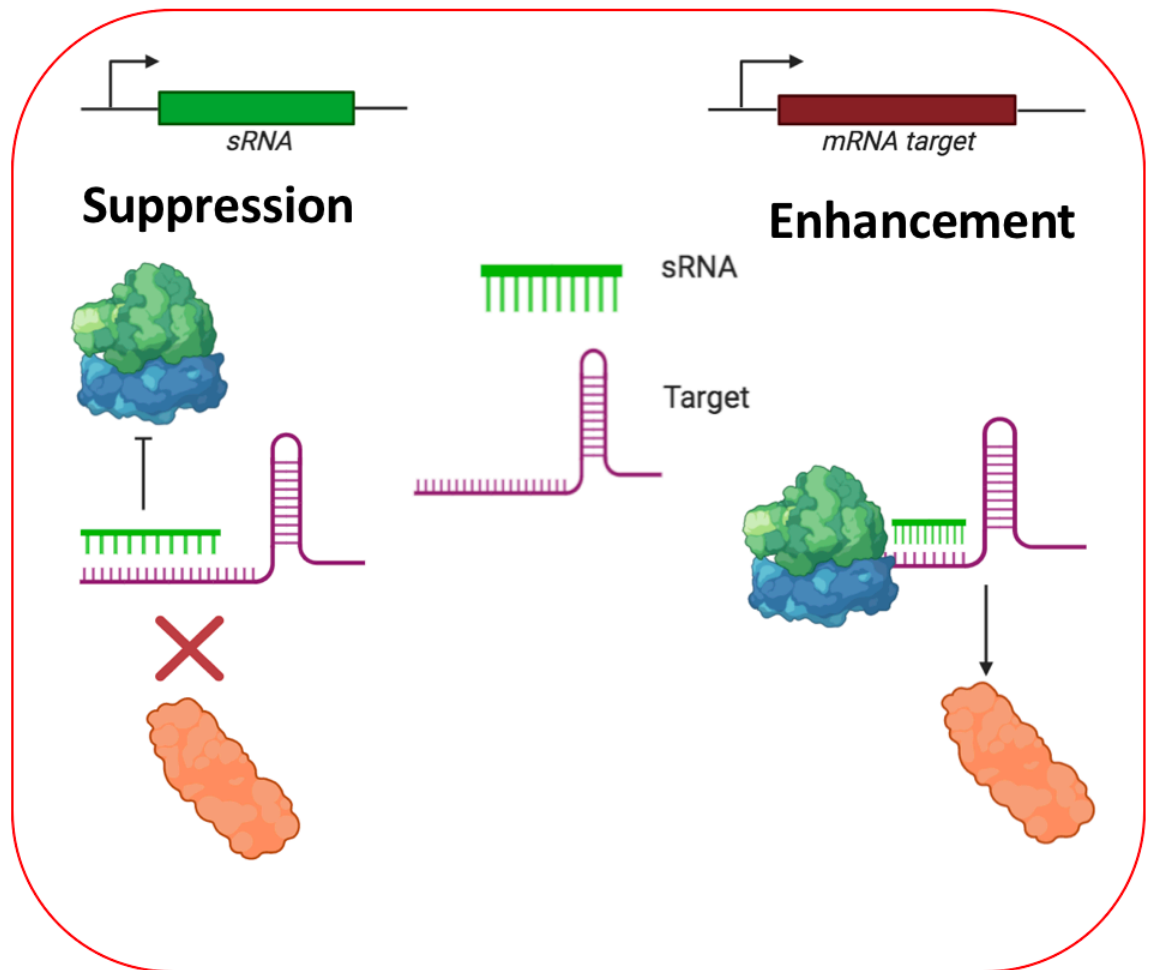


Figure 1.2 Bacterial *trans*-encoded sRNA mechanisms of action

Bacterial *trans*-encoded sRNAs are capable of either binding to their mRNA target, preventing ribosomes from binding to their 5' flank, stopping translation or binding to their mRNA target causing a conformational change that removes an inhibitory structure, increasing expression of their target.

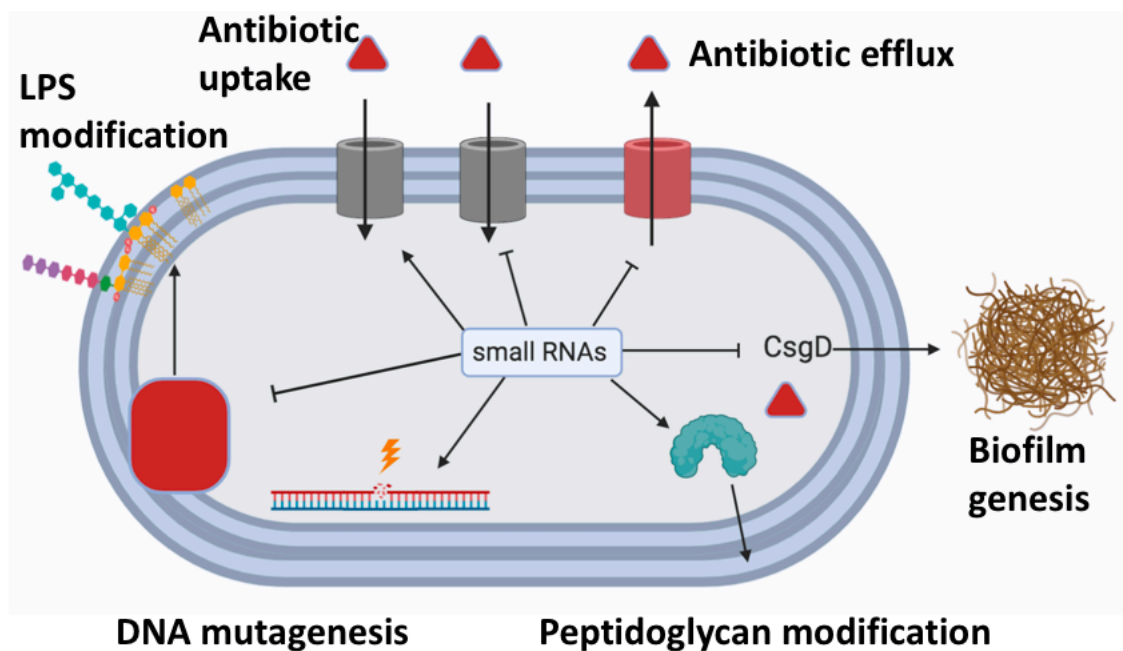


Figure 1.3 Regulation of antimicrobial resistance mechanisms by sRNAs

Bacterial sRNAs are capable of regulating antimicrobial resistance by altering antibiotic uptake, antibiotic efflux, expression of biofilm genes, peptidoglycan biosynthesis, mutagenesis and LPS modifications. Figure adapted from Dersch (Dersch et al., 2017). The sRNAs that are capable of suppressing the expression are denoted by the flatheaded lines while those that enhance expression are denoted by the arrows.

1.3 Characterisation of posttranscriptional regulation in *A. baumannii*

The mechanistic and physiological properties of *trans*-encoded sRNAs in *A. baumannii* remain ambiguous compared to other Gram-negative species (Kröger et al., 2017). A first *Acinetobacter* specific sRNA, *Acinetobacter* amino acid regulator (Aar), was identified through *in silico* comparative analysis of thermodynamically conserved loci in the non-pathogenic relative *Acinetobacter baylyi* (Schilling et al., 2010). Overexpression of Aar was observed to upregulate seven mRNAs, six of which are involved in amino acid metabolism; including pyruvate metabolism, branched chain-amino acid synthesis, branched-chain amino acid degradation, glycine degradation and nitrogen fixation into glutamine. A combination of computational analyses and Northern blotting assays were used to predict three *A. baumannii* sRNA candidates in the ATCC 15308 strain (Sharma et al., 2014). One of these putative sRNAs is suggested to negatively regulate a major facilitator superfamily efflux pump, however, the mechanisms underlying this interaction are not defined. The Shaw group employed the use of RNA-seq to identify 78 sRNAs in the multidrug resistant *A. baumannii* strain AB5075 (Weiss et al., 2016). This group identified the homologues of Aar and one of the three ATCC 15308 candidate sRNAs. The Kröger group improved the resolution of sRNA discovery by using differential RNA-seq (dRNA-seq) pooled from sixteen different growth conditions to detect *de novo* sRNAs in *A. baumannii* ATCC17978 (Kröger et al., 2018). This enabled discovery of transcriptional start sites (TSS), sRNAs located at the 3' end of coding genes facilitating future functional characterisation and led to the discovery of 110 potential sRNAs, the majority of which were conserved within *A. baumannii* and to a lesser extent within *A. nosocomialis* and *A. pittii* as shown in **Figure 1.4**. More recently, a comparative sRNA transcriptome analysis between colistin resistant and sensitive strains of *A. baumannii*

was performed (Cafiso et al., 2020). This led to the identification of three *cis*-encoded sRNAs and two microRNAs that are predicted to regulate colistin resistance.

Unlike in the *Enterobacteriaceae*, the involvement of Hfq and other potential RNA binding proteins in mediating sRNA-mRNA interactions in *Pseudomonas aeruginosa*, a closer relative of *A. baumannii* is unclear. The deletion of Hfq decreases the stability of the transcriptome of *P. aeruginosa* and attenuates virulence, however, there is a lack of experimental evidence linking the chaperone to sRNA-mRNA annealing (Sonnleitner et al., 2012). Analysis of Hfq in *A. baylyi* and *A. baumannii* ATCC 17978 reveal that this molecule has an enlarged glycine rich C-terminal domain relative to other bacteria (Schilling et al., 2009; Sharma et al., 2018). Deletion of *A. baumannii* Hfq impeded growth relative to the wild-type strain and increased susceptibility to environmental stressors, including desiccation, decreased carbon metabolism and restricted host cell adhesion and virulence (Kuo et al., 2017). While it appears that Hfq is a vital virulence factor in *A. baumannii*, it remains unclear how this chaperone is involved in mediating sRNA-mRNA interactions.

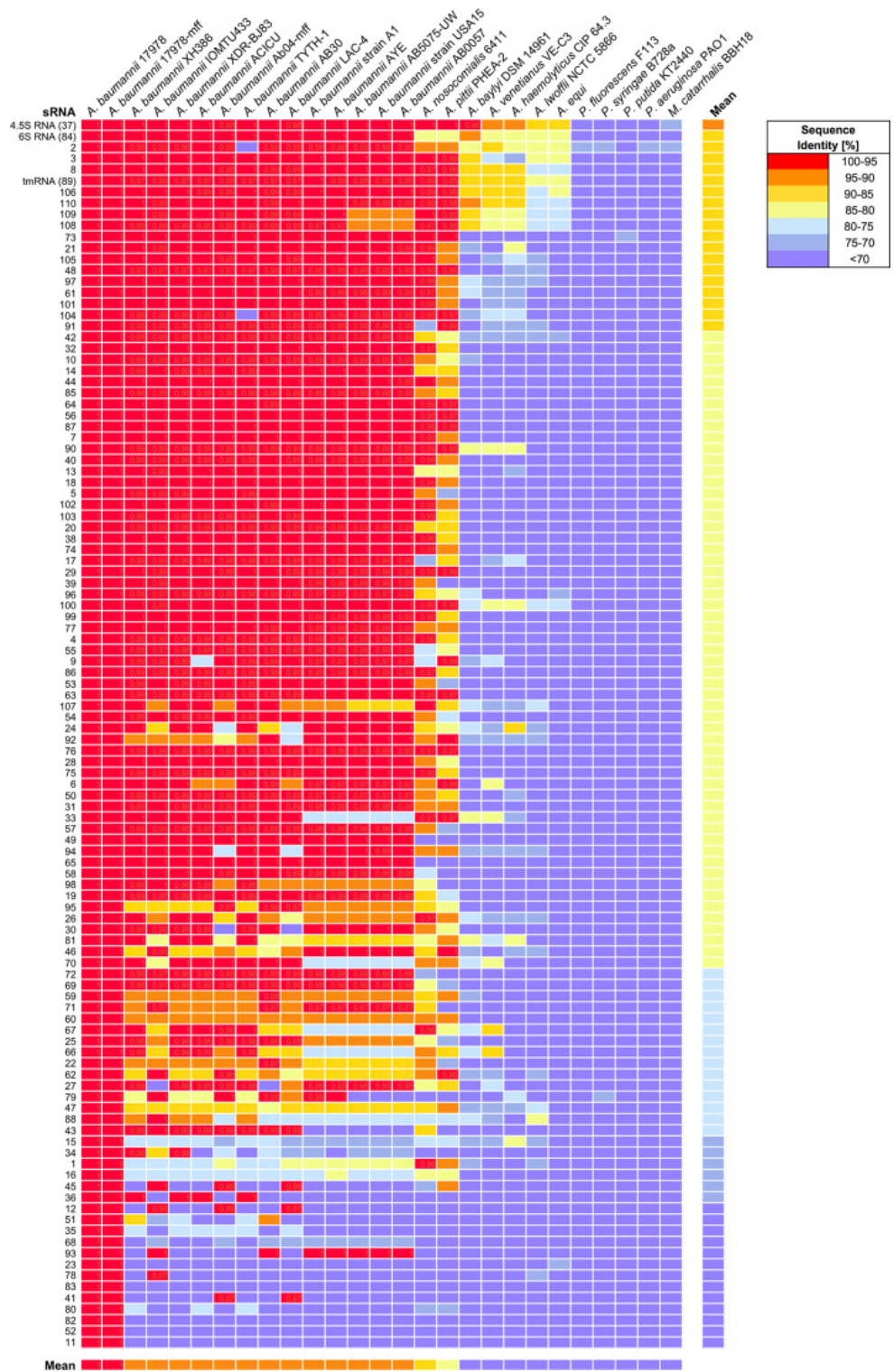


Figure 1.4 *A. baumannii* candidate sRNAs predicted by dRNA-seq

The *A. baumannii* sRNA candidates predicted by Kröger using differential RNA-sequencing (Kröger et al., 2018). These candidates were predicted in the ATCC 17978 and the conservation for each candidate among *Acb* complex organisms, *Pseudomonas* species and *Moraxella catarrhalis* was compared. This figure was modified from Kröger et al., 2018.

1.4 Identification of sRNA-mRNA interactions

To characterise the role potential *A. baumannii* sRNAs play in *A. baumannii* physiology, AMR and pathogenesis, their interaction partners must be predicted and validated. Identification of sRNA-mRNA interactions in other bacterial species relies on computational and experimental approaches (Wagner et al., 2015). Using computational approaches to predict interactions between sRNA candidates and mRNAs allows cheap and efficient definition of posttranscriptional regulation (Georg et al., 2020). These predictions simulate RNA-RNA interactions *in silico* by using algorithms that consider intramolecular and intermolecular structures based on the thermodynamics of complementary base-pairing (Wright et al., 2018). Certain prediction tools are optimised to uncover the exact target sequence that interacts with the sRNA seed sequence. These tools reliably predict experimentally-defined sRNA-mRNA duplex structures, for instance IntaRNA accurately predicts 62% of known interactions, however, these tools often poorly predict novel interactions (Busch et al., 2008; Lai et al., 2015). The development of comparative prediction tools, such as CopraRNA and TargetRNA2, allow identification of RNA-RNA interactions across entire sRNA “targetomes” (Wright et al., 2013). CopraRNA compares conserved target interactions in multiple species with homologous sRNAs, allowing specific and sensitive detection of novel sRNA-mRNA interaction pairs, this has previously detected mRNA targets in pathogenic species (Lu et al., 2016; Wright et al., 2014). However, CopraRNA only investigates complementarity within the 5' UTR and the first 100 nucleotides of mRNA limiting interaction discovery outside this region and ignoring interactions with non-protein coding mRNA targets (Georg et al., 2020).

Experimental approaches to functionally characterise sRNAs require genome-wide target identification systems. The earliest global target identification screen was performed *in*

vitro using direct-capture and pulse overexpression whole-genome microarray target hunts (Vogel et al., 2007). The direct capture method uses streptavidin beads to capture labelled sRNA-mRNA complexes, followed by conversion of these complexes to cDNA using reverse-transcription and hybridisation to a whole-genome microarray. This was used to determine that *ompA* and *ompC* are targets of the sRNA RseX (Douchin et al., 2006). Pulse overexpression compares the transcription profile of an sRNA overexpression strain to an sRNA deficient strain. Following sRNA overexpression, mRNA is extracted from both strains, differentially labelled, converted to cDNA and hybridised to the microarray. This strategy was used to determine that *sodB* is a RyhB target (Massé et al., 2005). These approaches are unable to detect changes in translation (Wang et al., 2015).

Proximity ligation assays facilitate the transcriptome-wide discovery of sRNA-mRNA interactions *in vivo*. These assays involve ligation of interacting RNA molecules to form RNA-RNA chimeras, which are then sequenced and compared to the genome of the organism under investigation. The sRNA-containing chimeras are analysed to determine which RNA molecules they are capable of interacting with, this often includes tRNAs, other sRNAs and functionally relevant mRNAs. Proximity ligation assays include; RNA interaction by ligation and sequencing (RIL-seq), Global sRNA target Identification by Ligation and Sequencing (GRIL-seq) and High-throughput Global sRNA target Identification by Ligation and Sequencing (Hi-GRIL-seq).

RIL-seq identifies sRNA-mRNA interactions that are bound to a chaperone molecule (Melamed et al., 2016). Melamed et al. established this method by crosslinking RNAs to tagged Hfq with UV light in three growth conditions in *E. coli*. Hfq was then coimmunoprecipitated and crosslinked RNAs were ligated, isolated, sequenced and

compared to the genome (Melamed et al., 2016). Approximately 2800 individual interactions were observed and this led to identification of 56% of previously known sRNA-target interactions and to the discovery of novel interactions. Despite the clear advantages, RIL-seq is reliant on a chaperone, restricting the discovery of chaperone independent sRNA-mRNA interactions.

The development of GRIL-seq and Hi-GRIL-seq enabled more extensive investigations of the global RNA interactome due to their chaperone independent methodology (Saliba et al., 2017). These protocols involve ligation of sRNA with their targets to form chimeras, which is accomplished through transient overexpression of a T4 RNA ligase—usually from a plasmid. In GRIL-seq, an sRNA and the T4 RNA ligase are overexpressed simultaneously from individual plasmids to create RNA chimeras (Han et al., 2016). The RNA is then isolated, sRNA chimeras are enriched by ligating sRNAs to a complementary polyadenylated tailed oligo which can be ligated to magnetic beads. The enriched chimeras are then reverse-transcribed to cDNA, sequenced and aligned to the genome. This has an improved ability to detect sRNA-mRNA interactions overlooked by pulse expression microarray assays (Lalaouna, Carrier, et al., 2015). Hi-GRIL-seq combined deep sequencing and computational analysis of chimeric RNA to grant a more global understanding of interactions between mRNA targets and endogenous sRNAs (Zhang et al., 2017). In Hi-GRIL-seq, T4 RNA ligase expression is induced to allow ligation of potentially all endogenous sRNAs and targets. The enrichment step of GRIL-seq is omitted after RNA isolation and rRNA is depleted prior to reverse-transcription and sequencing. The sRNA-mRNA chimeras were identified using a BLAST-based pipeline and mapped on the genome to identify mRNA targets (**Figure 1.5**). This strategy enabled the identification of targets involved in antimicrobial resistance and virulence that are regulated by sRNAs in *Pseudomonas aeruginosa*.

Experimental strategies other than the proximity ligation assays have also been developed to identify transcriptome-wide sRNA-mRNA interactions *in vivo*. For instance, MS2-affinity purification coupled with RNA-sequencing (MAPS) combines RNA affinity purification with RNA-sequencing to identify sRNA interaction partners (Carrier et al., 2016). This protocol is reliant on the highly specific interactions between the bacteriophage MS2 coat protein with the MS2 stem-loop aptamer. MAPS involves *in vivo* expression of MS2 aptamer-tagged sRNAs prior to cell lysis and purification of tagged sRNAs using affinity chromatography (Lalaouna & Massé, 2015). Purified RNA molecules are then analysed using high throughput RNA-sequencing. The ratio of enriched mRNAs in tagged sRNA experiments compared to untagged controls enables identification of sRNA-mRNA interactions. This approach has been reliably used to independently validate known interaction pairs and to identify novel mRNA target molecules (Lalaouna et al., 2019). While MAPS enables high resolution discovery of novel sRNA-mRNA interaction pairs, it cannot simultaneously identify interaction pairs between numerous sRNA candidates and their mRNA interaction partners unlike the proximity ligation assays.

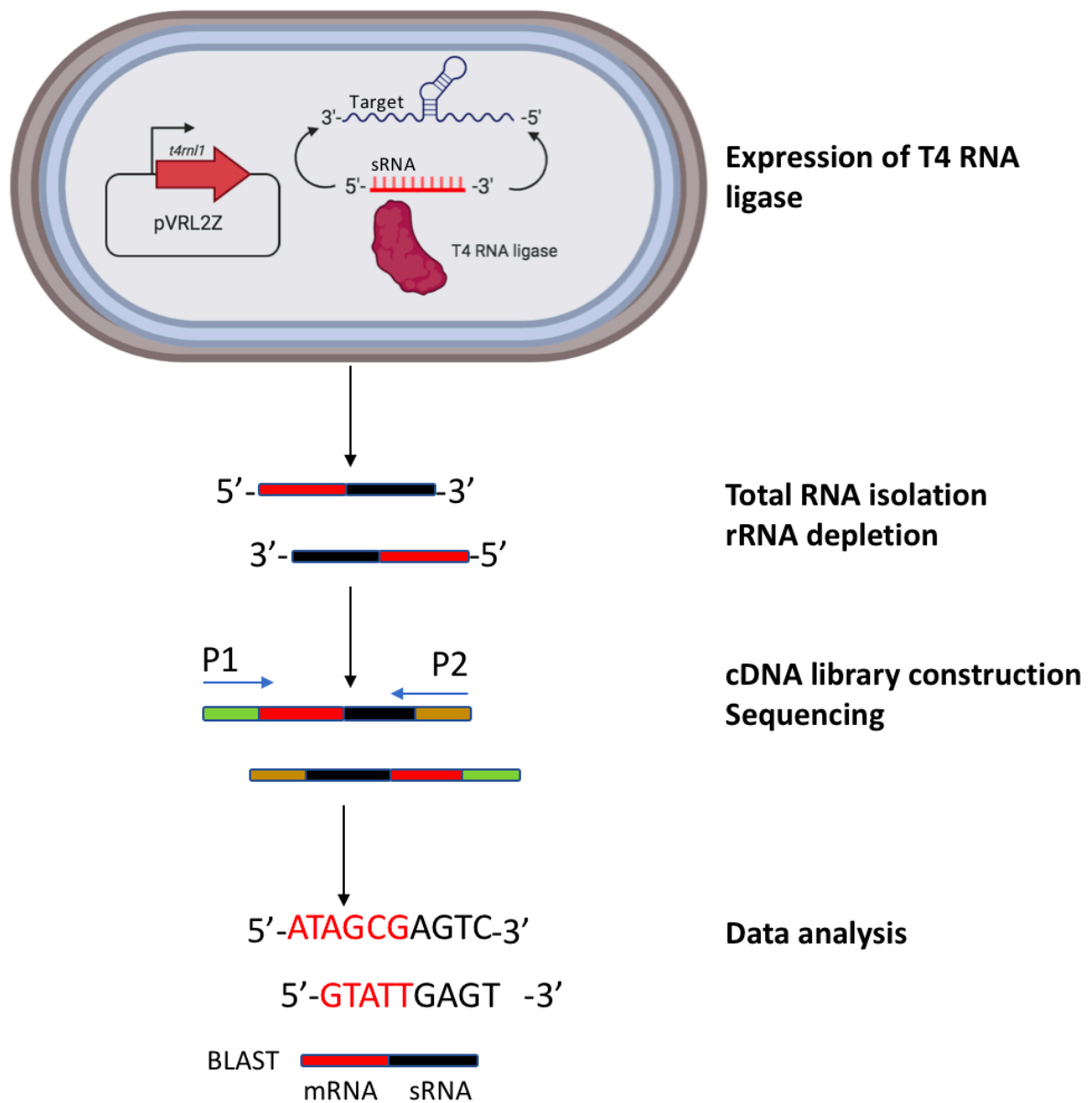


Figure 1.5 Hi-GRIL-seq protocol

The expression of pVRL2Z-*t4rn11* allows expression of T4 RNA ligase, which in turn ligates sRNA and mRNA target molecules forming chimeric molecules. The total RNA is then extracted, rRNA is depleted. Chimeric molecules are subsequently used for cDNA library construction and sequenced. These sequences are mapped to the genome using a BLAST-based pipeline, allowing identification of the sRNA-mRNA interaction pairs in chimeric molecules. Figure adapted from Zhang et al., 2017.

1.5 Aims and Experimental approach

In order to determine the biological importance sRNAs play in regulating gene expression in *A. baumannii*, it is vital to functionally characterise the candidate sRNAs identified so far (Kröger et al., 2018). This project seeks to explore posttranscriptional regulation of gene expression with a focus on AMR and pathogenesis in *A. baumannii* by using Hi-GRIL-seq to predict, analyse and experimentally investigate sRNA-mRNA interactions. Hi-GRIL-seq was chosen to investigate interactions because it is a chaperone independent target identification system and because Hfq plays an unclear role in RNA-RNA interactions in Pseudomonadales.

Hi-GRIL-seq was carried out in the *A. baumannii* strain AB5075 due to its increased virulence and multidrug resistance and due to the fact that it is susceptible to hygromycin and tetracycline, facilitating genetic manipulations (Jacobs et al., 2014). Hi-GRIL-seq was performed in four different conditions to uncover sRNA-mRNA interactions, this included; during induction and non-induction of T4 RNA ligase, during exposure to the antibiotic imipenem and during iron-limiting conditions. The T4 RNA ligase expressing gene was placed under control of the arabinose-inducible pBAD promoter on the pVRL2Z plasmid. The level of basal expression of T4 RNA ligase in the uninduced conditions was not characterised prior to performing the Hi-GRIL-seq analysis. Inappropriate expression of T4 RNA ligase was not expected due to the relative strength of the pBAD promoter. In order to determine the appropriate concentration of arabinose to induce T4 RNA ligase expression, the impact of various concentrations of arabinose on cell density was examined. This did not consider the ligase activity levels limiting the scope of the Hi-GRIL-seq analysis. Biologically important sRNA-mRNA chimeras were selected and analysed.

These interactions were subsequently verified using a fluorescent two-plasmid reporter in *E. coli* to confirm direct interaction between putative interaction pairs (Urban et al., 2007). This two-plasmid reporter assay assumes that sRNA-mRNA interactions translates into altered steady-state levels of the corresponding protein and that these effects can be reconstituted in a heterologous system. The lack of an effect in the reporter assay may not contradict the Hi-GRIL-seq results for these reasons and simply suggest that these are low-confidence interactions. While this independent validation assay measures a relatively indirect GFP readout compared to more direct *in vitro* strategies such as Electrophoretic Motility Shift Assays (EMSA), it outlines RNA-RNA interactions that are more representative of conditions encountered *in vivo* in *A. baumannii* (Morita et al., 2012).

2 Materials and Methods

2.1 General laboratory techniques

2.1.1 *Media*

All cells used in this study were cultivated in liquid and solid media using Lennox broth (L-broth) and Lennox agar (L-agar) respectively. They were prepared by dissolving Bacto-Tryptone (10 g/L), NaCl (5 g/L) and Bacto-Yeast extract (5 g/L), and 1.5% (w/v) Bacto-Agar for L-Agar, in deionised water (dH₂O) and autoclaved. L-agar plates were prepared by adding the required antibiotics in cooled molten L-agar before pouring this in petri dishes.

2.1.2 *Bacterial strains and plasmids*

The bacterial strains and plasmids used in this study are shown in **Table 2.1** and **Table 2.2** respectively. Bacterial strains were stored at -80°C and when needed they were streak out on L-agar, colonies from this were used to make overnight cultures.

2.1.3 *Bacterial culture conditions*

L-broth and L-agar plates were incubated at 37°C for 16-18 hours in this study. Overnight cultures were inoculated in 5 ml L-broth and cultured in a G24 environmental incubator shaker (New Brunswick Scientific). When larger liquid

cultures were needed, L-broth was sub-cultured with overnight cultures and incubated in an Innova3100 (New Brunswick Scientific) incubator. Agar plates were incubated in a Memmert Incubator Oven INB200.

Table 2.1 Bacterial strains used in study

| Strain | Genotype | Reference/source |
|---------------|--|---|
| AB5075 | <i>A. baumannii</i> wild-type | Salcedo Lab (Lyon) (Jacobs et al., 2014) |
| TOP10 | <i>E. coli</i> K12 mcrA Δ (mrr hsdRMS mcrBC) F80lacZ Δ M15 Δ lacX74 deoR recA1 araD139 Δ (ara leu)7697 galU galK rpsL endA1 nupG | Invitrogen |

Table 2.2 Plasmids used in study

| Plasmid | Stored in strain | Reference/source |
|-------------------------|-------------------------------|-------------------------|
| pVRL2Z | <i>A. baumannii</i> AB5075 | (Lucidi et al., 2018) |
| pVRL2Z- T4rn11 | <i>A. baumannii</i> AB5075 | Carsten Kröger |
| pJV300 | <i>E. coli</i> TOP10 | (Urban et al., 2007) |
| pP _L -RybB | <i>E. coli</i> TOP10 | (Vogel et al., 2006) |
| pXG10-OmpC | <i>E. coli</i> TOP10 | (Vogel et al., 2006) |
| pP _L -sRNA21 | <i>E. coli</i> TOP10 | Prepared in this study |
| pP _L -sRNA65 | <i>E. coli</i> TOP10 | Prepared in this study |
| pP _L -sRNA76 | <i>E. coli</i> TOP10 | Prepared in this study |
| pP _L -sRNA85 | <i>E. coli</i> TOP10 | Prepared in this study |
| pP _L -sRNA97 | <i>E. coli</i> TOP10 | Prepared in this study |
| pP _L -sRNA99 | <i>E. coli</i> TOP10 | Prepared in this study |
| pXG10 sf-RsuA | <i>E. coli</i> TOP10 | Prepared in this study |
| pXG10sf-NIF3 | <i>E. coli</i> TOP10 | Prepared in this study |
| pXG10sf-MSc | <i>E. coli</i> TOP10 | Prepared in this study |
| pXG10sf-TrpD | <i>E. coli</i> TOP10 | Prepared in this study |
| pXG10sf-FeoB | <i>E. coli</i> TOP10 | Prepared in this study |
| pXG10sf-CSP | <i>E. coli</i> TOP10 | Prepared in this study |
| pXG10sf-Kdc | <i>E. coli</i> TOP10 | Prepared in this study |
| pXG10sf- OmpH | <i>E. coli</i> TOP10 | Prepared in this study |

2.1.4 Preparation of antibiotics

Ampicillin (150 µg/ml) and chloramphenicol (25 µg/ml), imipenem (16 µg/ml) and zeocin (250 µg/ml and 10 µg/ml for *A. baumannii* and *E. coli* respectively) were used in this study. Antibiotic stock solutions were prepared from their powdered forms by dissolving these powders in 70% ethanol (for chloramphenicol) or in dH₂O and sterilised by filtration through a 0.22 µm filter pore. The strains carrying plasmids pP_L and pXG10 were cultured with ampicillin and chloramphenicol respectively.

2.1.5 Plasmid preparations

All plasmids were extracted from plasmid-containing *E. coli* using the E.Z.N.A.® Plasmid DNA Mini Kit 1 (Omega Bio-Tek). Plasmids were isolated from overnight L-broth cultures supplemented with the desired antibiotic. Cultures were then pelleted by centrifugation (13000 × g) and plasmids were isolated and purified following manufacturer's description (Omega Bio-Tek, 2018). Plasmid concentration and isolation was quantified using the Nanodrop™ spectrophotometer (eNovix V3.00 DS-II Spectrophotometer, Thermo Scientific).

2.1.6 Genomic DNA extraction

Genomic DNA extracted from *A. baumannii* AB5075 was used as a PCR template. An overnight culture (400 µl) was centrifuged (21,100 × g for 1 min). The supernatant was then removed and the pellet was resuspended in water (200

μl), boiled (100°C for 10 min) and vortexed. This sample was then centrifuged ($21,100 \times g$ for 5 min) and the contents were transferred to a new tube. Chloroform (approx. $200 \mu\text{l}$) was added to the suspension, vortexed and centrifuged ($21,100 \times g$ for 10 min). The aqueous phase was then removed, and the concentration was measured using the NanodropTM. The concentration was then adjusted to $100 \text{ ng}/\mu\text{l}$ in water and stored at -20°C .

2.1.7 Polymerase Chain Reactions

PCR was used to amplify genomic and plasmid DNA in this study, the primers used are shown in **Table 2.3**. This project used Taq DNA polymerase (New England Biolabs) and $2 \times$ Ranger-Mix (Bioline) to amplify DNA molecules. The ingredients used in these reactions are shown in **Table 2.4** and **Table 2.5**. The Taq DNA polymerase master mix was made by combining 10 X Standard Taq (Mg-free) Reaction Buffer ($5 \mu\text{l}$), 10 mM deoxynucleotides (dNTP) solution mix ($1 \mu\text{l}$) and 25 mM Magnesium chloride (MgCl_2) solution ($3 \mu\text{l}$).

Table 2.3 Primers used in this study

| Name | Primer Sequence (5'→3') | Use | Source |
|--------------|--|----------------------------|------------------------|
| BB_pPL_for | GCTAGCAAAGGAGAAGAAGCTTTTCAC | pPL backbone for cloning | Carsten Kröger |
| BB_pPL_rev | TCTAGAGGCATCAAATAAAACGAAAGGC | | |
| BB_pXG10_for | GTGAAAAGTTCTTCTCCTTTGCTAGCGGCTTCGAGCAGGATGACC | pXG10 backbone for cloning | Carsten Kröger |
| BB_pXG10_rev | GTGCTCAGTATCTTGTTATCCGCTCAC | | |
| pPL-sRNA21fw | GTGAGCGGATAACAAGATACTGAGCACGTAGGTTGATATGAACC | sRNA21 cloning | Prepared in this study |
| pPL-sRNA21rv | GCCTTTCGTTTTATTTGATGCCTCTAGAAGTTATCAAACAAAGGCGC | | |
| pPL-sRNA65fw | GTGAGCGGATAACAAGATACTGAGCACTCCTTTTAAATCATGTG | sRNA65 cloning | Prepared in this study |
| pPL-sRNA65rv | GCCTTTCGTTTTATTTGATGCCTCTAGACATAATTCACCTGTTACCTGC | | |
| pPL-sRNA76fw | GTGAGCGGATAACAAGATACTGAGCACTAAATGTACCCTTAATAAAA | sRNA76 cloning | Prepared in this study |
| pPL-sRNA76rv | GCCTTTCGTTTTATTTGATGCCTCTAGATTGTCAGGCATATCGTGC | | |
| pPL-sRNA85fw | GTGAGCGGATAACAAGATACTGAGCACGTAAAACGGTCTGTCACGG | sRNA85 cloning | Prepared in this study |
| pPL-sRNA85rv | GCCTTTCGTTTTATTTGATGCCTCTAGATTGGGATCAACCGTTAGATG | | |
| pPL-sRNA97fw | GTGAGCGGATAACAAGATACTGAGCACATCGGCACACGGAAGC | sRNA97 cloning | Prepared in this study |
| pPL-sRNA97rs | GCCTTTCGTTTTATTTGATGCCTCTAGAACGATTACTTATAATTAAGTAG | | |
| pPL-sRNA99fw | GTGAGCGGATAACAAGATACTGAGCACATAAGGAAATAGAACTAAAAC | sRNA99 cloning | Prepared in this study |
| pPL-sRNA99rs | GCCTTTCGTTTTATTTGATGCCTCTAGAATTCGACTCAATGTCCAC | | |

| Name | Primer Sequence (5'→3') | Use | Source |
|--------------|---|-----------------|------------------------------|
| pXG10-RsuAfw | ACTGAGCACATGCATGTTTCGTTTTAA AGAGAAAGC | RsuA cloning | Prepared in this study |
| pXG10-RsuArv | AGCGGATCCGCTAGCAACCTCCCCAT CAATAATTAC | | |
| pXG10-NIF3fw | ACTGAGCACATGCATTGCTGTTGGTTC AATTTTTGC | NIF3 cloning | Prepared in this study |
| pXG10-NIF3rv | AGCGGATCCGCTAGCCTCAGGTACGT AATAAATCAGC | | |
| pXG10-MSCFw | ACTGAGCACATGCATACTATTTTCATGC CACGTTG | MSC cloning | Prepared in this study |
| pXG10-MSCrv | AGCGGATCCGCTAGCAAACCTGAGCGC CGCGAGG | | |
| pXG10-TrpDfw | ACTGAGCACATGCATTAGCTAGTGAA TCATGGAACGC | TrpD cloning | Prepared in this study |
| pXG10-TrpDrv | AGCGGATCCGCTAGCATGAATGTTCTT GGTAATGTGG | | |
| pXG10-FeoBfw | ACTGAGCACATGCATCTTCCTCTAAAC CACTGTAC | FeoB cloning | Prepared in this study |
| pXG10-FeoBrv | AGCGGATCCGCTAGCCTGCGAAGCTG TAATCTATAG | | |
| pXG10-CSPfw | ACTGAGCACATGCATGTTTTAGGAATT ACCACACAG | CSP cloning | Prepared in this study |
| pXG10-CSPrv | AGCGGATCCGCTAGCTACATCGTCGC CGCCGTTACG | | |
| pXG10-Kdcfw | ACTGAGCACATGCATTATGGAATAAA AATTGGTCTC | Kdc cloning | Prepared in this study |
| pXG10-Kdcrv | AGCGGATCCGCTAGCGAGTTGTGGGT CTGCTTCAAC | | |
| pXG10-OmpHfw | ACTGAGCACATGCATAAGCTTTTGAA ATGGCAC | OmpH cloning | Prepared in this study |
| pXG10-OmpHrv | AGCGGATCCGCTAGCCCCATAACCAG CTGCATTAG | | |

| Name | Primer Sequence (5'→3') | Use | Source |
|--------------------|---------------------------------------|-----------------------------|----------------|
| BB_pVRL2_F | CGCGGAGTTGTTCCGGTAAATTG | pVRL2Z backbone for cloning | Carsten Kröger |
| BB_pVRL2_R | TGCGTTCGGTCAAGGTTCTG | | |
| qPCR_T4rnl1_R | CCATCTTTCATCACAGCAACATAG | T4 RNA ligase cloning | Carsten Kröger |
| ApraR_long_pVRL2_F | CAGAACCTTGACCGAACGCAGTATCTGCGCTCTGCTG | | |
| pPL_con_for | CGTATCACGAGGCCCTTTCGTC | pPL Colony PCR | Carsten Kröger |
| pPL_con_rev | GCGGCGGATTTGTCCTACTCAG | | |
| pXG10_con_for | GCCGTAATATCCAGCTGAAC | pXG10 Colony PCR | Carsten Kröger |
| pXG10_con_rev | CTCATGAATTCGCCAGAACC | | |
| pPL-seq_rev | GCGGATTTGTCCTACTCAG | Sanger sequencing | Carsten Kröger |
| pXG10-seq_F | AAATAGGCGTATCACGAGGC | | |

Table 2.4 Taq polymerase PCR reactants

| Components | Standard PCR | Standard PCR | Control |
|-------------------------|--------------|---------------|--------------|
| Taq master mix | 9.25 µl | 9.25 µl | 9.25 µl |
| Forward primer (0.2 µM) | 0.5 µl | 0.5 µl | 0.5 µl |
| Reverse primer (0.2 µM) | 0.5 µl | 0.5 µl | 0.5 µl |
| Template DNA (50 ng) | 0.5 µl | Single colony | 0 µl |
| dH ₂ O | 39.25 µl | 39.75 µl | 39.75 µl |
| Total Volume | 50 µl | 50 µl | 50 µl |

Table 2.5 Ranger-Mix PCR reactants

| Components | PCR | Control |
|-------------------------|--------------|----------------|
| Ranger master mix | 25 µl | 25 µl |
| Forward primer (0.2 µM) | 1 µl | 1 µl |
| Reverse primer (0.2 µM) | 1 µl | 1 µl |
| Template DNA | 10 ng/µl | 0 ng/µl |
| dH ₂ O | 41.75 µl | 40.75 µl |
| Total Volume | 50 µl | 50 µl |

All PCR reactions were prepared in PCR tubes and placed in the SimpliAmp™ Thermal Cycler for amplification using the cycles listed in **Table 2.6**. The annealing temperature and extension time are variable depending on the amplicon fragment sizes.

Table 2.6 PCR cycling conditions

| Step | Temperature | Time | Cycles |
|--------------|--------------------|-------------|---------------|
| Denaturation | 95°C | 2 min | 1 |
| Denaturation | 95°C | 15 s | 35 |
| Annealing | Variable | 30 s | |
| Extension | 72°C | Variable | |
| Extension | 72°C | 2 min | 1 |

Colony PCR was used to identify the presence of specific DNA sequences in bacterial colonies. These assays used Taq DNA polymerase for amplification, a single bacterial colony was selected and added to the Taq DNA polymerase reaction mixture. The cycling conditions primers used for colony PCR are shown in **Table 2.7**.

Table 2.7 Colony PCR cycling conditions

| Step | Temperature | Time | Cycles |
|--------------|-------------|----------|--------|
| Denaturation | 95°C | 10 min | 1 |
| Denaturation | 95°C | 15 s | 35 |
| Annealing | 50°C | 30 s | |
| Extension | 72°C | Variable | |
| Extension | 72°C | 2 min | 1 |

2.1.8 Agarose gel electrophoresis

The fragment sizes of PCR amplicons were measured using agarose gel electrophoresis. Agarose gels (1%) were prepared by melting agarose powder (1 g/100ml) in 1× TAE (40 mM Tris-acetate, 1 mM EDTA). A volume of SYBR™ Safe (Thermo Fisher Scientific) DNA gel stain (2 µl) was then added to the molten agarose (20 ml) and this was poured into a gel mould. A comb was used to create sample wells. Aliquots (5 µl) of PCR products were mixed with 6× orange DNA loading dye (Thermo Scientific), the total mixtures were loaded into the agarose gel wells. DNA ladders (5 µl) were also loaded into wells as comparators. Hyperladder 1 kb and Hyperladder IV (Bioline) were used to compare fragments over and under 1 kb respectively. The gel was then submerged in 1X TAE and gels was subjected to an electrical charge (120 V for 35 min) to separate fragments based on size. The gels were then removed and imaged under blue light (400–525 nm) using AlphaImager 2200.

2.1.9 PCR purification

Electrophoresis verified PCR products were purified using the Monarch PCR Cleanup Kit (New England BioLabs) to remove PCR reactants and other impurities. PCR replicates were pooled and purified using DNA spin columns as specified in the manufacturer's instructions (New England Biolabs Inc., 2016).

2.1.10 SLiCE cloning procedure

The SLiCE cloning procedure used recombination to integrate DNA inserts into linearised plasmid vectors (Zhang et al., 2014). This was made possible due to ~20 base-pairs homology of sequences at both ends of the insert to the ends of their target plasmid. The volumes and concentrations of reactants for this procedure is depicted in **Table 2.8**. These mixtures were then incubated at 37°C for 1h. The SLiCE extract was prepared prior to the start of this project. This was accomplished by lysing *E. coli* cells that are overexpressing λ prophage protein Red α system.

Table 2.8 SLiCE reaction components

| Component | SLiCE Reaction | SLiCE Control |
|---------------------|-----------------------------|-----------------------------|
| Ligation buffer | 1 μ l | 1 μ l |
| SLiC extract | 1 μ l | 1 μ l |
| Linearised plasmid | 100 ng | 100 ng |
| Target | 100 ng | 0 ng |
| Water | Variable | Variable |
| Total Volume | 10 μl | 10 μl |

2.1.11 Preparation and transformation of competent *E. coli*

To prepare strains competent for transformation with plasmid DNA, overnight cultures were inoculated with the required *E. coli* strains. This (50 µl) was used to inoculate a larger culture (50 ml) which was grown at 37°C until it reached exponential phase (OD 0.4-0.8). This culture was then centrifuged (2000 × g, 10 min, 4°C), resuspended in ice-cold CaCl₂ (30 mM, 40 ml). It was then centrifuged again, resuspended and incubated on ice for 20 min. It was centrifuged again and resuspended in 10 ml CaCl₂ with 87% glycerol (1.25 ml). This was aliquoted in microcentrifuge tubes and stored at -80°C.

To transform competent cells by heat shock, aliquots removed from the freezer, defrosted on ice and mixed with DNA (100 ng plasmids or 5 µl SLiCE products). Following this, cells were incubated on ice for 20 min, placed at 42°C for 2 min and re-incubated on ice for 2 min. Cells were then mixed with L-broth (800 µl) and incubated at 37°C for 90 min. 100 µl of the transformation mixture was then plated on L-agar plates with the required antibiotics and incubated at 37°C.

2.1.12 Sanger sequencing of plasmid DNA

The pP_L-sRNA and pXG10-target plasmids were sent to Eurofins Genomics for Sanger sequencing with primers listed in Table 2.3.

2.1.13 Measurement of fluorescence in 96-well plates

Cells grown in 96-well plates were used to identify posttranscriptional regulation by measuring fluorescence (GFP). A 1:100 dilution of overnight cultures was prepared by diluting the overnight culture (10 μ l) in an L-broth containing Eppendorf (1 ml). Aliquots (200 μ l) were transferred to individual wells as required. Fluorescence was measured (arbitrary units) for 24 hours in a Synergy H1™ Hybrid Multi-Mode microplate fluorometer at 37°C with continuous orbital shaking and excitation at 485 nm and emission at 508 nm.

2.2 Hi-GRIL-seq in *A. baumannii* AB5075

2.2.1 Generation of chimeric molecules

Chimeras were generated by ectopic expression of T4 RNA ligase on the pVRL2Z plasmid (Lucidi et al., 2018). This procedure was carried out by Carsten Kröger prior to this Master's project start. Purified T4 phage was kindly provided by Dr Siân Owen (University of Liverpool, UK). The T4 RNA ligase encoding-gene was amplified from the purified T4 phage using SLiCE primers with 20 nucleotides homologous to the linearised pVRL2Z backbone ends. The T4 RNA ligase-encoding gene amplicons were then cloned into the pVRL2Z backbone using the SLiCE cloning method, transformed into TOP10 *E. coli*, which were selected on zeocin-containing plasmids. The SLiCE plasmids were then isolated, purified and transformed into *A. baumannii* using zeocin selection.

The T4 RNA ligase encoding-gene was placed under control of the L-arabinose inducible P_{BAD} promoter and expression was induced through addition of L-arabinose. The influence of various concentrations of L-arabinose (0 mM, 1 mM, 5mM, 10 mM, 25 mM, 50 mM and 100 mM) on cell density was used to find the optimal concentration required. This induced expression of T4 RNA ligase in pVRL2Z-*t4rnII* using pVRL2Z as a control. For Hi-GRIL-seq, T4 RNA ligase expression was induced by addition of 50 mM L-arabinose in late exponential phase for one hour (OD₆₀₀=1). The generation of chimeric molecules in uninduced conditions was used as a comparator to examine the effectiveness of this promoter. Chimeric molecules were also generated following the addition of

subinhibitory concentration of β -lactam imipenem (16 $\mu\text{g/ml}$) and 0.2 mM 2,2'-dipyridyl (n=2 for each condition) at $\text{OD}_{600}=1$.

2.2.2 RNA isolation, reverse-transcription and sequencing

RNA was isolated using the TRIzol protocol previously described for *Salmonella enterica* serovar Typhimurium and *Acinetobacter baumannii* (Kröger et al., 2012, 2018). Total RNA for each condition was sent to Vertis Biotechnologie AG for DNase digestion, cDNA library preparation and sequencing using pair-ended sequencing. Ribosomal RNA was depleted using in-house depletion probes at Vertis Biotechnologie AG. The ribosomal RNA was hybridised with these specific DNA probes followed by RNase-mediated degradation. The DNA probes were then degraded using DNase I treatment, the remaining RNA molecules were then bead purified. The details of these samples submitted before and after rRNA depletion is shown in **Table 2.9**.

Table 2.9 Details of samples supplied to Vertis Biotechnologie AG

| Sample | Conc. (ng/ μl) | Amount (μg) | Ratio 23S/16S | Recovery after rRNA depletion (%) |
|--------|----------------------------|--------------------------|---------------|-----------------------------------|
| NI-1 | 456 | 8,7 | 1,3 | 7,2 |
| NI-2 | 475 | 9,0 | 1,4 | 9,4 |
| IND-1 | 517 | 9,8 | 1,3 | 5,3 |
| IND-2 | 509 | 9,7 | 1,1 | 7,2 |
| DIP-1 | 487 | 9,3 | 1,2 | 8,6 |
| DIP-2 | 453 | 8,6 | 1,2 | 4,9 |
| IMIP-1 | 436 | 8,3 | 1,5 | 9,1 |
| IMIP-2 | 504 | 9,6 | 1,5 | 7,1 |

The RNA was fragmented using ultrasound (four pulses of 30s at 4°C). Oligonucleotide adapters were ligated to 3' ends of the RNA molecules and first strand synthesis was performed with M-MLV reverse transcriptase and the 3' adapter as the primer. The first strand cDNA was purified and the 5' Illumina TruSeq sequencing adapter was ligated to the 3' end of the antisense cDNA. The resulting cDNA was PCR amplified to 10-20 ng/μl using high fidelity DNA polymerase for 12-13 cycles. The exact adapter details for cDNA synthesis and the cycles involved are depicted in **Table 2.10**.

Table 2.10 Properties of cDNA samples

| Sample | 5' barcode | 3' barcode | PCR cycles |
|---------------|-------------------|-------------------|-------------------|
| NI-1 | ATAGAGAG | ATTACTCG | 12 |
| NI-2 | AGAGGATA | ATTACTCG | 12 |
| IND-1 | CTCCTTAC | ATTACTCG | 13 |
| IND-2 | TATGCAGT | ATTACTCG | 12 |
| DIP-1 | TACTCCTT | ATTACTCG | 12 |
| DIP-2 | AGGCTTAG | ATTACTCG | 12 |
| IMIP-1 | ATTAGACG | ATTACTCG | 13 |
| IMIP-2 | CGGAGAGA | ATTACTCG | 13 |

The cDNA was purified using an Agencourt AMPure XP kit (Beckman Coulter Genomics) and analysed by capillary electrophoresis on a Shimadzu MultiNA microchip. The samples were then pooled in equimolar amounts and cDNA was fractionated based on size (200-500 bp) using a preparative agarose gel. The cDNA was then sequenced on an Illumina NextSeq 500 machine (75 bp read length).

2.2.3 *Hi-GRIL-seq analysis*

The chimera generated from Hi-GRIL-seq were analysed by Karsten Hokamp using a BLAST-based chimera pipeline similarly to that described by Zhang (Zhang et al., 2017). The first and last 20 nucleotides of the Illumina sequence reads were mapped to the *A. baumannii* AB5075-UW genome (NZ_CP008706.1) to identify to location of potential chimeric reads. Once one end of the read mapped to an annotated sRNA, the location of the other end was analysed, the distance to the sRNA mapping event measured and the nearest (or overlapping) gene reported as potential interaction partner.

2.2.4 *Bioinformatic analysis*

The sRNA-chimeras were further analysed using Microsoft Excel. Chimeras with under 10 ligated targets and those that ligated to mRNAs encoding hypothetical proteins were excluded from analysis. The frequency of specific sRNA and mRNA nucleotides appearing in ligation junctions was mapped on the sRNA and mRNA transcript structures respectively. The sRNA candidate structures were assessed using NUPACK: Nucleic Acid Package (www.nupack.org) using default settings.

Hi-GRIL-seq derived targets were compared to those obtained by TargetRNA2 (cs.wellesley.edu/~btjaden/TargetRNA2) and CopraRNA (<http://rna.informatik.uni-freiburg.de/CopraRNA>) using default settings (Kery et al., 2014; Wright et al., 2014). TargetRNA2 used the ATCC 17978 strain

(NZ_CP018664.1) to find novel targets, while CopraRNA used the strains *A. baumannii* AB5075-UW (NZ_CP008706.1), *A. baumannii* AYE (NC_010410.1), *A. baumannii* AB0057 (NC_011586.1), *A. nosocomialis* 6411 (NZ_CP010368.1) and *A. pittii* PHEA-2 (NC_016603.1) to find targets.

The sRNA-mRNA duplex structures were predicted using the default settings on IntaRNA (<http://rna.informatik.uni-freiburg.de/IntaRNA>). Sequences encompassing the target ligation sites were entered into this prediction software (Wright et al., 2014).

2.3 Construction of plasmids

2.3.1 Amplification of pP_L backbone

The pP_L plasmid was extracted from *E. coli* stock and used as the DNA template to amplify the pP_L backbone. The pP_L backbone was PCR amplified in triplicate using Ranger-Mix and a negative control was included. The PCRs were performed using the Ranger-mix reagents listed above and the BB_pP_L_for and BB_pP_L_rev primers. It was then cycled in the conditions listed in **Table 2.11**.

Table 2.11 pP_L modified PCR cycling condition

| Step | Temperature | Time | Cycles |
|-------------------------|-------------|-------|--------|
| Denaturation | 95°C | 2 min | 1 |
| Denaturation | 95°C | 15 s | 35 |
| Annealing and extension | 65°C | 3 min | |
| Extension | 72°C | 2 min | 1 |

The PCR products were analysed using gel electrophoresis and purified. The purified pP_L backbone was digested with DpnI (New England Biolabs) to remove the pP_L template by cleaving methylated DNA. This was achieved by incubating the pP_L backbone purified PCR products (5 µl) with DpnI (1 µl), 10×CutSmart Buffer (5 µl) and water (39 µl) at 37°C for 5 min. This plasmid was then diluted to 100 ng/µl in dH₂O.

2.3.2 Amplification of pXG10 backbone

The pXG10 plasmid was extracted from *E. coli* and used as the DNA template to amplify the pXG10 backbone. The pXG10 backbone was PCR amplified in triplicate using Ranger-Mix and a negative control was included. The PCRs were performed using the Ranger-mix reagents listed above and the BB_pXG10_for and BB_pXG10_rev primers. It was then cycled in the conditions listed in **Table 2.12**.

Table 2.12 pXG10 modified PCR cycling condition

| Step | Temperature | Time | Cycles |
|-------------------------|-------------|-------|--------|
| Denaturation | 95°C | 2 min | 1 |
| Denaturation | 95°C | 15 s | 35 |
| Annealing and extension | 65°C | 5 min | |
| Extension | 72°C | 2 min | 1 |

The PCR products were analysed using gel electrophoresis and purified using the PCR purification protocol. The purified pXG10 backbone was digested with DpnI to remove the pXG10 template by cleaving methylated DNA. This was achieved by incubating the pXG10 backbone purified PCR products (5 µl) with DpnI (1 µl), 10× CutSmart Buffer (5 µl) and water (39 µl) at 37°C for 5 min. This plasmid was then diluted to 100 ng/µl in dH₂O.

2.3.3 Amplification of candidate sRNAs

The sRNA candidate genes were amplified using the *A. baumannii* AB5075 genomic DNA as a template. The sRNA genes were PCR amplified using Taq DNA polymerase with the reagents listed above, with the pP_L-sRNA forward and reverse primers. The PCR reaction tubes were then cycled using the annealing temperatures and extension times listed in **Table 2.13**. The PCR products were then analysed using gel electrophoresis and purified using the PCR purification protocol.

Table 2.13 sRNA amplification cycling conditions

| sRNA | Annealing Temperature (tm) | Extension time |
|--------|----------------------------|----------------|
| sRNA21 | 62°C | 30 s |
| sRNA65 | 57°C | 30 s |
| sRNA85 | 55°C | 30 s |
| sRNA76 | 50°C | 30 s |
| sRNA97 | 57°C | 30 s |
| sRNA99 | 60°C | 30 s |

2.3.4 Amplification of mRNA targets

The mRNA target genes and their 5'-UTRs were then amplified from *A. baumannii* AB5075 genomic DNA. The target genes were PCR amplified using Taq DNA polymerase with the reagents listed above and the pXG10-target forward and reverse primers. The PCR reaction tubes were then cycled using the

annealing temperatures and extension times listed in **Table 2.14**. The PCR products were then analysed using gel electrophoresis and purified.

Table 2.14 Target amplification cycling conditions

| Target | Annealing Temperature (tm) | Extension time |
|--------|----------------------------|----------------|
| RsuA | 41°C | 30 s |
| Nif3 | 41°C | 30 s |
| MSC | 47°C | 2 min |
| CSP | 45°C | 30 s |
| TrpD | 47°C | 30 s |
| FeoB | 46°C | 2 min |
| Kdc | 41°C | 30 s |
| OmpH | 63°C | 2 min 56 s |

2.3.5 Cloning sRNAs into pP_L backbone

Purified sRNAs amplified by PCR were cloned into the DpnI digested pP_L backbone using the SLiCE cloning protocol described. The volumes of sRNA amplicons, pP_L and dH₂O reactants are shown in **Table 2.15**. The SLiCE products were then transformed into TOP10 *E. coli*, cultured on ampicillin containing L-agar plates and confirmed using colony PCR with the pP_L_con_for and pP_L_con_rev primers and Sanger sequencing.

Table 2.15 sRNA SLiCE cloning

| sRNA | sRNA Volume | pPL Volume (100 ng/μl) | dH₂O Volume |
|-------------|--------------------|--|-------------------------------|
| sRNA21 | 2.9 μ l | 1 μ l | 3.9 μ l |
| sRNA65 | 1 μ l | 1 μ l | 2 μ l |
| sRNA85 | 1.84 μ l | 1 μ l | 2.84 μ l |
| sRNA76 | 1.44 μ l | 1 μ l | 2.44 μ l |
| sRNA97 | 1 μ l | 1 μ l | 2 μ l |
| sRNA99 | 2.4 μ l | 1 μ l | 3.4 μ l |

2.3.6 Cloning targets into pXG10 backbone

Purified mRNA targets amplified by PCR were then cloned into the DpnI digested pXG10 backbone using the SLiCE cloning protocol described. The volumes of target amplicons, pXG10 and dH₂O reactants are shown in **Table 2.16**. The SLiCE products were then transformed into TOP10 *E. coli*, cultured on chloramphenicol containing L-agar plates and confirmed using colony PCR using the pXG10_con_for and pXG10_con_rev primers and Sanger sequencing.

Table 2.16 Target SLiCE cloning

| sRNA | Target Volume | pXG10 Volume (100ng/μl) | dH₂O Volume |
|-------------|----------------------|---|-------------------------------|
| RsuA | 2.6 μ l | 1 μ l | 4.4 μ l |
| Nif3 | 1.74 μ l | 1 μ l | 5.26 μ l |
| MSC | 0.81 μ l | 1 μ l | 6.19 μ l |
| CSP | 3.47 μ l | 1 μ l | 3.53 μ l |
| TrpD | 2.1 μ l | 1 μ l | 4.9 μ l |
| FeoB | 1.6 μ l | 1 μ l | 5.4 μ l |
| Kdc | 1.62 μ l | 1 μ l | 5.38 μ l |
| OmpH | 0.82 μ l | 1 μ l | 6.18 μ l |

2.4 GFP based two-plasmid sRNA and target validation

2.4.1 *Plasmids*

The p_{PL}-sRNA and pXG10-target plasmids were used to identify posttranscriptional interactions in this study. The pXG10-target plasmids were capable of expressing GFP allowing them to be used in this experiment. The co-expression of these plasmids was used to identify posttranscriptional interactions. To do this, GFP expression in pXG10-target with the pJV300 was used as a comparator.

2.4.2 *Validation of sRNA-mRNA interactions*

The pXG10-target plasmids were transformed into p_{PL}-sRNA and pJV300 competent *E. coli*. The expression of GFP these two group was measured overnight in 96-well plates, as described 2.1.13, to investigate posttranscriptional regulation.

3 Analysis of RNA-RNA interactions using Hi-GRIL-seq

3.1 Identification of potential sRNA-mRNA interactions

To investigate the RNA-RNA interactome of *A. baumannii* AB5075 and to identify potential mRNA targets of sRNAs that may be involved in AMR or pathogenesis, we performed a Hi-GRIL-seq experiment (Zhang et al., 2017). This analysis allowed us to capture possible sRNA-mRNA interactions for the sRNA candidates conserved in AB5075 identified previously by the Kröger group in the antibiotic sensitive strain ATCC17978 (Kröger et al., 2018).

To identify sRNAs and target mRNAs that play essential roles in mediating antibiotic survival and iron stress responses that are critical for clinical and environmental persistence (Cardoso et al., 2010; Nwugo et al., 2011), AB5075 cells were exposed to the an antibiotic and in iron deprivation conditions for 15 minutes after reaching OD 1 (late exponential phase; LEP) prior to induction of T4 RNA ligase. These stressful conditions were instigated by exposing AB5075 cells to the β -lactam antibiotic imipenem and the iron chelator 2,2'-dipyridyl (2,2'-DIP) respectively. As a control experiment and to study sRNAs involved in gene regulation of cells growing in rich medium (L-broth), Hi-GRIL-seq was also performed in AB5075 at LEP without applying any stress. Chimeras were generated through ectopic expression of T4 RNA ligase with an arabinose inducible promoter from the pVRL2Z plasmid in LEP for one hour (Lucidi et al., 2018). Additionally, a T4 RNA ligase non-inducing control experiment was used as another comparator.

Prior to performing the Hi-GRIL-seq experiment, Carsten Kröger measured the impact of different concentrations of L-arabinose on *A. baumannii* viability to determine the optimal concentration of L-arabinose needed for T4 RNA ligase induction (**Figure 3.1**).

This was accomplished by comparing the optical density of overnight cultures of *A. baumannii* cells expressing either pVRL2Z-*t4rnI1* or the pVRL2Z control upon addition of the L-arabinose concentrations indicated. Because RNA-RNA ligation over time is lethal for bacterial cells, reduced growth should indicate substantial RNA-RNA ligation in comparison to the control strain that harboured the empty plasmid. It was determined that 50 mM L-arabinose was needed to induce T4 RNA ligase to cause a severe reduction in growth indicating RNA-RNA ligation was occurring (**Figure 3.1**).

In the Hi-GRIL-seq experiment, after T4 RNA ligase expression, the total RNA was isolated from each condition in duplicate, converted to cDNA and deep sequenced (Zhang et al., 2017). Approximately 60 million RNA reads were obtained per conditions and sRNA sequence containing-chimeras accounted for approximately 3% of all sequenced RNA molecules compared to the 0.26-0.29% sRNA containing-chimeras identified in *P. aeruginosa* (Zhang et al., 2017). A deeper sequencing strategy was used in this study to enhance the identification of potential targets, accounting for this discrepancy, however, it might also increase the number of false-positive results. The sequencing reads for each condition are summarised in **Table 3.1**. The 5' and 3' ends of each sRNA-containing chimera reads were mapped to the AB5075 genome to identify the location of their mRNA interaction partners.

Table 3.1 Total number of Hi-GRIL-seq reads per condition

| Condition | Total No. Of Reads Sequenced |
|---------------------------|-------------------------------------|
| Non-induced (NI-1) | 52160911 |
| Non-induced (NI-2) | 59069637 |
| Induced (IND-1) | 59809291 |
| Induced (IND-2) | 59043850 |
| Low Iron (DIP-1) | 54233135 |
| Low Iron (DIP-2) | 56807880 |
| Antibiotic shock (IMIP-1) | 55235231 |
| Antibiotic shock (IMIP-2) | 57183653 |

The identification of sRNA-mRNA interaction pairs using Hi-GRIL-seq reads was achieved by filtering sRNA-containing chimeras based on frequency. The combined read count of sRNA-containing chimeras from all growth conditions with under 10 sequencing reads were excluded from further analysis to improve identification. This was performed to ensure that transcripts highly expressed in individual conditions that ligated to sRNAs regardless of complementarity were not overrepresented in the analysis. Genes encoding hypothetical proteins were also excluded to find targets with defined biological functions. Of the 110 sRNA candidates analysed in this manner, only 32 generated chimeras with over 10 sequencing reads that mapped to mRNA targets. Chimeras were generated in all conditions, including the uninduced condition, for each sRNA. The potential mRNA targets present in these chimera were subsequently analysed, there were over 1600 potential targets among the 32 chimera. This led to the identification of over 1600 potential targets, however, out of the 110 sRNA candidates, only 32 met the chimera criteria for further analysis. The global sRNA-mRNA chimeras identified in this analysis were then mapped to the AB5075 genome to facilitate selection of interaction pairs for further analysis (**Figure 3.2**). This was achieved by mapping the genomic coordinates of the 5' and 3' ends of these chimeras to the X-axis and Y-axis respectively, proportionally to the frequency of sequencing reads.

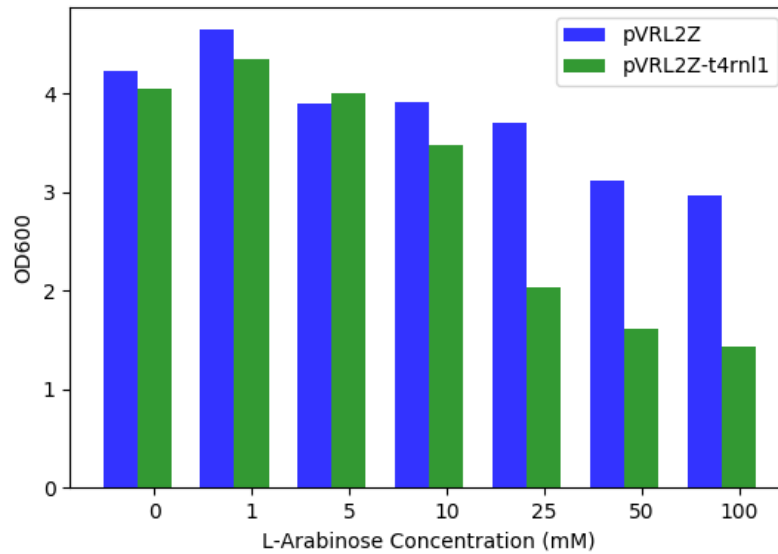


Figure 3.1 Identification of optimal L-arabinose concentration for T4 RNA ligase expression

The impact of adding various concentrations of L-arabinose on *A. baumannii* AB5075 cell density was used to determine the optimal L-arabinose concentration for ligating sRNA and mRNA molecules during the Hi-GRIL-seq experiment without causing excessive cell death. Cell density was compared in cells carrying the T4 RNA ligase-encoding plasmid (pVRL2Z-*t4rnI1*) to those carrying a control plasmid (pVRL2Z).

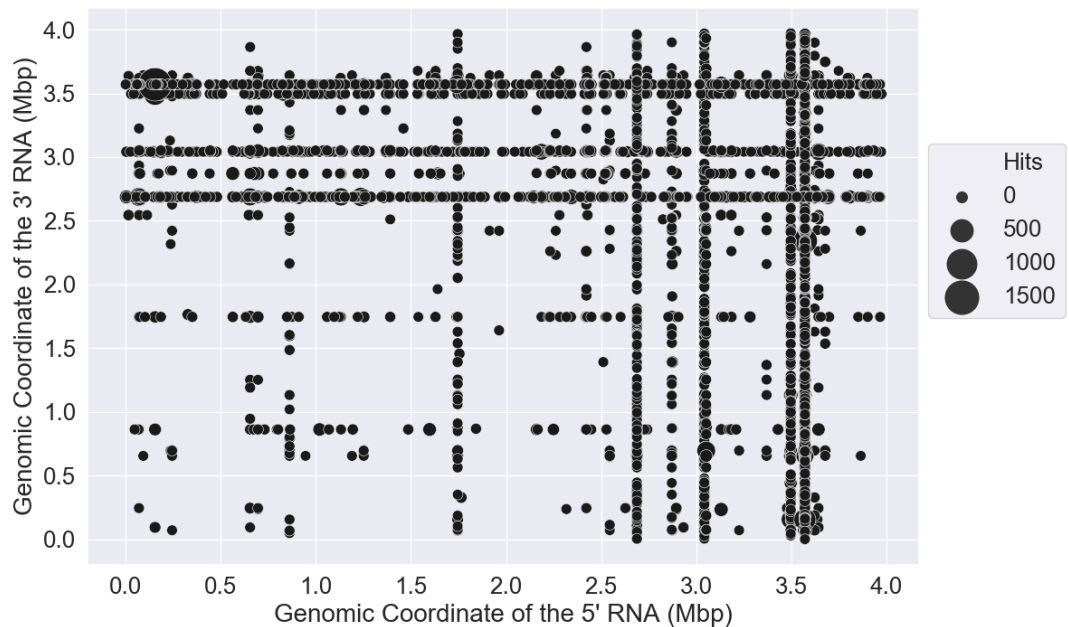


Figure 3.2 Two-dimensional display of chimeras identified by Hi-GRIL-seq

The 5' and 3' ends of sRNA-sequence containing chimeras were mapped to the *A. baumannii* AB5075 genome to identify the genomic location of the constituent sRNA and mRNA molecules. The 5' chimera ends were mapped to the x-axis, while the 3' ends of chimeras were mapped to the y-axis. The size of the dots are proportional to the number of the corresponding chimeras.

3.2 Characterisation of candidate sRNAs

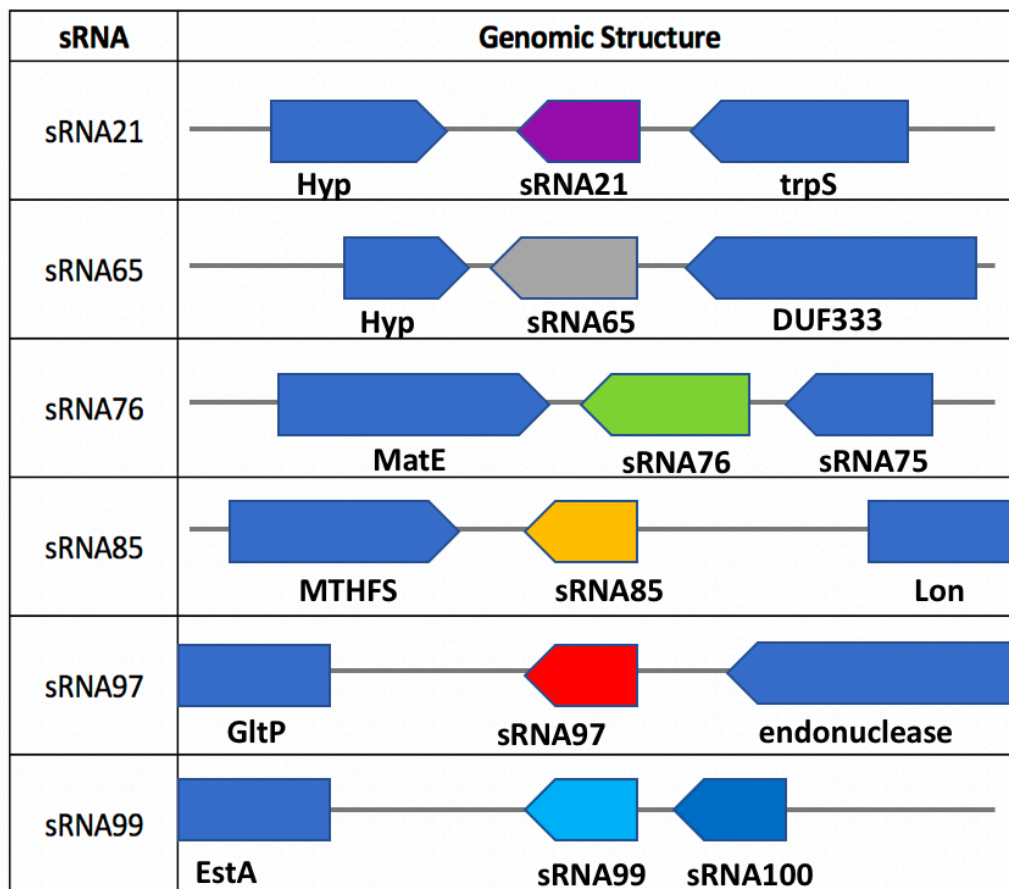
Several sRNA candidates that were anticipated to regulate targets important in the maintenance of *A. baumannii* physiology were selected for further investigation. From the 32 candidates predicted to regulate mRNA targets in the Hi-GRIL-seq analysis, only 6 putative sRNAs were chosen, this included; sRNA21, sRNA65, sRNA76, sRNA85, sRNA97 and sRNA99. While these sRNAs were selected based on the abundance and perceived importance of their targets, three candidates are the homologues of sRNAs previously suggested to play regulatory roles in *Acinetobacter*. The sRNAs sRNA21 and sRNA97 are homologues of the *A. baylyi* sRNAs Aar and the putative RsmY respectively (Kulkarni et al., 2006; Schilling et al., 2010). The sRNA65 is a homologue of the putative sRNA AbsR25 identified in *A. baumannii* ATCC 17978 (Sharma et al., 2011).

The potential sRNAs selected are well conserved among *A. baumannii*, *A. nosocomialis* 6411 and *A. pittii* PHEA-2 (100-90% sequence identity), as indicated in **Figure 1.4**. The sRNAs Aar (75-70%) and RsmY (80-75%) also share high sequence similarity with their *A. baylyi* DSM 14961 homologues. The genomic structures of each of these sRNAs is shown in **Table 3.2**. The sRNA21 gene is located at the 3' end of tryptophan-tRNA ligase gene similarly to the *aar* gene, however, the synteny of genes downstream of the sRNA21 encoding-gene is disrupted. The location of the sRNA97- and sRNA65-encoding genes and their homologues is conserved between AB5075 and *A. baylyi* ADP1 or ATCC 17978 respectively.

The chimera junction site for each sRNA was defined to locate the seed regions of the putative sRNAs. The sRNA sequence reads from sRNA-containing chimeras were used to determine which base-pairs of the sRNAs ligated to each target under investigation (**Figure 3.3**). The individual sRNA base-pairs that were located at junction sites are

highlighted by peaks that are proportional to their frequency. These junction sites are assumed to be near the sRNA seed regions involved in sRNA-mRNA interactions. They are localised to the 5' tails of sRNA21 (for *rsuA*), sRNA65, sRNA85, sRNA97 and sRNA99, which is a common for sRNA-mRNA interaction site (Hoekzema et al., 2019). The sRNA76 (for both *trpD* and *feoB*) and sRNA21 (for *nif3*) juncture sites were located in the 3' tail of sRNAs. The secondary structures of each sRNAs were also predicted using NUPACK. This prediction suggests that sRNA97 harbours three GGA motifs in the loop section of separate stem-loop structures. This is characteristic of the RsmY secondary structure in *Pseudomonas* species (Janssen et al., 2018)

Table 3.2 Genomic structure of sRNAs under investigation



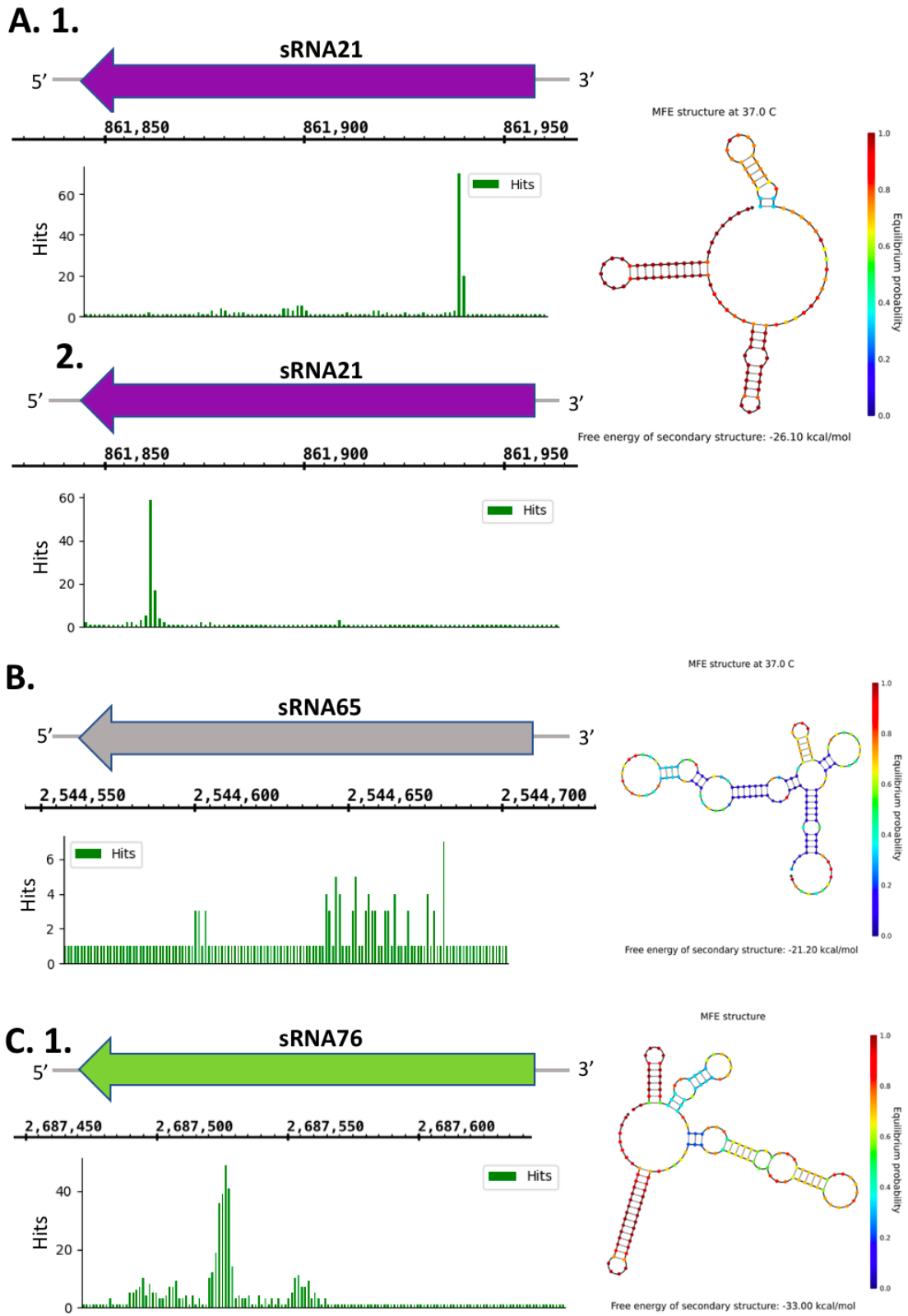


Figure 3.3 Mapping Hi-GRIL-seq ligation sites to sRNAs under investigation

The ligation junctions of chimeras generated from Hi-GRIL-seq were used to map the ligation sites of sRNA21 for RsuA and NIF3 (A.1. and A.2. respectively), sRNA65 for MSC (B.), sRNA76 for TrpD and FeoB (C.1. and C.2. respectively), sRNA85 for CSP (D.), sRNA97 for Kd (E.) and sRNA99 for OmpH (F.)

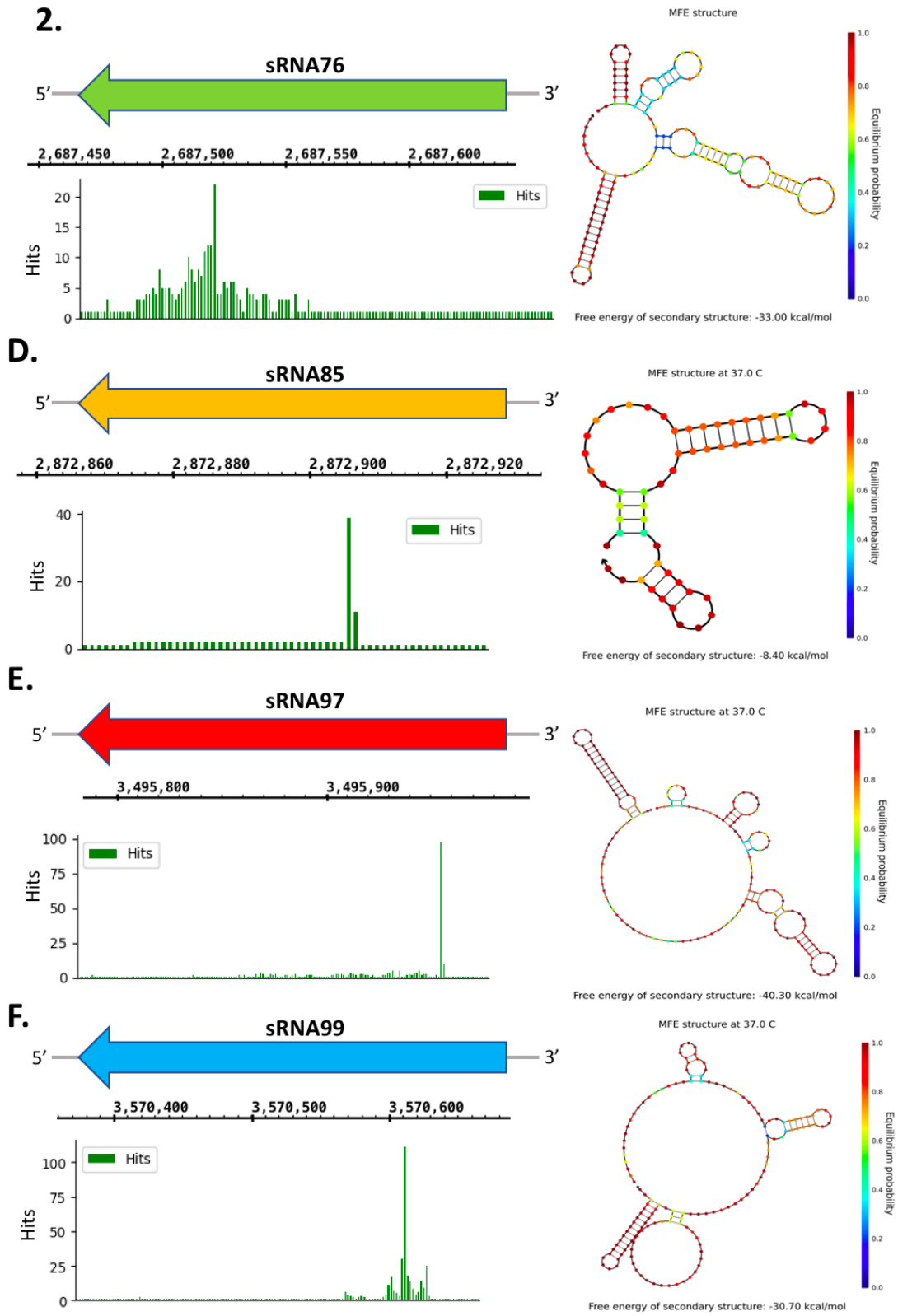


Figure 3.3 Mapping Hi-GRIL-seq ligation sites to sRNAs under investigation (continued)

3.3 Characterisation of potential mRNA targets

As mentioned, the mRNA targets were selected based on their frequency and their predicted biological importance. Many of the most frequent targets were shared amongst multiple sRNA candidates, complicating the decision of which targets should have been investigated. For this reason, four of the overall most abundant targets present in their respective sRNA were selected regardless of uniqueness and four of the most abundant, unique targets were chosen as comparators (**Table 3.3**). The non-unique targets included 16S rRNA pseudouridine synthase (RsuA) for sRNA21, anthranilate phosphoribosyltransferase (TrpD) for sRNA76, α -keto acid decarboxylase family protein (Kdc) for sRNA97 and outer membrane protein H (OmpH) for sRNA99. The unique targets included; NIF3-containing protein (NIF3) for sRNA21, mechanosensitive ion channel (MSC) for sRNA65, ferrous iron transport protein B (FeoB) for sRNA76 and cold-shock protein (Csp) for sRNA85. These two groups were compared to offer a preliminary insight into the importance of unique or non-unique Hi-GRIL-seq targets for defining sRNA-mRNA interactions.

Table 3.3 Hi-GRIL-seq Targets under investigation

| sRNA | Target | Unique/Non-unique | Potential Biological Function |
|--------|--------|-------------------|-------------------------------|
| sRNA21 | RsuA | Non-unique | Ribosome biogenesis |
| | NIF3 | Unique | Virulence |
| sRNA65 | MSC | Unique | Osmoregulation |
| sRNA76 | TrpD | Non-unique | Tryptophan biosynthesis |
| | FeoB | Unique | Iron acquisition |
| sRNA85 | CSP | Unique | Stress response |
| sRNA97 | Kdc | Non-unique | Amino acid metabolism |
| sRNA99 | OmpH | Non-unique | Colistin resistance |

These targets were also selected based on their potential roles in mediating *A. baumannii* AMR and persistence. MSCs are cytoplasmic pores that release osmolytes to relieve

turgor pressure associated with cell division or when the organism is subjected to a hypotonic shock (Kung et al., 2010). They are suggested to be important osmolarity regulators in *A. baumannii* and are desirable antimicrobial targets (Nguyen et al., 2005; Zeidler et al., 2019a). FeoB is a member of the ferrous iron transport system, it is a cytoplasmic membrane protein that is responsible for transporting iron molecules across the cytoplasmic membrane (Lau et al., 2016; Sestok et al., 2018). FeoB is dispensable for iron acquisition in *A. baumannii*, however, it is essential for survival in human serum and providing resistance to antimicrobial peptides (Runci et al., 2019; Subashchandrabose et al., 2016). As hosts deplete amino acids to restrict pathogen growth, *A. baumannii* lung infections alter the expression of genes involved in amino acid metabolism (Peng et al., 2010; Wang et al., 2014). TrpD is a key component of the tryptophan biosynthesis operon that was previously described to be negatively regulated by an sRNA in *Sinorhizobium meliloti* (Melior et al., 2019). Kdc catalyses the decarboxylation of alpha-keto acids, such as pyruvate and α -ketoglutarate, important Krebs cycle substrates. It is essential in *Listeria monocytogenes* for replication and macrophage survival by mediating branched-chain fatty acid biosynthesis (Sun et al., 2010). 16S rRNA Pseudouridine synthase (RsuA), modifies U516 of 16S rRNA to Pseudouridine in *E. coli* (Jayalath et al., 2020). It preferentially binds to and modifies a 16S rRNA intermediate in a complex with the ribosomal protein S17 to streamline ribosomal assembly. These ribosomes are suggested to have improved function in stressful conditions. Expression of cold-shock proteins (CSPs) is induced when cells encounter sudden temperature decreases, these proteins are capable of interacting with DNA and RNA, highlighting their role as potential *trans*-encoded sRNA chaperones (Keto-Timonen et al., 2016). Outer membrane proteins (OMPs) are typically secreted in Outer Membrane Vesicles (OMVs) by Gram-negative pathogens to host cells where they are involved in virulence (Jin et al., 2011). OmpH is

an outer membrane protein that is secreted via OMVs in colistin resistant *A. baumannii* strains, suggesting a potential role in either colistin resistance or virulence (Lee et al., 2020). Outer membrane proteins are also classical sRNA targets in *Enterobacteriaceae*, increasing our interest in this target.

The sRNA-mRNA ligation sites were examined for each target to determine the location that sRNAs bind to their prospective targets. This was accomplished by comparing the ligation junctures of the target sequence-containing chimeras under investigation. The high frequency of the same ligation junctions increased our confidence that these were biologically relevant targets. The frequency and location of ligation junctions for each target is indicated in **Figure 3.4**. The TSS and adjacent genes for each target were also depicted to help consider the sRNA binding site in the resulting transcript. A number of the predicted sRNA-mRNA ligation sites are located in the 5'-UTR of their target transcripts; this is observed for the RsuA, Nif3, TrpD and CSP, which is consistent with the predominant sRNA binding mechanism (Wagner et al., 2015). The predicted ligation sites in MSC, FeoB, Kdc and OmpH are intragenic. Several target genes are in operons with other genes; *trpD* is located upstream of *trpE*, *MSC* is in operon with the genes encoding ferredoxin—NADP reductase and a hypothetical protein, *feoB* is located downstream of *feoA*, *kdc* is located upstream of an amino acid permease encoding gene and *ompH* is located downstream of the outer membrane protein assembly factor gene *bamA*. The posttranscriptional regulation of targets within polycistronic mRNA can indirectly regulate other cistrons opening the possibility that these adjacent genes play a role in mediating *A. baumannii* pathogenesis (Balasubramanian et al., 2013).

We subsequently sought to determine whether any of these potential targets are regulated in condition-specific manners. To determine whether this was the case, we compared the

total number of sRNA-mRNA chimeras generated in each condition for each interaction pair under investigation (**Figure 3.5**). It is evident that the sRNA76-FeoB interaction pair was enriched in the iron starvation condition leading us to speculate that this potential interaction was vital for iron acquisition. We also noticed that the sRNA65-MSc, sRNA97-Kdc and sRNA99-OmpH interaction pairs were enriched in the uninduced conditions, while the remaining interaction pairs were rarely identified in this condition, which warrants further investigation.

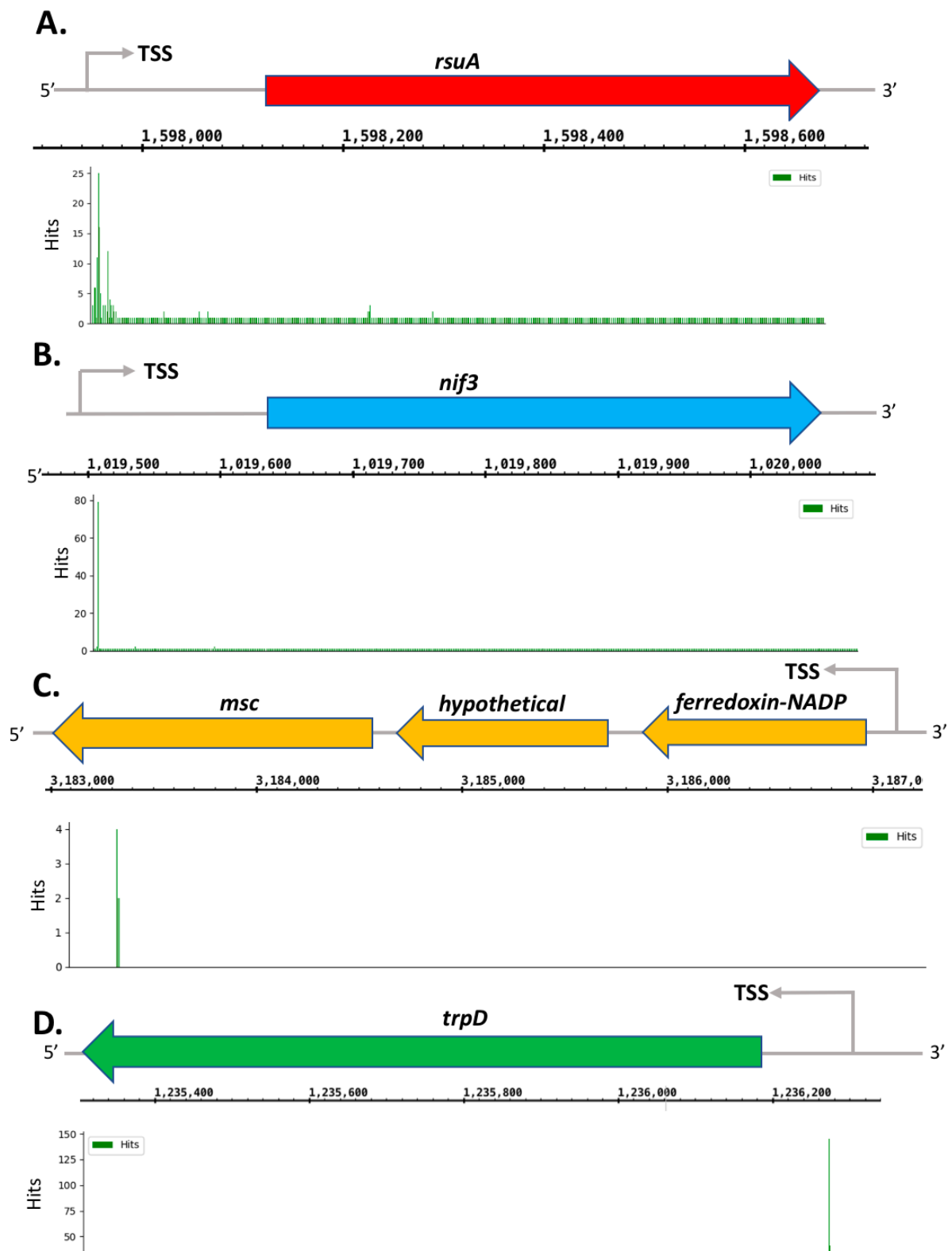


Figure 3.4 Mapping Hi-GRIL-seq ligation sites to targets under investigation

The ligation junctions of chimeras generated from Hi-GRIL-seq were used to map the *RsuA* (A.), *NIF3* (B.) *MSC* (C.), *TrpD* (D.) *FoB* (E.), *CSP* (G.), *Kdc* (F.) and *OmpH* (G.) ligation sites.

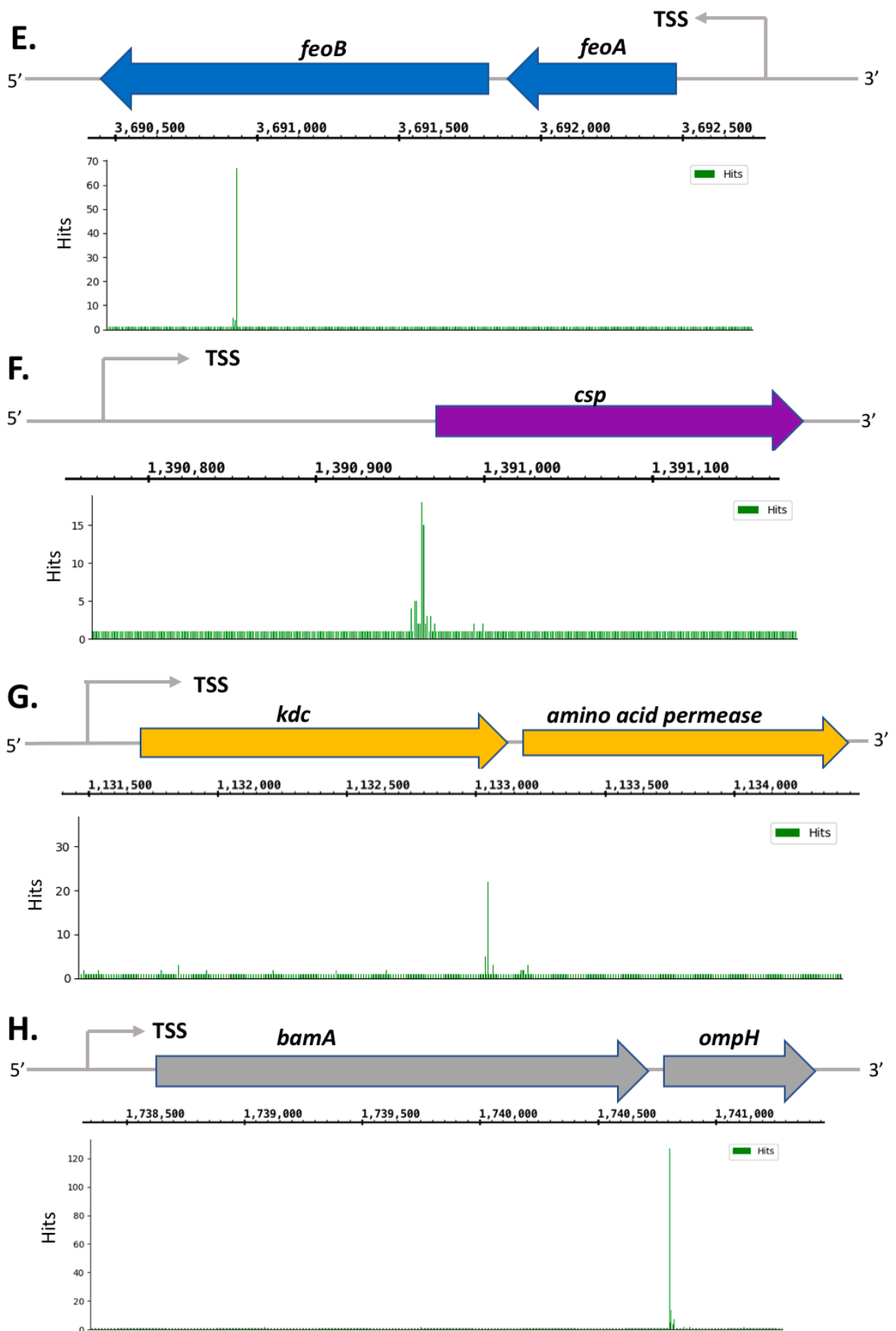


Figure 3.4 Mapping Hi-GRIL-seq ligation sites to targets under investigation (continued)

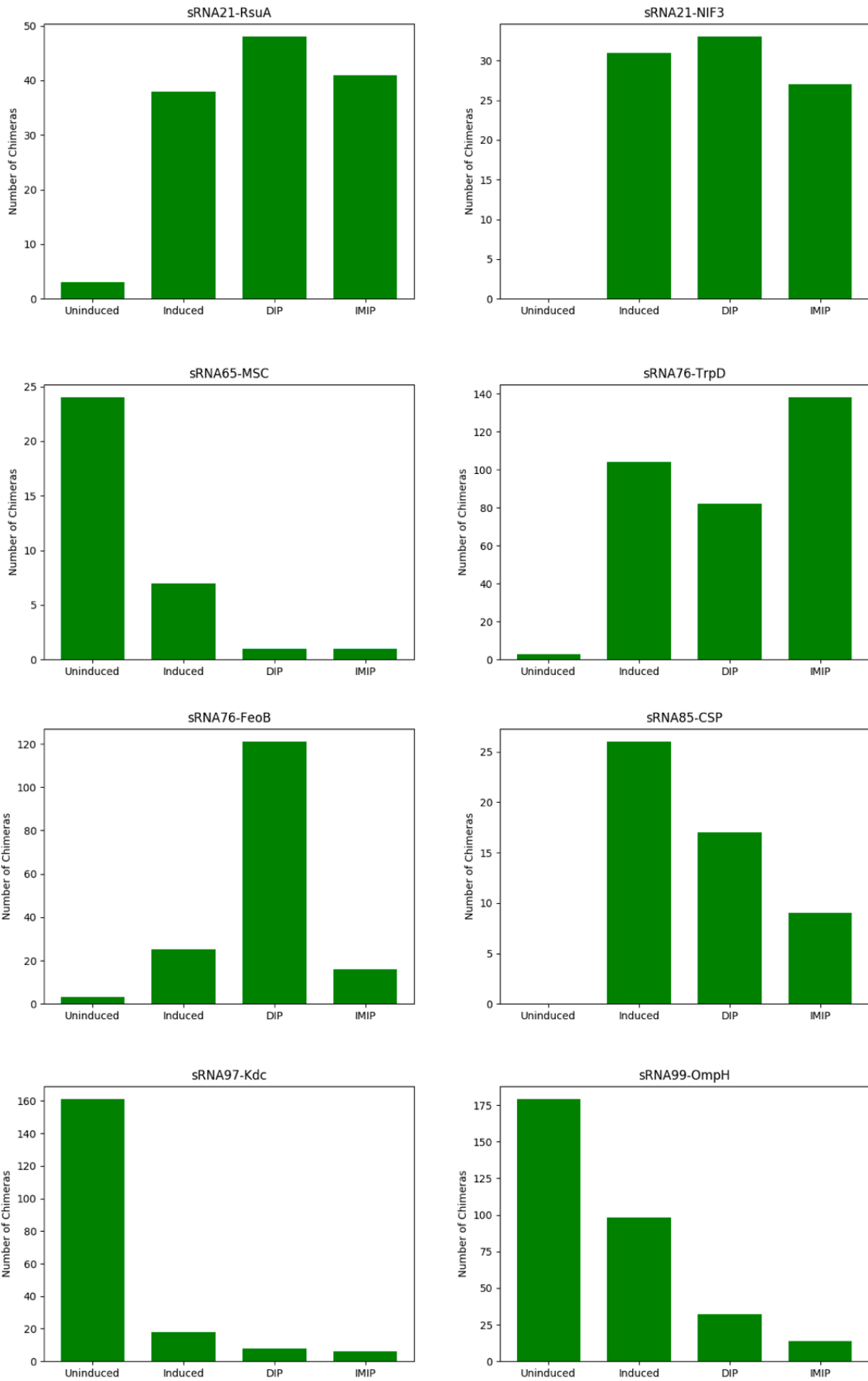


Figure 3.5 Number of chimera formed in each condition

The total number of sRNA-mRNA chimeras generated in each experimental condition is depicted.

3.4 Prediction of sRNA-mRNA duplex structures

While the examination of chimera junction sites provides an estimate of where the sRNA and their cognate mRNA target base-pair, it provides no insight into the dynamics of the potential sRNA-mRNA interactions. For this reason, we used the computational prediction tool IntaRNA to predict the sRNA-mRNA hybridisation structure (Busch et al., 2008). This software was capable of predicting the duplex structure for each interaction pair (**Figure 3.6**). The sRNA-mRNA interaction pair hybridisation strengths are depicted in **Table 3.4**, the sRNA76-TrpD interaction pair had the strongest hybridisation energy. There is generally a relationship between strength of hybridisation and strength of sRNA-mRNA interactions, this was considered while performing the experimental analysis (Vazquez-Anderson et al., 2017). All of the predicted duplexes were located within or in close proximity to their ligation junctures, this feature played a role in their selection.

Table 3.4 Interaction pair hybridisation strengths

| Interaction pair | Hybridisation energy |
|-------------------------|-----------------------------|
| sRNA21-RsuA | -14.47 kcal/mol |
| sRNA21-NIF3 | -9 kcal/mol |
| sRNA65-MSc | -16.97 kcal/mol |
| sRNA76-TrpD | -22.16 kcal/mol |
| sRNA76-FeoB | -14.8 kcal/mol |
| sRNA85-CSP | -7.98 kcal/mol |
| sRNA97-Kdc | -16.12 kcal/mol |
| sRNA99-OmpH | -7.8 kcal/mol |

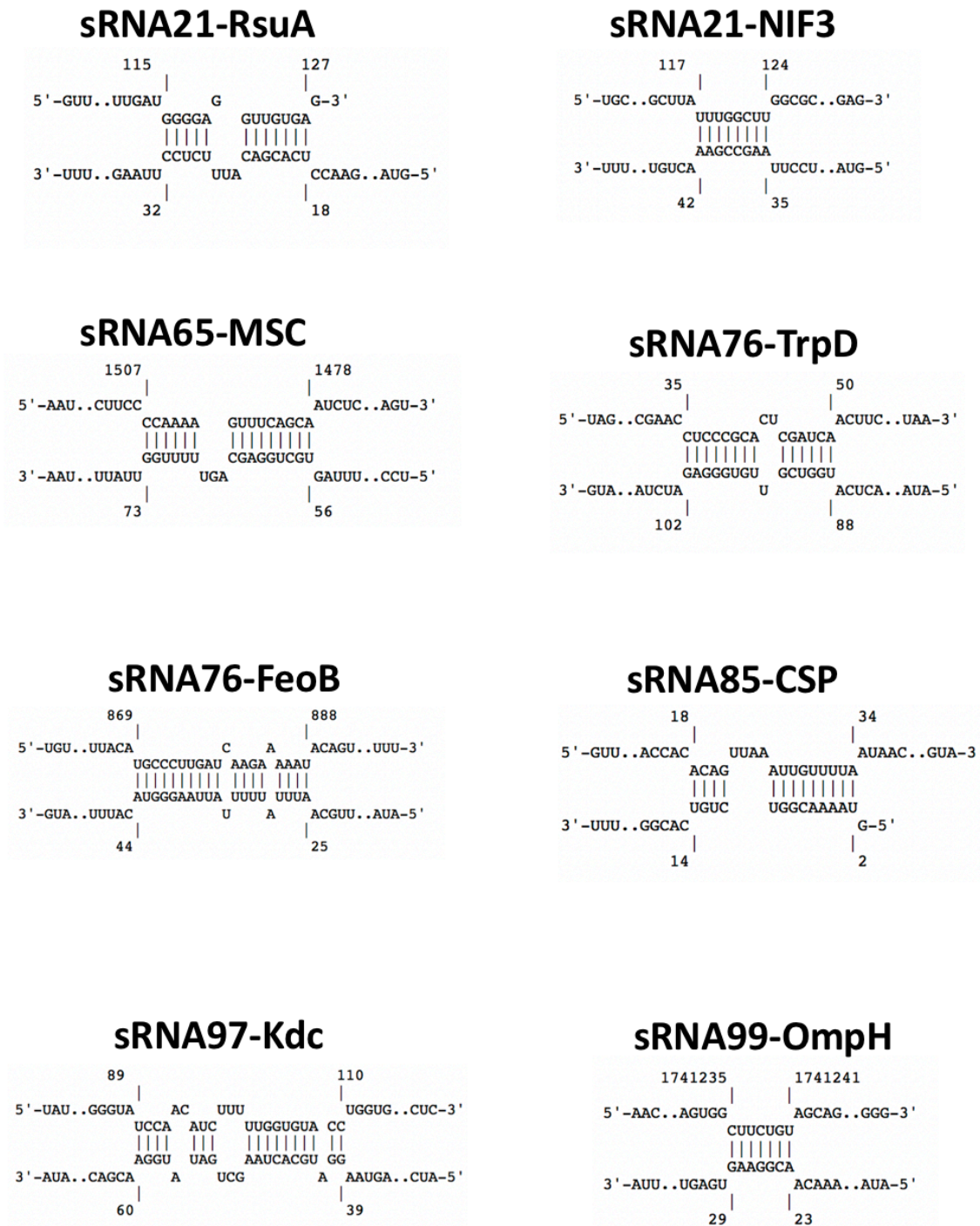


Figure 3.6 Duplex structure of sRNA-mRNA interactions under investigation

The duplex structures of putative sRNA-mRNA interaction partners were obtained using the computational sRNA target prediction tool IntaRNA (Busch et al., 2008). This identifies likely base-pairing interactions between the mRNA target, depicted as the top interaction partner for each interaction, and the sRNA candidate, depicted as the bottom interaction partner. The location of the predicted interaction sites for each mRNA target and sRNA candidate is represented by the numbers above or below the interaction respectively.

3.5 Comparison of Hi-GRIL-seq to target prediction tools

Targets identified by Hi-GRIL-seq based on abundance were compared to those identified *in silico* by prediction tools TargetRNA2 and CopraRNA (Kery et al., 2014; Wright et al., 2014). This enabled us to find common targets and to determine whether the combination of *in silico* and experimental selection of targets is more efficient than those obtained based on abundance. TargetRNA2 predicted targets based on the *A. baumannii* ATCC 17978 genome, while CopraRNA identified conserved potential targets in *A. nosocomialis* 6411, *A. pittii* PHEA-2, *A. baumannii* AB5075, *A. baumannii* AYE and *A. baumannii* AB0057.

A comparison of the targets predicted by TargetRNA2, CopraRNA and Hi-GRIL-seq is summarised in **Figure 3.7**. There were few targets shared by only TargetRNA2 and Hi-GRIL-seq, 2 targets were shared with sRNA76 and sRNA97, this included elongation factor G and F0F1 ATP synthase subunit beta for sRNA76 and bacterioferritin and glyceraldehyde-3-phosphate dehydrogenase respectively. There were multiple targets shared between CopraRNA and Hi-GRIL-seq, including 13 targets shared for sRNA21, 34 targets shared for sRNA76, 10 targets shared for sRNA97 and 23 targets shared for sRNA99. A single target was shared between all methods for sRNA85, a gene encoding 3-oxoadipyl-CoA thiolase. RsuA was the only target that was examined in this study and shared with the CopraRNA prediction tool.

Many of the targets shared between Hi-GRIL-seq and the target prediction tools are involved in vital *A. baumannii* metabolic, resistance and virulence pathways. 3-oxoadipyl-CoA thiolase is a member of the phenylacetic acid catabolism operon, system essential for neutrophil evasion (Bhuiyan et al., 2016). Superoxide dismutase and OmpA were predicted by CopraRNA and are highly abundant in sRNA76 Hi-GRIL-seq, these

proteins play critical roles in oxidative stress resistance and multidrug resistance in *A. baumannii* respectively (Heindorf et al., 2014; Nie et al., 2020). *A. baumannii* OmpA is also involved in host epithelial cell adherence and invasion (Choi et al., 2008). Similarly, peptidoglycan-binding protein LysM which is involved in biofilm formation in *A. baumannii* (Cabral et al., 2011) was abundantly ligated to sRNA65 in Hi-GRIL-seq and predicted by CopraRNA. The RNA binding protein CsrA was also predicted by CopraRNA and was an abundant sRNA97 target in the Hi-GRIL-seq analysis. CsrA was previously suggested to be regulated by the *A. baylyi* ADP1 sRNA97-homologue RsmY (Kulkarni et al., 2006; Müller et al., 2019). A gene involved in amino acid metabolism, phosphoenolpyruvate synthase, was predicted for sRNA21 (Aar), thus the role of Aar in amino acid metabolism in *A. baylyi* might be conserved in *A. baumannii*. These are valuable sRNA targets that warrant further investigation.

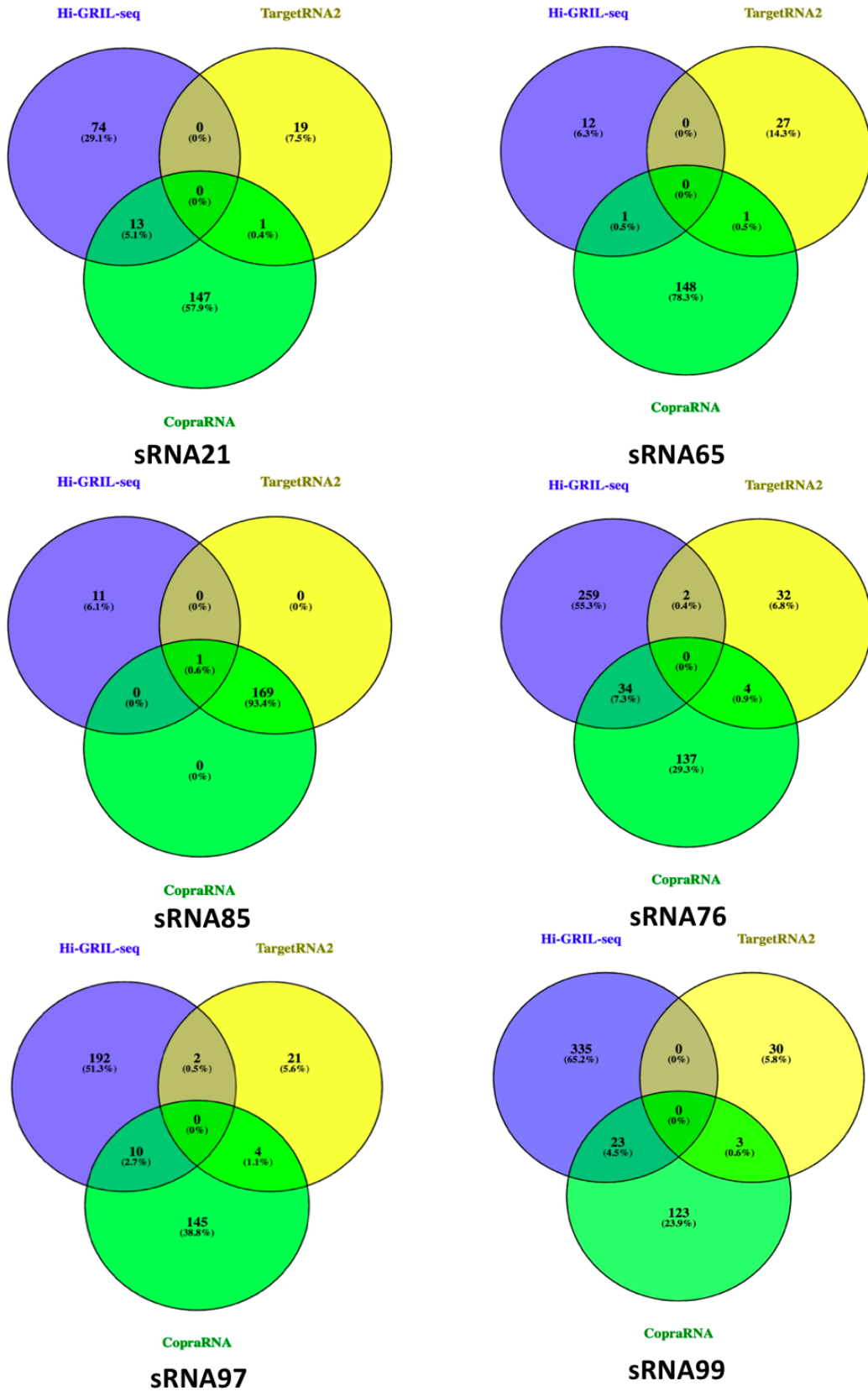


Figure 3.7 Comparison of computational and experimental target predictions
 The mRNA targets of various sRNA candidates identified experimentally were compared to targets identified *in silico* by the sRNA target prediction tools CopraRNA and TargetRNA2.

4 Validation of sRNA-mRNA interactions

4.1 Construction of overexpression vectors

The sRNA-mRNA interactions predicted by Hi-GRIL-seq and investigated *in silico* may not be the result of posttranscriptional interactions but may rather be caused by indirect sRNA-mRNA interactions in *A. baumannii* (Wagner et al., 2015). To ensure the veracity of these interactions, we employed a previously described fluorescence based, two-plasmid target reporter system in *E. coli*. This system enabled investigation of interactions of heterologous sRNAs and their targets, derived from other Gram-negative species, *in trans* in *E. coli* (Liu et al., 2015; Urban et al., 2007).

The sRNAs under investigation and their cognate mRNA targets were cloned into the pP_L and pXG10 plasmids respectively, where they were constitutively expressed (**Figure 4.1**). The mRNA targets are translationally fused to GFP in the pXG10 plasmids forming the basis of this fluorescence-based reporter system (Urban et al., 2007). The sRNAs and their targets were cloned into the pP_L and pXG10 plasmids using the Seamless Ligation Cloning Extract (SLiCE) cloning protocol (Zhang et al., 2012, 2014). Extracts from *E. coli* expressing λ prophage Red recombination system allowed recombination between identical SLiCE sequences (of approximately 25 base-pairs) at the 5' and 3' ends of the interaction partners being studied and the ends of their respective linearised vectors.

The pP_L and pXG10 plasmids were linearised by carrying out a plasmid backbone PCR. These PCR reactions were performed in triplicate for both plasmids. Negative controls were included to ensure amplification occurred as intended (**Figure 4.2**). This resulted in the generation of amplicons of 2159 and 4145 base-pairs respectively as expected (**Table 4.1**). The remainder of the backbone PCR reactions for both plasmids were pooled

together, purified and digested with DpnI to remove methylated template DNA and prepare them for them for the SLiCE reaction.

The sRNAs and their targets were prepared for the SLiCE reaction by PCR amplifying them with primers that contained their respective SLiCE sequences at their 5' ends. The sRNA primers were designed to amplify the entire sRNA genes and 100 base-pairs downstream to ensure termination. The region between the TSSs and the Hi-GRIL-seq indicated ligation junctions of the targets under investigation was amplified using SLiCE modified primers. The amplified targets were designed to include their start codon and to retain the proper codon sequence order needed to allow GFP expression. The PCR amplified sRNAs and mRNA target sequences are demonstrated in **Figure 4.3** and **Figure 4.4** respectively. The amplicon fragment sizes obtained from both reactions are in line with the estimated amplicon sizes (**Table 4.2** and **Table 4.3**).

The sRNAs and target sequences were then integrated into the pP_L and pXG10 expression vectors using the SLiCE reaction. After this, competent *E. coli* cells were transformed with the SLiCE reactions and recovered on ampicillin or chloramphenicol containing L-plates respectively. The resulting plasmids were confirmed to contain the sRNAs and target sequences through colony PCR and Sanger sequencing. Colonies of cells expressing the pXG10-target vectors were assessed for GFP fluorescence using a GFP-detecting CCD camera. All of the pXG10-target plasmids demonstrated fluorescence, suggesting that GFP was successfully being translated. This ensured that we could determine posttranscriptional interactions between sRNAs and their targets by monitoring GFP expression.

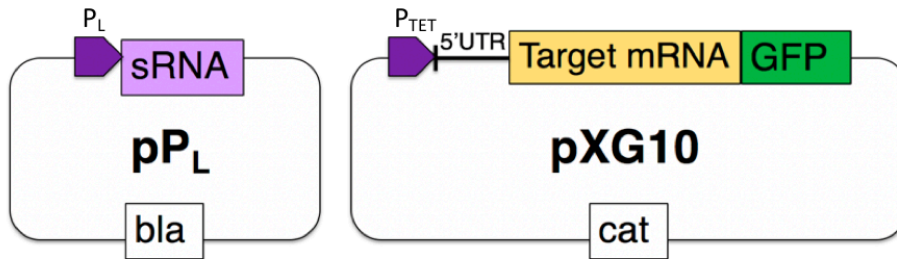


Figure 4.1 Model of the two-plasmid RNA-RNA interaction confirmation system

The sRNAs and their targets under investigation in this experiment are constitutively expressed by the P_L and P_{TET} in pP_L and pXG10 plasmids respectively. The target under investigation is translationally fused to GFP which enables use of a fluorescence based two plasmid report system to detect posttranscriptional interactions.

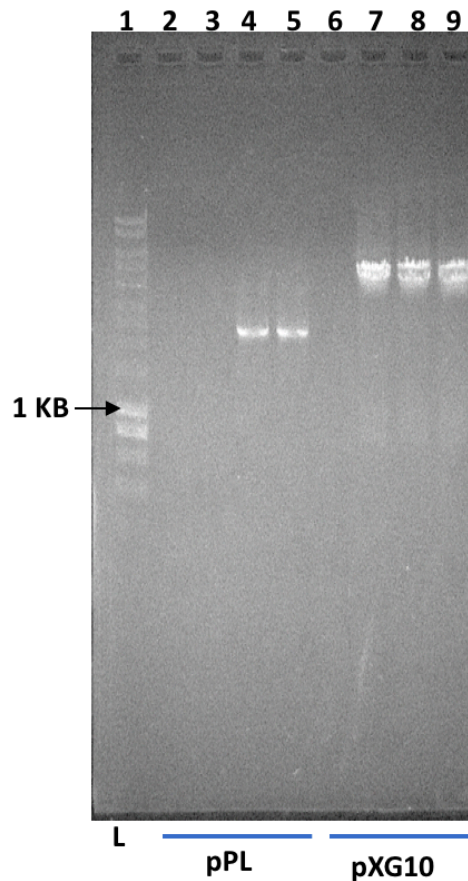


Figure 4.2 Backbone amplification of pP_L and pXG10

| Lane | Sample | Sample size | Expected size |
|------|------------------|-------------|---------------|
| 1 | Hyperladder 1 Kb | N/A | N/A |
| 2 | control | 0 bp | 0 bp |
| 3 | pPL backbone | 0 bp | 2159 bp |
| 4 | pPL backbone | 2325 bp | 2159 bp |
| 5 | pPL backbone | 2315 bp | 2159 bp |
| 6 | control | 0 bp | 0 bp |
| 7 | pXG10 backbone | 4048 bp | 4145 bp |
| 8 | pXG10 backbone | 4061 bp | 4145 bp |
| 9 | pXG10 backbone | 4038 bp | 4145 bp |

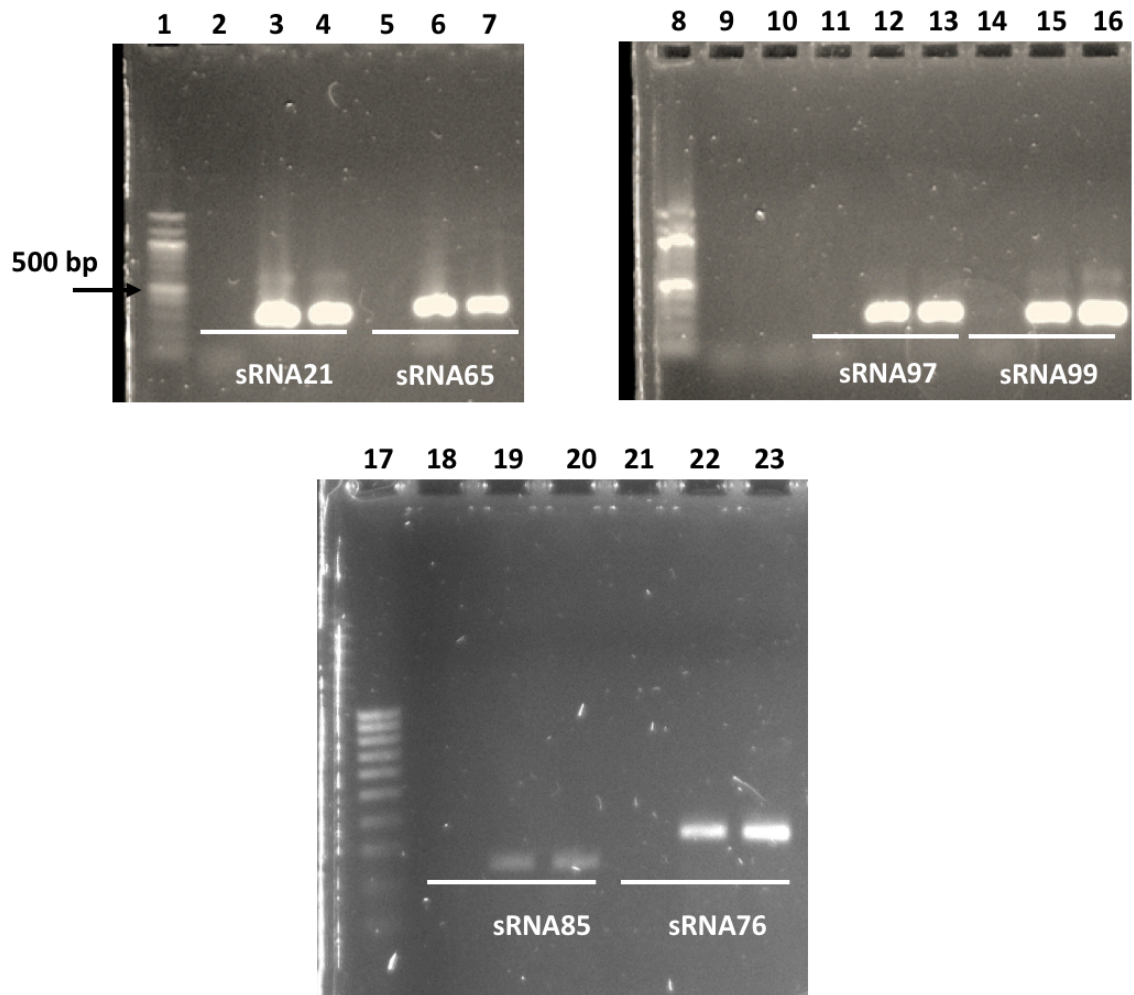


Figure 4.3 Amplification of sRNAs under investigation

Table 4.2 sRNA amplification results

| Lane | Sample | Sample size | Expected size |
|-------------|---------------------|--------------------|----------------------|
| 1 | 100 bp ladder (NEB) | N/A | N/A |
| 2 | Control (sRNA21) | 0 bp | 0 bp |
| 3 | sRNA21 | 269 bp | 246 bp |
| 4 | sRNA21 | 269 bp | 246 bp |
| 5 | Control (sRNA65) | 0 bp | 0 bp |
| 6 | sRNA65 | 314 bp | 275 bp |
| 7 | sRNA65 | 314 bp | 275 bp |
| 8 | 100 bp ladder (NEB) | N/A | N/A |
| 9 | blank | N/A | N/A |
| 10 | blank | N/A | N/A |
| 11 | Control (sRNA97) | 0 bp | 0 bp |
| 12 | sRN97 | 266 bp | 261 bp |
| 13 | sRNA97 | 266 bp | 261 bp |
| 14 | Control (sRNA99) | 0 bp | 0 bp |
| 15 | sRNA99 | 247 bp | 256 bp |
| 16 | sRNA99 | 247 bp | 256 bp |
| 17 | Hyperladder IV | N/A | N/A |
| 18 | Control (sRNA85) | 0 bp | 0 bp |
| 19 | sRNA85 | 153 bp | 176 bp |
| 20 | sRNA85 | 153 bp | 176 bp |
| 21 | Control (sRNA76) | 0 bp | 0 bp |
| 22 | sRNA76 | 260 bp | 275 bp |
| 23 | sRNA76 | 260 bp | 275 bp |

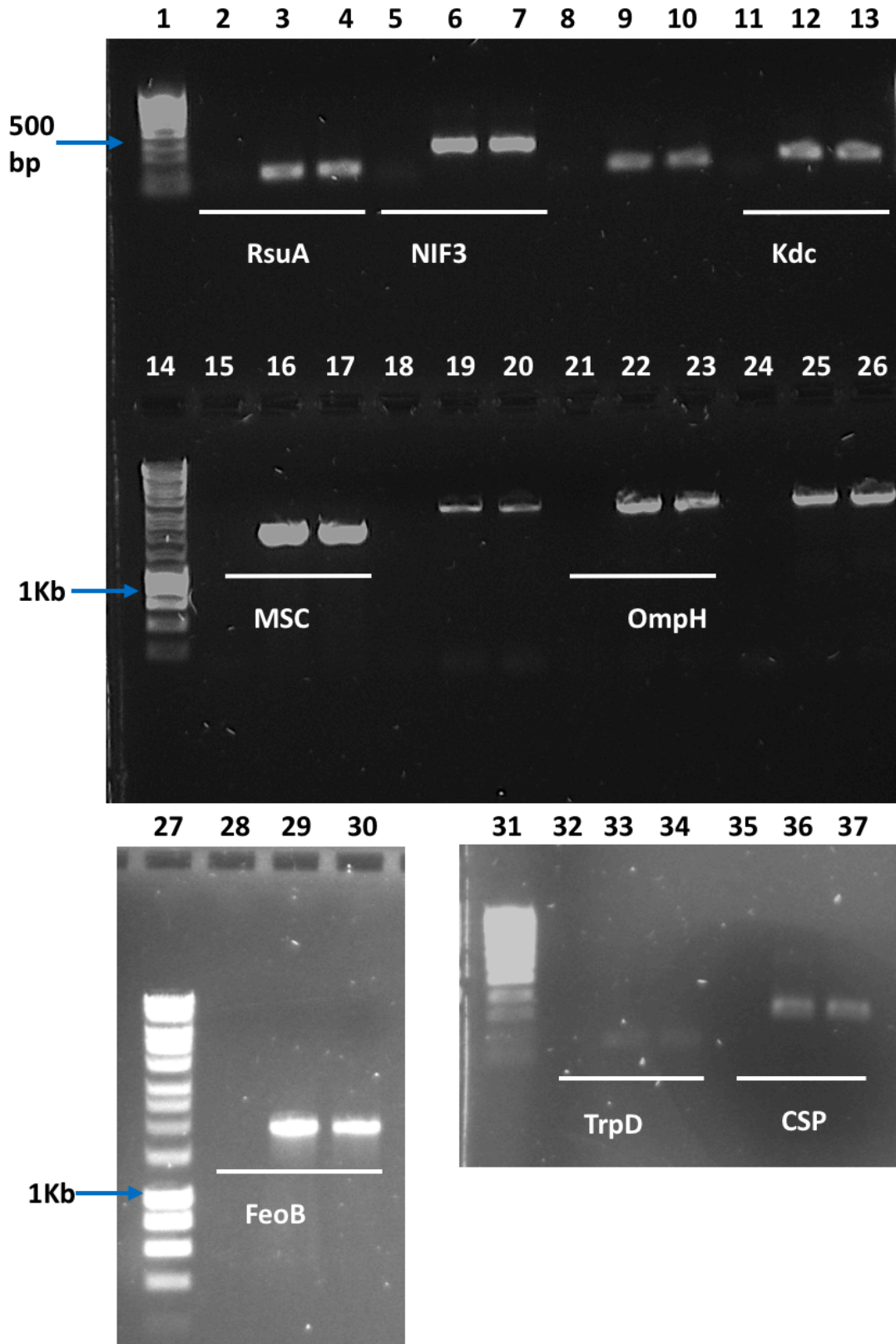


Figure 4.4 Amplification of targets under investigation

Table 4.3 Target amplification results

| Lane | Sample | Sample size | Expected size |
|-------------|---------------------|--------------------|----------------------|
| 1 | 100 bp ladder (NEB) | N/A | N/A |
| 2 | Control (RsuA) | 0 bp | 0 bp |
| 3 | RsuA | 162 bp | 153 bp |
| 4 | RsuA | 167 bp | 153 bp |
| 5 | Control (NIF3) | 0 bp | 0 bp |
| 6 | NIF3 | 323 bp | 310 bp |
| 7 | NIF3 | 325 bp | 310 bp |
| 8 | N/A | N/A | N/A |
| 9 | N/A | N/A | N/A |
| 10 | N/A | N/A | N/A |
| 11 | Control (Kdc) | 0 bp | 0 bp |
| 12 | Kdc | 204 bp | 192 bp |
| 13 | Kdc | 212 bp | 192 bp |
| 14 | Hyperladder 1 Kb | N/A | N/A |
| 15 | Control (MSC) | 0 bp | 0 bp |
| 16 | MSC | 2036 bp | 2073 bp |
| 17 | MSC | 2036 bp | 2073 bp |
| 18 | N/A | N/A | N/A |
| 19 | N/A | N/A | N/A |
| 20 | N/A | N/A | N/A |
| 21 | Control (OmpH) | 0 bp | 0 bp |
| 22 | OmpH | 3200 bp | 3092 bp |
| 23 | OmpH | 3127 bp | 3092 bp |
| 24 | N/A | N/A | N/A |
| 25 | N/A | N/A | N/A |
| 26 | N/A | N/A | N/A |
| 27 | Hyperladder 1 Kb | N/A | N/A |
| 28 | Control (FeoB) | 0 bp | 0 bp |
| 29 | FeoB | 2084 bp | 1862 bp |
| 30 | FeoB | 2084 bp | 1862 bp |
| 31 | Hyperladder IV | N/A | N/A |
| 32 | Control (TrpD) | 0 bp | 0 bp |
| 33 | TrpD | 100 bp | 139 bp |
| 34 | TrpD | 100 bp | 139 bp |
| 35 | Control (CSP) | 0 bp | 0 bp |
| 36 | CSP | 248 bp | 244 bp |
| 37 | CSP | 248 bp | 244 |

4.2 Verification of sRNA-mRNA interactions

Posttranscriptional interactions between the *A. baumannii* sRNAs and their cognate mRNA targets were confirmed in *E. coli* using a two-plasmid fluorescence reporter system previously mentioned (Urban et al., 2007). We used heterologous expression of the predicted *A. baumannii* sRNA-mRNA interaction pairs *in trans* in *E. coli* because there are currently not two plasmids that are compatible and replicated in *A. baumannii*. This reporter system examines the change in GFP fluorescence levels in cells co-expressing a pXG10-target vector with their respective pP_L-sRNA vector compared to cells expressing the pXG10-target vector with the pJV300 control vector. The pJV300 vector transcribes a nonsense RNA molecule that is incapable of interacting with the transcribed target::GFP mRNA (Papenfort et al., 2010). If the pP_L-sRNA interacts with target, it will change the *target::GFP* mRNA levels, and therefore alter GFP expression. The expression of GFP for each sRNA-mRNA interaction pair and their respective controls was quantified over twenty four hours using a microplate fluorometer. The GFP expression levels between the sRNA-mRNA interaction pairs and between the control group were compared after this growth time (**Figure 4.5**). The interaction between the sRNA RybB and OmpC was used as a positive control, due to the fact that RybB is a known suppressor of OmpC (Papenfort et al., 2010). From this experiment, we observed that two sRNA alter the abundance of GFP; the Aar-homologue sRNA21 significantly negatively regulates RsuA expression compared to the control group (P=0.0068) and sRNA97 significantly upregulates Kdc expression compared to the control group (P=0.0001). The sRNA21 also appears to reduce expression of Nif3, however, this reduction is not statistically significant (P= 0.0515). None of the other targets have significantly altered GFP abundance compared to their control groups.

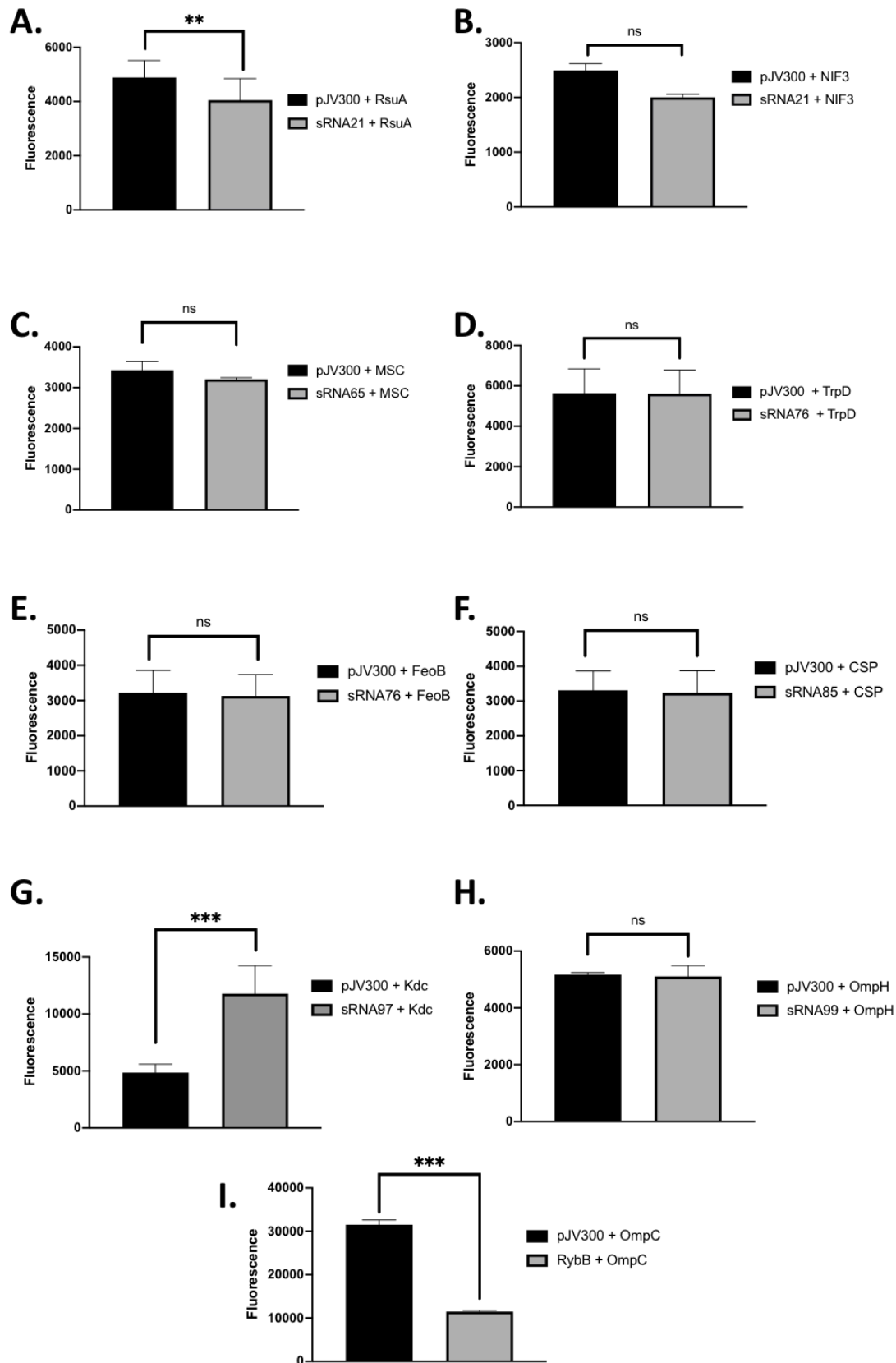


Figure 4.5 Co-expression of sRNA and target vectors compared to pJV300 control

The expression of GFP in *E. coli* co-expressing the pPL-sRNA and pXG10-target vectors was compared to *E. coli* co-expressing the pJV300 control vector with the pXG10-target vector. Data is shown as mean \pm SD. Statistical comparisons were performed using Student's T-test. Differences were considered statistically significant when $P < 0.5$ where ** denotes $P < 0.01$ and *** denotes $P < 0.001$

5 Discussion

Bacterial sRNAs are a critical class of regulatory molecules that can modulate vital cellular mechanisms by directly base-pairing with complementary mRNA targets (Storz et al., 2011). The emergence of high-throughput RNA-sequencing technologies combined with the improvement of computational prediction software has promoted the detection of novel *trans*-encoded sRNAs (Diallo et al., 2020). Despite these improved sRNA characterisation methods, the discovery of their targets remains elusive. The advent of the proximity ligation method Hi-GRIL-seq promises to accelerate the detection of new targets (Zhang et al., 2017). Hi-GRIL-seq is dependent on the ectopic expression of T4 RNA ligase, to ligate endogenous sRNA-mRNA interaction pairs into chimeric molecules. Here, we apply Hi-GRIL-seq to investigate the posttranscriptional regulation of *A. baumannii* physiology by attempting to define the targets of 110 sRNA candidates previously described (Kröger et al., 2018). The Hfq-independent nature of Hi-GRIL-seq is attractive due to the unclear role Hfq plays in regulating *A. baumannii* sRNA-mRNA interactions (Kröger et al., 2017; Sharma et al., 2018). This study sought to investigate targets that play essential roles in survival and antimicrobial resistance by analysis sRNA-mRNA interaction pairs for each sRNA candidate. This was accomplished by performing ligations in diverse growth conditions including iron depletion, antibiotic exposure and T4 RNA ligase induced and uninduced conditions. Targets that were suspected to play promising roles in modulating *A. baumannii* physiological properties that promote virulence and environmental persistence mechanisms were prioritised. This study shows that Hi-GRIL-seq offers a promising role in defining the *A. baumannii* targetome and in identifying sRNA-mRNA interaction pairs in this pathogen.

Hi-GRIL-seq has proven to be a very effective way of investigating the entire *A. baumannii* targetome. The sequencing depth of this study was twice as high as that used in the *P. aeruginosa* Hi-GRIL-seq experiment (Zhang et al., 2017). This led to the identification of ten times more potential sRNA-containing chimeras, highlighting the power of this approach. The selection of Hi-GRIL-seq targets for each sRNA based on their abundance, uniqueness and biological potential allowed identification of eight putative sRNA-mRNA interaction pairs, including sRNA21–16 rRNA Pseudouridine synthase, sRNA21–NIF3 domain containing protein, sRNA65–Mechanosensitive ion channel, sRNA76–Anthranilate phosphoribosyltransferase, sRNA76–ferrous iron transporter B, sRNA85–cold-shock protein, sRNA97– α -keto acid decarboxylase family protein and sRNA99–outer membrane protein H. We also determined that the sRNA21 and the sRNA65 are homologues of the *A. baylyi* ADP1 sRNA Aar and the *A. baumannii* ATCC 17978 putative sRNA AbsR25 respectively (Schilling et al., 2010; Sharma et al., 2014). Similarly, the sRNA97 is a homologue if the potential *A. baylyi* ADP1 sRNA RsmY (Kulkarni et al., 2006). Many of these putative targets were predicted to play important roles in regulating iron metabolism, antibiotic resistance, pathogenesis and osmolarity.

Despite these clear advantages, this Hi-GRIL-seq analysis had certain limitations. There was a large number of low-confidence targets identified by this approach. This may be due to the promiscuous nature of the P_{BAD} promoter, which allowed excessive ligation of RNA molecules, even under uninduced conditions. The targets identified were also not overrepresented in individual ligation conditions. This hinders our ability to define condition specific interactions using this approach. Future analyses warrant the inclusion

of Hi-GRIL-seq experiments using an empty pVRL2Z vector as additional negative control to determine the extent of leaky T4 RNA ligase expression. Another limitation of this study was that there were no targets identified for the majority of sRNA candidates. This may imply that the number of sequencing reads used to filter potential chimeras was unnecessarily high and may have ignored potential interactions with sparse targets. A lower sequencing read cut-off may be worth investigating in future analyses. In addition, the 110 sRNAs identified previously were obtained by growing cells in 16 different conditions, thus it is conceivable that not all sRNAs were expressed in the three conditions used in this study.

Interrogation of the sRNA-mRNA junction sites, for each of the chimeric molecules, revealed that these ligation sites encompass the sRNA-mRNA duplex structures predicted by the computational interaction prediction tool IntaRNA. This lends further credence to the notion that these sRNA candidates and predicted target molecules are capable of direct base-pairing interactions. We were able to assess the target detection ability of Hi-GRIL-seq by comparing all the targets suggested in our analysis with those outlined by computational prediction tools TargetRNA2 and CopraRNA for the sRNAs under investigation (Kery et al., 2014; Wright et al., 2014). It is evident that CopraRNA was better capable of identifying targets in common with those obtained from Hi-GRIL-seq than TargetRNA2. This may suggest that CopraRNA has improved target detection abilities. RsuA was the only target under investigation identified by both Hi-GRIL-seq and CopraRNA. This is partially due to the nature of the prediction tools that identify targets in close proximity to the start codon, ignoring putative intragenic targets. Despite this limitation, CopraRNA and Hi-GRIL-seq identified additional targets that justify further experimental investigations. These targets worthy of further investigation include superoxide dismutase, OmpA, LysM and the potential RNA chaperone CsrA (Cabral et

al., 2011; Müller et al., 2019; Nie et al., 2020; Shin et al., 2020). The combination of computational target prediction with experimental target discovery may offer a more refined approach to target discovery, the combination of CopraRNA with MAPS and RIL-seq enabled more detailed discovery of RyhB targets (Georg et al., 2020). This would help eliminate low-confidence targets.

In vivo co-expression of the *A. baumannii* sRNAs and their cognate mRNA targets using a previously defined 2-plasmid fluorescent reporter system in *E. coli* was used to identify sRNA-mRNA interactions (Urban et al., 2007). Co-expression of these plasmids in *E. coli* was used due to the fact that two plasmids cannot currently be maintained at the same time in *A. baumannii* (Lucidi et al., 2018). The *A. baumannii* sRNAs and mRNA targets were amplified and cloned into the pP_L overexpression vector and the pXG10 overexpression vector respectively using the SLiCE cloning method (Zhang et al., 2014). This cloning method enabled rapid construction of these overexpression vectors. The pXG10-target vectors were co-expressed in *E. coli* with either their cognate pP_L-sRNA vector or a pJV300 control, that transcribes a small nonsense RNA molecule (Urban et al., 2007). By comparing the expression of GFP in *E. coli* cells co-expressed with the pP_L-sRNA vector or the pJV300 control over twenty four hours, we were able to identify two likely interaction pairs; sRNA21–RsuA and sRNA97–Kdc. It appears that sRNA21 negatively regulates RsuA, while sRNA97 dramatically upregulates Kdc. As the Kdc-encoding gene is directly upstream of an amino acid permease in an operon, sRNA97 may upregulate this amino acid permease indirectly by base-pairing to polycistronic mRNA (Balasubramanian et al., 2013).

The interactions suggested in this study imply that *A. baumannii* AB5075 sRNAs are capable of occurring utilising endogenous *E. coli* systems, this opens up the possibility

that *E. coli* Hfq may support sRNA-mRNA interaction from *A. baumannii*. However, it is possible that the other sRNA-mRNA interaction pairs were incapable of effecting GFP expression due to the heterologous *E. coli* systems. These interactions should also be examined in *A. baumannii* once a detection system is established. The role of Hfq in mediating these interactions should be further characterised by assessing base-pairing in Hfq deficient *E. coli* (Moon et al., 2011). If the involvement of Hfq is established, interactions in the presence of recombinant *A. baumannii* Hfq should also be investigated. The enlarged, glycine rich C-terminal of *A. baumannii* Hfq may alter the loading of sRNAs, potentially changing the sRNA-mRNA interaction properties (Schilling et al., 2009; Sharma et al., 2018). To confirm the mechanistic of these identified interactions, point mutations should be induced in nucleotides in the sRNA that are predicted to disrupt the sRNA-mRNA duplex. A compensatory mutation in the complementary mRNA nucleotide should be induced to restore the duplex.

This study is the first to confirm *A. baumannii* sRNA candidates by identifying their targets. It also confirms that sRNA-mediated gene regulation exists in *A. baumannii*. The use of Hi-GRIL-seq to identify these targets also improve our understanding of the mechanistic that underlie their interactions. These sRNA-mRNA interactions may play integral roles in the regulation of *A. baumannii* physiology. As mentioned, the α -keto acid decarboxylase family protein decarboxylates α -keto acids, including pyruvate and α -ketoglutarate. As sRNA97 upregulates this enzyme, it may be a critical regulator of central metabolism in this pathogen. The potential upregulation of the amino acid permease downstream of this gene may be essential for overcoming host amino acid deprivation during pulmonary infections (Peng et al., 2010; Wang et al., 2014). Since both the α -keto acid decarboxylase and the sRNA Aar regulate pyruvate metabolism, this

suggests that pyruvate metabolism is an important *A. baumannii* virulence factor. This is supported by recent evidence that suggests that pyruvate is an inducer of *A. baumannii* virulence in the presence of human pleural fluid (Rodman et al., 2019) suggesting that sRNA97 may be negatively regulated during infection to prevent degradation of pyruvate. A transcriptomic analysis of *A. baumannii* ATCC 17978 also suggested that α -keto acid decarboxylase is more highly expressed in biofilms than in planktonic cells, suggesting that sRNA97 may promote biofilm formation (Rumbo-Feal et al., 2013). As mentioned CsrA was a target predicted by CopraRNA that was abundant in the sRNA97 Hi-GRIL-seq data. CsrA is an RNA-binding protein and posttranscriptional regulator of quorum sensing, biofilm formation, host cell invasion and carbon metabolism (Altier et al., 2000; Wei et al., 2000; Yang et al., 1996). Many sRNAs act as “sponges” by binding with CsrA, preventing this chaperone from interacting with its target mRNAs (Holmqvist et al., 2013). It seems that sRNA97 is a homologue of RsmY, a negative RsmA regulator involved in quorum sensing in *P. aeruginosa* (Kay et al., 2006). Rsm is the *P. aeruginosa* CsrA homologue. Furthermore, prediction of the secondary structure of sRNA97 revealed the presence of three GGA sequences located in the loops of three separate stem-loop structures. This motif is critical for CsrA/RsmA binding and for maintaining stability of RsmY in *Pseudomonas* species (Janssen et al., 2018; Valverde et al., 2004). It is worth investigating sRNA97-CsrA interactions to determine the importance this regulator plays in modulating pathogenesis. There are no homologues of the sRNAs CsrB and CsrC in *A. baumannii*, however, homologues of RsmX, RsmY and RsmZ have been predicted (Sobrero et al., 2020). These sRNAs are regulators of RsmA and may be functional analogues of CsrB and CsrC.

Persister cells are a subpopulation of slow-growing, phenotypically heterogeneous cells that are capable of surviving high concentrations of antibiotics (Fisher et al., 2017). This

enables them to re-establish infection following treatment. *A. baumannii* employs this strategy to overcome antimicrobial therapy (Chung et al., 2019). A transcriptomic analysis of *A. baumannii* ATCC 19606 treated with ceftazidime suggested that α -keto acid decarboxylase is overexpressed during persister cell formation, however this requires further evaluation (Alkasir et al., 2018). The sRNA21 downregulates RsuA, the role of RsuA in pseudouridylation of 16S rRNA is previously discussed (Jayalath et al., 2020). A study in *E. coli* demonstrated that the synthesis RsuA is a critical for survival of a subpopulation of cells after induction of the MazF toxin (Amitai et al., 2009). The author suggests that RsuA is involved in reactive oxygen species detoxification, however, this putative mechanism is not defined. The 23S rRNA Pseudouridine synthase RluD was shown to be involved in the resuscitation of persister cells in *E. coli*, it was even negatively regulated by the sRNA RybB (Song et al., 2020). This suggests that both sRNA97 and sRNA21 may be involved in the formation or regrowth of persister cells respectively. This could explain the heterologous nature of *A. baumannii* persistent cells, however, this requires further study.

In conclusion, this work demonstrates that Hi-GRIL-seq is an invaluable tool for defining the *A. baumannii* targetome. It has enabled determination of sRNA-mRNA mechanisms, which has not been previously demonstrated in *A. baumannii*. The Hfq-independent nature of the protocol allows definition of target without relying on this RNA chaperone that plays an unclear role in *Pseudomonades species*. Further work should seek to confirm the mechanisms of interaction proposed in this work, investigate the role of chaperones in depth and fully characterise the biological importance of these interactions observed. Additionally, the other sRNA-mRNA chimeras outlined in this study should be investigated for more targets.

6 Bibliography

- Alkasir, R., Ma, Y., Liu, F., Li, J., Lv, N., Xue, Y., Hu, Y., & Zhu, B. (2018). Characterization and transcriptome analysis of *Acinetobacter baumannii* persister cells. *Microbial Drug Resistance*, *24*(10), 1466–1474. <https://doi.org/10.1089/mdr.2017.0341>
- Altier, C., Suyemoto, M., & Lawhon, S. D. (2000). Regulation of *Salmonella enterica* serovar typhimurium invasion genes by *csrA*. *Infection and Immunity*, *68*(12), 6790–6797. <https://doi.org/10.1128/IAI.68.12.6790-6797.2000>
- Amitai, S., Kolodkin-Gal, I., Hananya-Meltabashi, M., Sacher, A., & Kulka, H. E. (2009). *Escherichia coli* MazF leads to the simultaneous selective synthesis of both “death proteins” and “survival proteins.” *PLoS Genetics*, *5*(3). <https://doi.org/10.1371/journal.pgen.1000390>
- Andreassen, P. R., Pettersen, J. S., Szczerba, M., Valentin-Hansen, P., Møller-Jensen, J., & Jørgensen, M. G. (2018). SRNA-dependent control of curli biosynthesis in *Escherichia coli*: McaS directs endonucleolytic cleavage of *csgD* mRNA. *Nucleic Acids Research*, *46*(13), 6746–6760. <https://doi.org/10.1093/nar/gky479>
- Antunes, L. C. S., Visca, P., & Towner, K. J. (2014). *Acinetobacter baumannii*: Evolution of a global pathogen. *Pathogens and Disease*, *71*(3), 292–301. <https://doi.org/10.1111/2049-632X.12125>
- Balasubramanian, D., & Vanderpool, C. K. (2013). New developments in post-transcriptional regulation for operons by small RNAs. *RNA Biology*, *10*(3), 337–341. <https://doi.org/10.4161/rna.23696>
- Bhuiyan, M. S., Ellett, F., Murray, G. L., Kostoulias, X., Cerqueira, G. M., Schulze, K. E., Maifiah, M. H. M., Li, J., Creek, D. J., Lieschke, G. J., & Peleg, A. Y. (2016). *Acinetobacter baumannii* phenylacetic acid metabolism influences infection

- outcome through a direct effect on neutrophil chemotaxis. *Proceedings of the National Academy of Sciences of the United States of America*, 113(34), 9599–9604. <https://doi.org/10.1073/pnas.1523116113>
- Busch, A., Richter, A. S., & Backofen, R. (2008). IntaRNA: Efficient prediction of bacterial sRNA targets incorporating target site accessibility and seed regions. *Bioinformatics*, 24(24), 2849–2856. <https://doi.org/10.1093/bioinformatics/btn544>
- Butler, D. A., Biagi, M., Tan, X., Qasmieh, S., Bulman, Z. P., & Wenzler, E. (2019). Multidrug Resistant *Acinetobacter baumannii*: Resistance by Any Other Name Would Still be Hard to Treat. *Current Infectious Disease Reports*, 21(12). <https://doi.org/10.1007/s11908-019-0706-5>
- Cabral, M. P., Soares, N. C., Aranda, J., Parreira, J. R., Rumbo, C., Poza, M., Valle, J., Calamia, V., Lasa, Í., & Bou, G. (2011). Proteomic and functional analyses reveal a unique lifestyle for *acinetobacter baumannii* biofilms and a key role for histidine metabolism. *Journal of Proteome Research*, 10(8), 3399–3417. <https://doi.org/10.1021/pr101299j>
- Cafiso, V., Stracquadiano, S., Lo Verde, F., Dovere, V., Zega, A., Pigola, G., Aranda, J., & Stefani, S. (2020). COLR *Acinetobacter baumannii* sRNA Signatures: Computational Comparative Identification and Biological Targets. *Frontiers in Microbiology*, 10(January), 1–9. <https://doi.org/10.3389/fmicb.2019.03075>
- Cardoso, K., Gandra, R. F., Wisniewski, E. S., Osaku, C. A., Kadowaki, M. K., Felipach-Neto, V., Haus, L. F. A. Á., & Simão, R. D. C. G. (2010). DnaK and GroEL are induced in response to antibiotic and heat shock in *Acinetobacter baumannii*. *Journal of Medical Microbiology*, 59(9), 1061–1068. <https://doi.org/10.1099/jmm.0.020339-0>
- Carrier, M. C., Lalaouna, D., & Massé, E. (2016). A game of tag: MAPS catches up on

- RNA interactomes. *RNA Biology*, 13(5), 473–476.
<https://doi.org/10.1080/15476286.2016.1156830>
- Centers for Disease Control and Prevention. (2019). *Antibiotic resistance threats in the United States. fcimb-07-00055.pdf*, 114. <https://doi.org/CS239559-B>
- Chao, Y., Papenfort, K., Reinhardt, R., Sharma, C. M., & Vogel, J. (2012). An atlas of Hfq-bound transcripts reveals 3' UTRs as a genomic reservoir of regulatory small RNAs. *EMBO Journal*, 31(20), 4005–4019.
<https://doi.org/10.1038/emboj.2012.229>
- Chareyre, S., & Mandin, P. (2018). Bacterial Iron Homeostasis Regulation by sRNAs. *Regulating with RNA in Bacteria and Archaea*, 267–281.
<https://doi.org/10.1128/9781683670247.ch16>
- Chen, S., Zhang, A., Blyn, L. B., & Storz, G. (2004). MicC, a second small-RNA regulator of omp protein expression in Escherichia coli. *Journal of Bacteriology*, 186(20), 6689–6697. <https://doi.org/10.1128/JB.186.20.6689-6697.2004>
- Choi, C. H., Lee, J. S., Lee, Y. C., Park, T. I., & Lee, J. C. (2008). Acinetobacter baumannii invades epithelial cells and outer membrane protein A mediates interactions with epithelial cells. *BMC Microbiology*, 8, 1–11.
<https://doi.org/10.1186/1471-2180-8-216>
- Chung, E. S., & Ko, K. S. (2019). Eradication of persister cells of Acinetobacter baumannii through combination of colistin and amikacin antibiotics. *Journal of Antimicrobial Chemotherapy*, 74(5), 1277–1283.
<https://doi.org/10.1093/jac/dkz034>
- Cornejo-Juárez, P., Cevallos, M. A., Castro-Jaimes, S., Castillo-Ramírez, S., Velázquez-Acosta, C., Martínez-Oliva, D., Pérez-Oseguera, A., Rivera-Buendía, F., & Volkow-Fernández, P. (2020). High mortality in an outbreak of multidrug

- resistant *Acinetobacter baumannii* infection introduced to an oncological hospital by a patient transferred from a general hospital. *PloS One*, *15*(7), e0234684.
<https://doi.org/10.1371/journal.pone.0234684>
- Dexter, C., Murray, G. L., Paulsen, I. T., & Peleg, A. Y. (2015). Community-acquired *Acinetobacter baumannii*: clinical characteristics, epidemiology and pathogenesis. *Expert Review of Anti-Infective Therapy*, *13*(5), 567–573.
<https://doi.org/10.1586/14787210.2015.1025055>
- Di Noto, G. P., Molina, M. C., & Quiroga, C. (2019). Insights into non-coding RNAs as novel antimicrobial drugs. *Frontiers in Genetics*, *10*(FEB), 1–7.
<https://doi.org/10.3389/fgene.2019.00057>
- Diallo, I., & Provost, P. (2020). RNA-sequencing analyses of small bacterial RNAs and their emergence as virulence factors in host pathogen interactions. *International Journal of Molecular Sciences*, *21*(5). <https://doi.org/10.3390/ijms21051627>
- Diancourt, L., Passet, V., Nemec, A., Dijkshoorn, L., & Brisse, S. (2010). The population structure of *Acinetobacter baumannii*: Expanding multiresistant clones from an ancestral susceptible genetic pool. *PLoS ONE*, *5*(4).
<https://doi.org/10.1371/journal.pone.0010034>
- Dijkshoorn, L., Nemec, A., & Seifert, H. (2007). An increasing threat in hospitals: Multidrug-resistant *Acinetobacter baumannii*. In *Nature Reviews Microbiology* (Vol. 5, Issue 12, pp. 939–951). <https://doi.org/10.1038/nrmicro1789>
- Douchin, V., Bohn, C., & Bouloc, P. (2006). Down-regulation of porins by a small RNA bypasses the essentiality of the regulated intramembrane proteolysis protease RseP in *Escherichia coli*. *Journal of Biological Chemistry*, *281*(18), 12253–12259.
<https://doi.org/10.1074/jbc.M600819200>
- Du, D., Wang-Kan, X., Neuberger, A., van Veen, H. W., Pos, K. M., Piddock, L. J. V.,

- & Luisi, B. F. (2018). Multidrug efflux pumps: structure, function and regulation. *Nature Reviews Microbiology*, *16*(9), 523–539. <https://doi.org/10.1038/s41579-018-0048-6>
- Eze, E. C., Chenia, H. Y., & El Zowalaty, M. E. (2018). *Acinetobacter baumannii* biofilms: Effects of physicochemical factors, virulence, antibiotic resistance determinants, gene regulation, and future antimicrobial treatments. *Infection and Drug Resistance*, *11*, 2277–2299. <https://doi.org/10.2147/IDR.S169894>
- Farrow, J. M., Wells, G., & Pesci, E. C. (2018). Desiccation tolerance in *Acinetobacter baumannii* is mediated by the two-component response regulator BfmR. *PLoS ONE*, *13*(10), 1–25. <https://doi.org/10.1371/journal.pone.0205638>
- Fiester, S. E., & Actis, L. A. (2013). Stress responses in the opportunistic pathogen *Acinetobacter baumannii*. *Future Microbiology*, *8*(3), 353–365. <https://doi.org/10.2217/fmb.12.150>
- Fily, F., Ronat, J. B., Malou, N., Kanapathipillai, R., Seguin, C., Hussein, N., Fakhri, R. M., & Langendorf, C. (2019). Post-traumatic osteomyelitis in Middle East war-wounded civilians: Resistance to first-line antibiotics in selected bacteria over the decade 2006-2016. *BMC Infectious Diseases*, *19*(1), 1–8. <https://doi.org/10.1186/s12879-019-3741-9>
- Fisher, R. A., Gollan, B., & Helaine, S. (2017). Persistent bacterial infections and persister cells. *Nature Reviews Microbiology*, *15*(8), 453–464. <https://doi.org/10.1038/nrmicro.2017.42>
- Fröhlich, K. S., Papenfort, K., Fekete, A., & Vogel, J. (2013). A small RNA activates CFA synthase by isoform-specific mRNA stabilization. *EMBO Journal*, *32*(22), 2963–2979. <https://doi.org/10.1038/emboj.2013.222>
- Fröhlich, K. S., & Vogel, J. (2009). Activation of gene expression by small RNA.

- Current Opinion in Microbiology*, 12(6), 674—682.
<https://doi.org/10.1016/j.mib.2009.09.009>
- Gaddy, J. A., & Actis, L. A. (2009). Regulation of *Acinetobacter baumannii* biofilm formation. *Future Microbiology*, 4, 273–278. <https://doi.org/10.1038/jid.2014.371>
- Georg, J., Lalaouna, D., Hou, S., Lott, S. C., Caldelari, I., Marzi, S., Hess, W. R., & Romby, P. (2020). The power of cooperation: Experimental and computational approaches in the functional characterization of bacterial sRNAs. *Molecular Microbiology*, 113(3), 603–612. <https://doi.org/10.1111/mmi.14420>
- Görke, B., & Vogel, J. (2008). Noncoding RNA control of the making and breaking of sugars. *Genes and Development*, 22(21), 2914–2925.
<https://doi.org/10.1101/gad.1717808>
- Gutierrez, A., Laureti, L., Crussard, S., Abida, H., Rodríguez-Rojas, A., Blázquez, J., Baharoglu, Z., Mazel, D., Darfeuille, F., Vogel, J., & Matic, I. (2013). β -lactam antibiotics promote bacterial mutagenesis via an RpoS-mediated reduction in replication fidelity. *Nature Communications*, 4.
<https://doi.org/10.1038/ncomms2607>
- Han, K., Tjaden, B., & Lory, S. (2016). GRIL-seq provides a method for identifying direct targets of bacterial small regulatory RNA by in vivo proximity ligation. *Nature Microbiology*, 2(0), 1–10. <https://doi.org/10.1038/nmicrobiol.2016.239>
- Heidrich, N., Bauriedl, S., Barquist, L., Li, L., Schoen, C., & Vogel, J. (2017). The primary transcriptome of *Neisseria meningitidis* and its interaction with the RNA chaperone Hfq. *Nucleic Acids Research*, 45(10), 6147–6167.
<https://doi.org/10.1093/nar/gkx168>
- Heindorf, M., Kadari, M., Heider, C., Skiebe, E., & Wilharm, G. (2014). Impact of *Acinetobacter baumannii* superoxide dismutase on motility, virulence, oxidative

- stress resistance and susceptibility to antibiotics. *PLoS ONE*, *9*(7), 1–11.
<https://doi.org/10.1371/journal.pone.0101033>
- Hoekzema, M., Romilly, C., Holmqvist, E., & Wagner, E. G. H. (2019). Hfq-dependent mRNA unfolding promotes sRNA -based inhibition of translation . *The EMBO Journal*, *38*(7), 1–14. <https://doi.org/10.15252/embj.2018101199>
- Holmqvist, E., & Vogel, J. (2013). A small RNA serving both the Hfq and CsrA regulons. *Genes and Development*, *27*(10), 1073–1078.
<https://doi.org/10.1101/gad.220178.113>
- Holmqvist, E., & Wagner, G. H. (2017). Impact of bacterial sRNAs in stress responses. *Biochemical Society Transactions*, *45*(6), 1203–1212.
<https://doi.org/10.1042/BST20160363>
- Holmqvist, E., Wright, P. R., Li, L., Bischler, T., Barquist, L., Reinhardt, R., Backofen, R., & Vogel, J. (2016). Global RNA recognition patterns of post-transcriptional regulators Hfq and CsrA revealed by UV crosslinking in vivo . *The EMBO Journal*, *35*(9), 991–1011. <https://doi.org/10.15252/embj.201593360>
- Hör, J., Gorski, S. A., & Vogel, J. (2018). Bacterial RNA Biology on a Genome Scale. *Molecular Cell*, *70*(5), 785–799. <https://doi.org/10.1016/j.molcel.2017.12.023>
- Jacobs, A. C., Thompson, M. G., Black, C. C., Kessler, J. L., Clark, L. P., McQueary, C. N., Gancz, H. Y., Corey, B. W., Moon, J. K., Si, Y., Owen, M. T., Hallock, J. D., Kwak, Y. I., Summers, A., Li, C. Z., Rasko, D. A., Penwell, W. F., Honnold, C. L., Wise, M. C., ... Zurawskia, D. V. (2014). AB5075, a Highly Virulent Isolate of *Acinetobacter baumannii*, as a Model Strain for the Evaluation of Pathogenesis and Antimicrobial Treatments. *Mbio*, *5*(3), 1–10.
<https://doi.org/10.1128/mBio.01076-14.Editor>
- Janssen, K. H., Diaz, M. R., Golden, M., Graham, J. W., Sanders, W., Wolfgang, M. C.,

- & Yahr, T. L. (2018). Functional analyses of the RsmY and RsmZ small noncoding regulatory RNAs in *Pseudomonas aeruginosa*. *Journal of Bacteriology*, *200*(11), 1–15. <https://doi.org/10.1128/JB.00736-17>
- Jayalath, K., Frisbie, S., To, M., & Abeysirigunawardena, S. (2020). Pseudouridine synthase rsua captures an assembly intermediate that is stabilized by ribosomal protein S17. *Biomolecules*, *10*(6). <https://doi.org/10.3390/biom10060841>
- Jin, J. S., Kwon, S. O., Moon, D. C., Gurung, M., Lee, J. H., Kim, S. Il, & Lee, J. C. (2011). *Acinetobacter baumannii* secretes cytotoxic outer membrane protein a via outer membrane vesicles. *PLoS ONE*, *6*(2). <https://doi.org/10.1371/journal.pone.0017027>
- Joly-Guillou, M. L. (2005). Clinical impact and pathogenicity of *Acinetobacter*. *Clinical Microbiology and Infection*, *11*(11), 868–873.
- Kay, E., Humair, B., Dénervaud, V., Riedel, K., Spahr, S., Eberl, L., Valverde, C., & Haas, D. (2006). Two GacA-dependent small RNAs modulate the quorum-sensing response in *Pseudomonas aeruginosa*. *Journal of Bacteriology*, *188*(16), 6026–6033. <https://doi.org/10.1128/JB.00409-06>
- Kery, M. B., Feldman, M., Livny, J., & Tjaden, B. (2014). TargetRNA2: Identifying targets of small regulatory RNAs in bacteria. *Nucleic Acids Research*, *42*(W1), 124–129. <https://doi.org/10.1093/nar/gku317>
- Keto-Timonen, R., Hietala, N., Palonen, E., Hakakorpi, A., Lindström, M., & Korkeala, H. (2016). Cold Shock Proteins: A Minireview with Special Emphasis on Csp-family of Enteropathogenic *Yersinia*. *Frontiers in Microbiology*, *7*(July), 1–7. <https://doi.org/10.3389/fmicb.2016.01151>
- Khan, M. A., Göpel, Y., Milewski, S., & Görke, B. (2016). Two small RNAs conserved in enterobacteriaceae provide intrinsic resistance to antibiotics targeting the cell

- wall biosynthesis enzyme glucosamine-6-phosphate synthase. *Frontiers in Microbiology*, 7(JUN), 1–13. <https://doi.org/10.3389/fmicb.2016.00908>
- Klein, G., & Raina, S. (2015). Regulated control of the assembly and diversity of lps by noncoding sRNAs. *BioMed Research International*, 2015. <https://doi.org/10.1155/2015/153561>
- Kröger, C., Dillon, S. C., Cameron, A. D. S., Papenfort, K., Sivasankaran, S. K., Hokamp, K., Chao, Y., Sittka, A., Hébrard, M., Händler, K., Colgan, A., Leekitcharoenphon, P., Langridge, G. C., Lohan, A. J., Loftus, B., Lucchini, S., Ussery, D. W., Dorman, C. J., Thomson, N. R., ... Hinton, J. C. D. (2012). The transcriptional landscape and small RNAs of *Salmonella enterica* serovar Typhimurium. *Proceedings of the National Academy of Sciences of the United States of America*, 109(20), 1277–1286. <https://doi.org/10.1073/pnas.1201061109>
- Kröger, C., Kary, S. C., Schauer, K., & Cameron, A. D. S. (2017). Genetic regulation of virulence and antibiotic resistance in *Acinetobacter baumannii*. *Genes*, 8(1). <https://doi.org/10.3390/genes8010012>
- Kröger, C., MacKenzie, K. D., Alshabib, E. Y., Kirzinger, M. W. B., Suchan, D. M., Chao, T. C., Akulova, V., Miranda-CasoLuengo, A. A., Monzon, V. A., Conway, T., Sivasankaran, S. K., Hinton, J. C. D., Hokamp, K., & Cameron, A. D. S. (2018). The primary transcriptome, small RNAs and regulation of antimicrobial resistance in *Acinetobacter baumannii* ATCC 17978. *Nucleic Acids Research*, 46(18), 9684–9698. <https://doi.org/10.1093/nar/gky603>
- Kulkarni, P. R., Cui, X., Williams, J. W., Stevens, A. M., & Kulkarni, R. V. (2006). Prediction of CsrA-regulating small RNAs in bacteria and their experimental verification in *Vibrio fischeri*. *Nucleic Acids Research*, 34(11), 3361–3369. <https://doi.org/10.1093/nar/gkl439>

- Kung, C., Martinac, B., & Sukharev, S. (2010). Mechanosensitive channels in microbes. *Annual Review of Microbiology*, *64*, 313–329.
<https://doi.org/10.1146/annurev.micro.112408.134106>
- Kuo, H. Y., Chao, H. H., Liao, P. C., Hsu, L., Chang, K. C., Tung, C. H., Chen, C. H., & Liou, M. L. (2017). Functional characterization of *Acinetobacter baumannii* Lacking the RNA chaperone Hfq. *Frontiers in Microbiology*, *8*(OCT), 1–12.
<https://doi.org/10.3389/fmicb.2017.02068>
- Lai, D., & Meyer, I. M. (2015). A comprehensive comparison of general RNA-RNA interaction prediction methods. *Nucleic Acids Research*, *44*(7), 1–13.
<https://doi.org/10.1093/nar/gkv1477>
- Lalaouna, D., Carrier, M. C., Semsey, S., Brouard, J. S., Wang, J., Wade, J. T., & Massé, E. (2015). A 3' external transcribed spacer in a tRNA transcript acts as a sponge for small RNAs to prevent transcriptional noise. *Molecular Cell*, *58*(3), 393–405. <https://doi.org/10.1016/j.molcel.2015.03.013>
- Lalaouna, D., Eyraud, A., Devinck, A., Prévost, K., & Massé, E. (2019). GcvB small RNA uses two distinct seed regions to regulate an extensive targetome. *Molecular Microbiology*, *111*(2), 473–486. <https://doi.org/10.1111/mmi.14168>
- Lalaouna, D., & Massé, E. (2015). Identification of sRNA interacting with a transcript of interest using MS2-affinity purification coupled with RNA sequencing (MAPS) technology. *Genomics Data*, *5*, 136–138.
<https://doi.org/10.1016/j.gdata.2015.05.033>
- Lau, C. K. Y., Krewulak, K. D., & Vogel, H. J. (2016). Bacterial ferrous iron transport: The Feo system. *FEMS Microbiology Reviews*, *40*(2), 273–298.
<https://doi.org/10.1093/femsre/fuv049>
- Lee, C. R., Lee, J. H., Park, M., Park, K. S., Bae, I. K., Kim, Y. B., Cha, C. J., Jeong, B.

- C., & Lee, S. H. (2017). Biology of *Acinetobacter baumannii*: Pathogenesis, antibiotic resistance mechanisms, and prospective treatment options. *Frontiers in Cellular and Infection Microbiology*, 7(MAR).
<https://doi.org/10.3389/fcimb.2017.00055>
- Lee, S. Y., Yun, S. H., Lee, H., Yi, Y. S., Park, E. C., Kim, W., Kim, H. Y., Lee, J. C., Kim, G. H., & Kim, S. Il. (2020). Analysis of the Extracellular Proteome of Colistin-Resistant Korean *Acinetobacter baumannii* Strains. *ACS Omega*, 5(11), 5713–5720. <https://doi.org/10.1021/acsomega.9b03723>
- Liu, H., Liu, W., He, X., Chen, X., Yang, J., Wang, Y., Li, Y., Ren, J., Xu, W., & Zhao, Y. (2020). Characterization of a cell density-dependent sRNA, Qrr, and its roles in the regulation of the quorum sensing and metabolism in *Vibrio alginolyticus*. *Applied Microbiology and Biotechnology*, 104(4), 1707–1720.
<https://doi.org/10.1007/s00253-019-10278-3>
- Liu, Z., Wang, H., Wang, H., Wang, J., Bi, Y., Wang, X., Yang, R., & Han, Y. (2015). Intrinsic plasmids influence MicF-mediated translational repression of ompF in *Yersinia pestis*. *Frontiers in Microbiology*, 6(August), 1–8.
<https://doi.org/10.3389/fmicb.2015.00862>
- Lob, S. H., Hoban, D. J., Sahm, D. F., & Badal, R. E. (2016). Regional differences and trends in antimicrobial susceptibility of *Acinetobacter baumannii*. *International Journal of Antimicrobial Agents*, 47(4), 317–323.
<https://doi.org/10.1016/j.ijantimicag.2016.01.015>
- Lu, P., Wang, Y., Zhang, Y., Hu, Y., Thompson, K. M., & Chen, S. (2016). RpoS-dependent sRNA RgsA regulates Fis and AcpP in *Pseudomonas aeruginosa*. *Molecular Microbiology*, 102(2), 244–259. <https://doi.org/10.1111/mmi.13458>
- Lucidi, M., Runci, F., Rampioni, G., Frangipani, E., Leoni, L., & Visca, P. (2018). New

- Shuttle Vectors for Gene Cloning and Expression in. *Antimicrobial Agents and Chemotherapy*, 62(4), 1–19.
- Magill, S. S., Edwards, J. R., Bamberg, W., Beldavs, Z. G., Dumyati, G., Kainer, M. A., Lynfield, R., Maloney, M., McAllister-Hollod, L., Nadle, J., Ray, S. M., Thompson, D. L., Wilson, L. E., & Fridkin, S. K. (2014). Multistate Point-Prevalence Survey of Health Care–Associated Infections. *New England Journal of Medicine*, 370(13), 1198–1208. <https://doi.org/10.1056/NEJMoa1306801>
- Massé, E., Vanderpool, C. K., & Gottesman, S. (2005). Effect of RyhB Small RNA on Global Iron Use in *Escherichia coli*. *Journal of Bacteriology*, 187(20), 6962 LP – 6971. <https://doi.org/10.1128/JB.187.20.6962-6971.2005>
- Matos, R. G., Casinhas, J., Bárria, C., Dos Santos, R. F., Silva, I. J., & Arraiano, C. M. (2017). The role of ribonucleases and sRNAs in the virulence of foodborne pathogens. *Frontiers in Microbiology*, 8(MAY), 1–7. <https://doi.org/10.3389/fmicb.2017.00910>
- Melamed, S., Peer, A., Faigenbaum-Romm, R., Gatt, Y. E., Reiss, N., Bar, A., Altuvia, Y., Argaman, L., & Margalit, H. (2016). Global Mapping of Small RNA-Target Interactions in Bacteria. *Molecular Cell*, 63(5), 884–897. <https://doi.org/10.1016/j.molcel.2016.07.026>
- Melior, H., Li, S., Madhugiri, R., Stötzel, M., Azarderakhsh, S., Barth-Weber, S., Baumgardt, K., Ziebuhr, J., & Evguenieva-Hackenberg, E. (2019). Transcription attenuation-derived small RNA rnrTrpL regulates tryptophan biosynthesis gene expression in trans. *Nucleic Acids Research*, 47(12), 6396–6410. <https://doi.org/10.1093/nar/gkz274>
- Michaux, C., Holmqvist, E., Vasicek, E., Sharan, M., Barquist, L., Westermann, A. J., Gunn, J. S., & Vogel, J. (2017). RNA target profiles direct the discovery of

- virulence functions for the cold-shock proteins CspC and CspE. *Proceedings of the National Academy of Sciences of the United States of America*, 114(26), 6824–6829. <https://doi.org/10.1073/pnas.1620772114>
- Miyakoshi, M., Chao, Y., & Vogel, J. (2015). Regulatory small RNAs from the 3' regions of bacterial mRNAs. *Current Opinion in Microbiology*, 24, 132–139. <https://doi.org/10.1016/j.mib.2015.01.013>
- Moon, K., & Gottesman, S. (2011). Competition among Hfq-binding small RNAs in *Escherichia coli*. *Molecular Microbiology*, 82(6), 1545–1562. <https://doi.org/10.1111/j.1365-2958.2011.07907.x>
- Morita, T., & Aiba, H. (2019). Mechanism and physiological significance of autoregulation of the *Escherichia coli* HFQ gene. *Rna*, 25(2), 264–276. <https://doi.org/10.1261/rna.068106.118>
- Morita, T., Maki, K., & Aiba, H. (2012). Detection of sRNA--mRNA Interactions by Electrophoretic Mobility Shift Assay. In K. C. Keiler (Ed.), *Bacterial Regulatory RNA: Methods and Protocols* (pp. 235–244). Humana Press. https://doi.org/10.1007/978-1-61779-949-5_15
- Müller, P., Gimpel, M., Wildenhain, T., & Brantl, S. (2019). A new role for CsrA: promotion of complex formation between an sRNA and its mRNA target in *Bacillus subtilis*. *RNA Biology*, 16(7), 972–987. <https://doi.org/10.1080/15476286.2019.1605811>
- Nelson, R. E., Schweizer, M. L., Perencevich, E. N., Nelson, S. D., Khader, K., Chiang, H. Y., Chorazy, M. L., Blevins, A., Ward, M. A., & Samore, M. H. (2016). Costs and mortality associated with multidrug-resistant healthcare-associated acinetobacter infections. *Infection Control and Hospital Epidemiology*, 37(10), 1212–1218. <https://doi.org/10.1017/ice.2016.145>

- New England Biolabs Inc. (2016). *Monarch*® PCR & DNA Cleanup Kit (5 µg). 1–5.
- Nguyen, T., Clare, B., Guo, W., & Martinac, B. (2005). The effects of parabens on the mechanosensitive channels of *E. coli*. *European Biophysics Journal*, 34(5), 389–395. <https://doi.org/10.1007/s00249-005-0468-x>
- Nie, D., Hu, Y., Chen, Z., Li, M., Hou, Z., Luo, X., Mao, X., & Xue, X. (2020). Outer membrane protein A (OmpA) as a potential therapeutic target for *Acinetobacter baumannii* infection. *Journal of Biomedical Science*, 27(1), 1–8. <https://doi.org/10.1186/s12929-020-0617-7>
- Nwugo, C. C., Gaddy, J. A., Zimble, D. L., & Actis, L. A. (2011). Deciphering the iron response in *Acinetobacter baumannii*: A proteomics approach. *Journal of Proteomics*, 74(1), 44–58. <https://doi.org/10.1016/j.jprot.2010.07.010>
- Oliva, G., Sahr, T., & Buchrieser, C. (2015). Small RNAs, 5' UTR elements and RNA-binding proteins in intracellular bacteria: Impact on metabolism and virulence. *FEMS Microbiology Reviews*, 39(3), 331–349. <https://doi.org/10.1093/femsre/fuv022>
- Omega Bio-Tek. (2018). *E. Z. N. A*® Plasmid DNA Mini Kit I Product Manual. July 2019, 6942–6943. <https://doi.org/10.1128/AEM.07230-11.Qi>
- Papenfort, K., Bouvier, M., Mika, F., Sharma, C. M., & Vogel, J. (2010). Evidence for an autonomous 5' target recognition domain in an Hfq-associated small RNA. *Proceedings of the National Academy of Sciences*, 107(47), 20435 LP – 20440. <https://doi.org/10.1073/pnas.1009784107>
- Papenfort, K., Podkaminski, D., Hinton, J. C. D., & Vogel, J. (2012). The ancestral SgrS RNA discriminates horizontally acquired Salmonella mRNAs through a single G-U wobble pair. *Proceedings of the National Academy of Sciences*, 109(13), E757 LP-E764. <https://doi.org/10.1073/pnas.1119414109>

- Papenfert, K., & Vogel, J. (2009). Multiple target regulation by small noncoding RNAs rewires gene expression at the post-transcriptional level. *Research in Microbiology*, 160(4), 278–287. <https://doi.org/10.1016/j.resmic.2009.03.004>
- Partridge, S. R., Kwong, S. M., Firth, N., & Jensen, S. O. (2018). Mobile genetic elements associated with antimicrobial resistance. *Clinical Microbiology Reviews*, 31(4), 1–61. <https://doi.org/10.1128/CMR.00088-17>
- Peng, K., & Monack, D. M. (2010). Indoleamine 2,3-dioxygenase 1 is a lung-specific innate immune defense mechanism that inhibits growth of *Francisella tularensis* tryptophan auxotrophs. *Infection and Immunity*, 78(6), 2723–2733. <https://doi.org/10.1128/IAI.00008-10>
- Reinhart, A. A., Nguyen, A. T., Brewer, L. K., Bever, J., Jones, J. W., Kane, M. A., Damron, F. H., Barbier, M., & Oglesby-Sherrouse, A. G. (2017). The *Pseudomonas aeruginosa* PrrF Small Acute Murine Lung Infection. *Infection and Immunity*, 85(5), 1–15. <https://doi.org/10.1128/IAI.00764-16>
- Roca, I., Espinal, P., Vila-Fanés, X., & Vila, J. (2012). The *Acinetobacter baumannii* oxymoron: Commensal hospital dweller turned pan-drug-resistant menace. *Frontiers in Microbiology*, 3(APR), 1–30. <https://doi.org/10.3389/fmicb.2012.00148>
- Rodman, N., Martinez, J., Fung, S., Nakanouchi, J., Myers, A. L., Harris, C. M., Dang, E., Fernandez, Jennifer S., Liu, Christine, Mendoza, A. M., Jimenez, V., Nikolaidis, N., A., B. C., Bonomo, R. A., Sieira, R., & Ramirez, M. S. (2019). Human Pleural Fluid Elicits Pyruvate and Phenylalanine Metabolism in *Acinetobacter baumannii* to Enhance Cytotoxicity and Immune Evasion. *Frontiers in Microbiology*, 10(JULY), 1–19. <https://doi.org/10.3389/fmicb.2019.01581>
- Rumbo-Feal, S., Gómez, M. J., Gayoso, C., Álvarez-Fraga, L., Cabral, M. P., Aransay,

- A. M., Rodríguez-Ezpeleta, N., Fullaondo, A., Valle, J., Tomás, M., Bou, G., & Poza, M. (2013). Whole Transcriptome Analysis of *Acinetobacter baumannii* Assessed by RNA-Sequencing Reveals Different mRNA Expression Profiles in Biofilm Compared to Planktonic Cells. *PLoS ONE*, *8*(8), 1–19.
<https://doi.org/10.1371/journal.pone.0072968>
- Runci, F., Gentile, V., Frangipani, E., Rampioni, G., Leoni, L., Lucidi, M., Visaggio, D., Harris, G., Chen, W., Stahl, J., Averhoff, B., & Visca, P. (2019). Contribution of active iron uptake to *acinetobacter baumannii* pathogenicity. *Infection and Immunity*, *87*(4), 1–16. <https://doi.org/10.1128/IAI.00755-18>
- Saliba, A. E., C Santos, S., & Vogel, J. (2017). New RNA-seq approaches for the study of bacterial pathogens. *Current Opinion in Microbiology*, *35*, 78–87.
<https://doi.org/10.1016/j.mib.2017.01.001>
- Santiago-Frangos, A., & Woodson, S. A. (2018). Hfq chaperone brings speed dating to bacterial sRNA. *Wiley Interdisciplinary Reviews: RNA*, *9*(4), 1–16.
<https://doi.org/10.1002/wrna.1475>
- Schilling, D., Findei, S., Richter, A. S., Taylor, J. A., & Gerischer, U. (2010). The small RNA Aar in *Acinetobacter baylyi*: A putative regulator of amino acid metabolism. *Archives of Microbiology*, *192*(9), 691–702. <https://doi.org/10.1007/s00203-010-0592-6>
- Schilling, D., & Gerischer, U. (2009). The *Acinetobacter baylyi* hfq gene encodes a large protein with an unusual C terminus. *Journal of Bacteriology*, *191*(17), 5553–5562. <https://doi.org/10.1128/JB.00490-09>
- Sestok, A. E., Linkous, R. O., & Smith, A. T. (2018). Toward a Mechanistic Understanding of Feo-Mediated Ferrous Iron Uptake Alexandria. *Metallomics*, *10*(7), 887–898. <https://doi.org/10.1016/j.physbeh.2017.03.040>

- Sharma, A., Dubey, V., Sharma, R., Devnath, K., Gupta, V. K., Akhter, J., Bhandu, T., Verma, A., Ambatipudi, K., Sarkar, M., & Pathania, R. (2018). The unusual glycine-rich C terminus of the *Acinetobacter baumannii* RNA chaperone Hfq plays an important role in bacterial physiology. *Journal of Biological Chemistry*, *293*(35), 13377–13388. <https://doi.org/10.1074/jbc.RA118.002921>
- Sharma, C. M., Papenfort, K., Pernitzsch, S. R., Mollenkopf, H. J., Hinton, J. C. D., & Vogel, J. (2011). Pervasive post-transcriptional control of genes involved in amino acid metabolism by the Hfq-dependent GcvB small RNA. *Molecular Microbiology*, *81*(5), 1144–1165. <https://doi.org/10.1111/j.1365-2958.2011.07751.x>
- Sharma, R., Arya, S., Patil, S. D., Sharma, A., Jain, P. K., Navani, N. K., & Pathania, R. (2014). Identification of novel regulatory small RNAs in *Acinetobacter baumannii*. *PLoS ONE*, *9*(4). <https://doi.org/10.1371/journal.pone.0093833>
- Shin, J.-H., Sulpizio, A. G., Kelley, A., Alvarez, L., Murphy, S. G., Fan, L., Cava, F., Mao, Y., Saper, M. A., & Dörr, T. (2020). Structural basis of peptidoglycan endopeptidase regulation. *Proceedings of the National Academy of Sciences*, *202001661*. <https://doi.org/10.1073/pnas.2001661117>
- Sievert, D., Ricks, P., Edwards, J. R., Schneider, A., Patel, J., Srinivasan, A., Kallen, A., Limbago, B., & Fridkin, S. (2013). Antimicrobial-Resistant Pathogens Associated with Healthcare-Associated Infections Summary of Data Reported to the National Healthcare Safety Network at the Centers for Disease Control and Prevention, 2009–2010. *Infection Control & Hospital Epidemiology*, *34*(1), 1–14. <https://doi.org/10.1086/668770>
- Smirnov, A., Förstner, K. U., Holmqvist, E., Otto, A., Günster, R., Becher, D., Reinhardt, R., & Vogel, J. (2016). Grad-seq guides the discovery of ProQ as a

- major small RNA-binding protein. *Proceedings of the National Academy of Sciences*, 113(41), 11591 LP – 11596. <https://doi.org/10.1073/pnas.1609981113>
- Smirnov, A., Wang, C., Drewry, L. L., & Vogel, J. (2017). Molecular mechanism of mRNA repression in trans by a ProQ-dependent small RNA. *The EMBO Journal*, 36(8), 1029–1045. <https://doi.org/10.15252/emj.201696127>
- Sobrero, P. M., & Valverde, C. (2020). Comparative Genomics and Evolutionary Analysis of RNA-Binding Proteins of the CsrA Family in the Genus *Pseudomonas*. *Frontiers in Molecular Biosciences*, 7(July), 1–22. <https://doi.org/10.3389/fmolb.2020.00127>
- Song, S., & Wood, T. K. (2020). Persister cells resuscitate via ribosome modification by 23S rRNA pseudouridine synthase RluD. *Environmental Microbiology*, 22(3), 850–857. <https://doi.org/10.1111/1462-2920.14828>
- Sonnleitner, E., Romeo, A., & Bläsi, U. (2012). Small regulatory RNAs in *Pseudomonas aeruginosa*. *RNA Biology*, 9(4), 364–371. <https://doi.org/10.4161/rna.19231>
- Storz, G., Vogel, J., & Wassarman, K. M. (2011). Regulation by Small RNAs in Bacteria: Expanding Frontiers. *Molecular Cell*, 43(6), 880–891. <https://doi.org/10.1016/j.molcel.2011.08.022>.Regulation
- Subashchandrabose, S., Smith, S., DeOrnellas, V., Crepin, S., Kole, M., Zahdeh, C., & Mobley, H. L. T. (2016). *Acinetobacter baumannii* Genes Required for Bacterial Survival during Bloodstream Infection. *MSphere*, 1(1), 1–12. <https://doi.org/10.1128/msphere.00013-15>
- Sun, Y., & Riordan, M. X. D. (2010). Branched-Chain Fatty Acids Promote *Listeria monocytogenes* Intracellular Infection and Virulence. *Infection and Immunity*, 78(11), 4667 LP – 4673. <https://doi.org/10.1128/IAI.00546-10>

- Tacconelli, E., Carrara, E., Savoldi, A., Harbarth, S., Mendelson, M., Monnet, D. L., Pulcini, C., Kahlmeter, G., Kluytmans, J., Carmeli, Y., Ouellette, M., Outtersson, K., Patel, J., Cavaleri, M., Cox, E. M., Houchens, C. R., Grayson, M. L., Hansen, P., Singh, N., ... Zorzet, A. (2018). Discovery, research, and development of new antibiotics: the WHO priority list of antibiotic-resistant bacteria and tuberculosis. *The Lancet Infectious Diseases*, *18*(3), 318–327. [https://doi.org/10.1016/S1473-3099\(17\)30753-3](https://doi.org/10.1016/S1473-3099(17)30753-3)
- Towner, K. J. (2009). Acinetobacter: an old friend, but a new enemy. *Journal of Hospital Infection*, *73*(4), 355–363. <https://doi.org/10.1016/j.jhin.2009.03.032>
- Urban, J. H., & Vogel, J. (2007). Translational control and target recognition by Escherichia coli small RNAs in vivo. *Nucleic Acids Research*, *35*(3), 1018–1037. <https://doi.org/10.1093/nar/gkl1040>
- Valverde, C., Lindell, M., Wagner, E. G. H., & Haas, D. (2004). A repeated GGA motif is critical for the activity and stability of the riboregulator RsmY of Pseudomonas fluorescens. *Journal of Biological Chemistry*, *279*(24), 25066–25074. <https://doi.org/10.1074/jbc.M401870200>
- Vazquez-Anderson, J., Mihailovic, M. K., Baldrige, K. C., Reyes, K. G., Haning, K., Cho, S. H., Amador, P., Powell, W. B., & Contreras, L. M. (2017). Optimization of a novel biophysical model using large scale in vivo antisense hybridization data displays improved prediction capabilities of structurally accessible RNA regions. *Nucleic Acids Research*, *45*(9), 5523–5538. <https://doi.org/10.1093/nar/gkx115>
- Vogel, J., & Papenfort, K. (2006). Small non-coding RNAs and the bacterial outer membrane. *Current Opinion in Microbiology*, *9*(6), 605–611. <https://doi.org/10.1016/j.mib.2006.10.006>
- Vogel, J., & Wagner, E. G. H. (2007). Target identification of small noncoding RNAs

- in bacteria. *Current Opinion in Microbiology*, 10(3), 262–270.
<https://doi.org/10.1016/j.mib.2007.06.001>
- Wagner, E. G. H., & Romby, P. (2015). Small RNAs in Bacteria and Archaea: Who They Are, What They Do, and How They Do It. In *Advances in Genetics* (Vol. 90). Elsevier Ltd. <https://doi.org/10.1016/bs.adgen.2015.05.001>
- Wang, J., Rennie, W., Liu, C., Carmack, C. S., Prévost, K., Caron, M. P., Massé, E., Ding, Y., & Wade, J. T. (2015). Identification of bacterial sRNA regulatory targets using ribosome profiling. *Nucleic Acids Research*, 43(21), 10308–10320.
<https://doi.org/10.1093/nar/gkv1158>
- Wang, N., Ozer, E. A., Mandel, M. J., & Hauser, A. R. (2014). Genome-wide identification of *Acinetobacter baumannii* genes necessary for persistence in the lung. *MBio*, 5(3), 1–8. <https://doi.org/10.1128/mBio.01163-14>
- Wassarman, K. M. (2018). 6S RNA, a Global Regulator of Transcription. *Regulating with RNA in Bacteria and Archaea*, 6(3), 355–367.
<https://doi.org/10.1128/9781683670247.ch20>
- Wei, B., Shin, S., Laporte, D., Wolfe, A. J., & Romeo, T. (2000). Global regulatory mutations in *csrA* and *rpoS* cause severe central carbon stress in *Escherichia coli* in the presence of acetate. *Journal of Bacteriology*, 182(6), 1632–1640.
<https://doi.org/10.1128/JB.182.6.1632-1640.2000>
- Weiner, L. M., Webb, A. K., Limbago, B., Dudeck, M. A., Patel, J., Kallen, A. J., Edwards, J. R., & Sievert, D. M. (2016). Antimicrobial-Resistant Pathogens Associated With Healthcare-Associated Infections: Summary of Data Reported to the National Healthcare Safety Network at the Centers for Disease Control and Prevention, 2011-2014. *Infection Control and Hospital Epidemiology*, 37(11), 1288–1301. <https://doi.org/10.1016/j.physbeh.2017.03.040>

- Weiss, A., Broach, W. H., Lee, M. C., & Shaw, L. N. (2016). Towards the complete small RNome of *Acinetobacter baumannii*. *Microbial Genomics*, 2(3), 1–18.
<https://doi.org/10.1099/mgen.0.000045>
- Westermann, A. J., Förstner, K. U., Amman, F., Barquist, L., Chao, Y., Schulte, L. N., Müller, L., Reinhardt, R., Stadler, P. F., & Vogel, J. (2016). Dual RNA-seq unveils noncoding RNA functions in host-pathogen interactions. *Nature*, 529(7587), 496–501. <https://doi.org/10.1038/nature16547>
- Westermann, A. J., Venturini, E., Sellin, M. E., Förstner, K. U., Hardt, W.-D., & Vogel, J. (2019). The Major RNA-Binding Protein ProQ Impacts Virulence Gene Expression in *Salmonella enterica* Serovar Typhimurium. *MBio*, 10(1), e02504-18.
<https://doi.org/10.1128/mBio.02504-18>
- Wood, C. R., Mack, L. E., & Actis, L. A. (2018). An Update on the *Acinetobacter baumannii* Regulatory Circuitry. *Trends in Microbiology*, 26(7), 560–562.
<https://doi.org/10.1016/j.tim.2018.05.005>
- Woodson, S. A., Panja, S., & Santiago-Frangos, A. (2018). Proteins That Chaperone RNA Regulation. *Regulating with RNA in Bacteria and Archaea*, 6(4), 383–397.
<https://doi.org/10.1128/9781683670247.ch22>
- Wright, P. R., Georg, J., Mann, M., Sorescu, D. A., Richter, A. S., Lott, S., Kleinkauf, R., Hess, W. R., & Backofen, R. (2014). CopraRNA and IntaRNA: Predicting small RNA targets, networks and interaction domains. *Nucleic Acids Research*, 42(W1), 119–123. <https://doi.org/10.1093/nar/gku359>
- Wright, P. R., Mann, M., & Backofen, R. (2018). Structure and Interaction Prediction in Prokaryotic RNA Biology. *Microbiology Spectrum*, 6(2), 1–17.
<https://doi.org/10.1128/microbiolspec>
- Wright, P. R., Richter, A. S., Papenfort, K., Mann, M., Vogel, J., Hess, W. R.,

- Backofen, R., & Georg, J. (2013). Comparative genomics boosts target prediction for bacterial small RNAs. *Proceedings of the National Academy of Sciences*, *110*(37), E3487 LP-E3496. <https://doi.org/10.1073/pnas.1303248110>
- Wu, F., & Hu, R. (2020). Risk factors for pneumonia caused by antimicrobial drug-resistant or drug-sensitive *Acinetobacter baumannii* infections: A retrospective study. *Medicine*, *99*(28), e21051. <https://doi.org/10.1097/MD.00000000000021051>
- Yamada, J., Yamasaki, S., Hirakawa, H., Hayashi-nishino, M., Yamaguchi, A., & Nishino, K. (2010). Impact of the RNA chaperone HFQ on multidrug resistance in *Escherichia coli*. *Journal of Antimicrobial Chemotherapy*, *65*(5), 853–858. <https://doi.org/10.1093/jac/dkq067>
- Yang, H., Liu, M. Y., & Romeo, T. (1996). Coordinate genetic regulation of glycogen catabolism and biosynthesis in *Escherichia coli* via the CsrA gene product. *Journal of Bacteriology*, *178*(4), 1012–1017. <https://doi.org/10.1128/jb.178.4.1012-1017.1996>
- Zeidler, S., & Müller, V. (2019a). Coping with low water activities and osmotic stress in *Acinetobacter baumannii*: significance, current status and perspectives. *Environmental Microbiology*, *21*(7), 2212–2230. <https://doi.org/10.1111/1462-2920.14565>
- Zeidler, S., & Müller, V. (2019b). The role of compatible solutes in desiccation resistance of *Acinetobacter baumannii*. *MicrobiologyOpen*, *8*(5), 1–9. <https://doi.org/10.1002/mbo3.740>
- Zhang, Y. F., Han, K., Chandler, C. E., Tjaden, B., Ernst, R. K., & Lory, S. (2017). Probing the sRNA regulatory landscape of *P. aeruginosa*: post-transcriptional control of determinants of pathogenicity and antibiotic susceptibility. *Molecular Microbiology*, *106*(6), 919–937. <https://doi.org/10.1111/mmi.13857>

Zhang, Y., Werling, U., & Edelman, W. (2012). SLiCE: A novel bacterial cell extract-based DNA cloning method. *Nucleic Acids Research*, *40*(8), 1–10.

<https://doi.org/10.1093/nar/gkr1288>

Zhang, Y., Werling, U., & Edelman, W. (2014). Seamless Ligation Cloning Extract (SLiCE) Cloning Method. *Methods in Molecular Biology*, *1116*(January), 1–24.

<https://doi.org/10.1007/978-1-62703-764-8>